

e-ISSN : 2320-0847

p-ISSN : 2320-0936



AJER

American Journal of Engineering Research

Volume-2 Issue-3



AJER

American Journal of Engineering Research

**American Journal of
Engineering Research**

Editorial Board

American Journal of Engineering Research (AJER)

**Dr. Jonathan Okeke
Chimakonam**

Qualification: PHD
Affiliation: University of Calabar
Specialization: Logic, Philosophy of
Maths and African Science,
Country: Nigeria

Dr. ABDUL KAREEM

Qualification: MBBS, DMRD, FCIP, FAGE
Affiliation: UNIVERSITI SAINS Malaysia
Country: Malaysia

Dr. sukhmander singh

Qualification: Phd
Affiliation: Indian Institute Of
Technology, Delhi
Specialization : PLASMA PHYSICS
Country: India

Dr. Nwachukwu Eugene Nnamdi

Qualification: Phd
Affiliation: Michael Okpara University of
Agriculture, Umudike, Nigeria
Specialization: Animal Genetics and
Breeding
Country: Nigeria

Dr. June II A. Kiblasan

Qualification : Phd
Specialization: Management, applied
sciences
Country: PHILIPPINES

Dr. Narendra Kumar Sharma

Qualification: PHD
Affiliation: Defence Institute of Physiology
and Allied Science, DRDO
Specialization: Proteomics, Molecular
biology, hypoxia
Country: India

Prof. Dr. Shafique Ahmed Arain

Qualification: Postdoc fellow, Phd
Affiliation: Shah Abdul Latif University
Khairpur (Mirs),
Specialization: Polymer science
Country: Pakistan

Dr. Alcides Chaux

Qualification: MD
Affiliation: Norte University, Paraguay,
South America
Specialization: Genitourinary Tumors
Country: Paraguay, South America

Dr. Md. Nazrul Islam Mondal

Qualification: Phd
Affiliation: Rajshahi University, Bangladesh
Specialization: Health and Epidemiology
Country: Bangladesh

CONTENTS

Volume-2 Issue-3

S.No.	Title Name	Page No.
01.	Influence of enhanced curing temperature of epoxy monomers structure on the electro-optical properties and morphology of polymer-dispersed liquid crystal films Mujtaba Ellahi, Yanzi Gao, M.Y.Rafique	01-06
02.	Advanced Linux Security Ranjit Nimbalkar, Paras Patel, Dr. B. B. Meshram	07-12
03.	Investigating Emission Values of a Passenger Vehicle in the Idle Mode and Comparison with Regulated Values O.N Aduagba, J. D. Amine, and M.I. Oseni	13-19
04.	Comparison of Performance of Standard Concrete And Fibre Reinforced Standard Concrete Exposed To Elevated Temperatures K.Srinivasa Rao, S.Rakesh kumar, A.Laxmi Narayana	20-26
05.	Compressive Study on Importance of Wind Power in India Dr. Srinivasa Rao Kasisomayajula	27-35
06.	Rheological Behavior of Tomato Fruits Affected By Various Loads Under Storage Conditions Nabil S. Albaloushi	36-43
07.	Dwt - Based Feature Extraction from ecg Signal V.K.Srivastava, Dr. Devendra Prasad	44-50
08.	Spatiotemporal Pattern of Crime Using Geographic Information System (GIS) Approach in Dala L.G.A of Kano State, Nigeria M. Ahmed and R. S. Salihu	51-58
09	Quality of Irrigation Water and Soil Characteristics of Watari Irrigation Project Adamu G.K	59-68

Influence of enhanced curing temperature of epoxy monomers structure on the electro-optical properties and morphology of polymer-dispersed liquid crystal films

Mujtaba Ellahi¹, Yanzi Gao², M.Y.Rafique³

^{1,2}(Department of Materials Physics and Chemistry, School of Materials Science and Engineering, University of Science and Technology Beijing, P.R.CHINA)

³(Department of Physics, University of Science and Technology Beijing, P.R.CHINA)

Abstract: The effect of enhanced curing temperature of epoxy monomers structure on the electro-optical properties and morphology of Polymer dispersed liquid crystal (PDLC) films has been studied. PDLC films were prepared by polymerization induced separation (PIPS) method with nematic liquid crystal (LC) content as low as 40 wt% and the electro-optical (E-O) properties were carefully investigated. To accomplish this, epoxy curable monomers structure with different molar ratio of two mixtures was examined in PDLC films. The LC domain size in the PDLC films decreased at first and then increased with the gradual raise of the curing temperature with lower LC content. Meanwhile, the E-O properties of the PDLC film depended strongly on the LC droplet size. The detailed characteristics and morphology of polymer network of PDLC films were analyzed by employing liquid crystal device (LCD) parameters tester and scanning electron microscopy (SEM). It was found that the LC domain size of the polymer network could be regulated by adjusting the curing temperature, structure and composition ratio of curable epoxy monomers, then the electro-optical of PDLC films could be optimized; which is beneficial to a novel generation of materials with sophisticated properties and new effects ready for use in various areas of modern technologies.

Keywords: Polymer dispersed liquid crystal, electro-optical, curable monomers, morphology, LC content.

I. INTRODUCTION

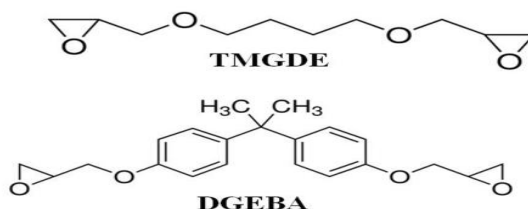
Polymer-dispersed liquid crystal (PDLC) films have been studied for many years. PDLC films constitute a high active research area in polymer science comparatively new technology of materials that consist of micron-sized LC droplets dispersed in a solid polymer matrix [1-3]. Usually, the E-O properties of PDLC films can be affected by the LC concentration, film thickness, separation degree and dimension, composition ratio of monomers and morphology of the LC domain size [4]. Four general methods have been developed for the formation of PDLC films, including encapsulation, PIPS (polymerization-induced phase separation), TIPS (thermal-induced phase separation) and SIPS (solvent-induced phase separation) methods [5-7]. However, the PIPS method with heat curing technique is more reliable to provide homogeneity and forms a uniform morphology of polymer networks that renders it insensitive to temperature changes. Epoxy resins are widely utilized for coatings and structural applications, adhesives and composites for microelectronic encapsulants. Among the various families of cross linking resins, epoxies are widely used due to their exceptional performance, coupled with very easy usage methods and limited cost. The effect of curing temperature on the electro-optic behavior and polymer network morphology has been studied by Dierking I et al [8]. In our group, Ping Song et al studied a UV polymerization temperature dependence of PDLCs based on epoxies/acrylates hybrid polymer matrix components by the PIPS method [9]. In the present experiments, PDLC films with LC content as low as 40 wt% were prepared by curable epoxy monomers with different temperatures, molecular structures and same weight%, to investigate briefly the combine effects of two mixtures on the altering morphology of polymer networks and the E-O properties of the PDLC films.

II. EXPERIMENTAL DETAILS

2.1 Materials

The heat curable epoxy monomers used were a mixture of bisphenol a diglycidyl ether (DGEBA, Alfa Aesar, A Johnson Matthey Company), Tetra methylene glycol diglycidyl ether (TMGDE, Sigma Aldrich Company) and Poly oxy propylene di amine (POPDA, Jeffamine D-400, Heowns Biochem Technologies Tianjin). POPDA is also used as a polyamine hardener for epoxy resins in this study. Figure 1 shows the chemical structures of these materials.

1. MONOMERS

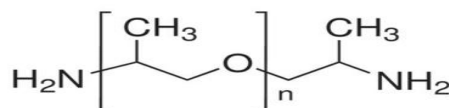


2. LC

SLC-1717

$T_{NI}=365.2K$ $n_o=1.519$ $n_e=1.720$

3. HARDENER



POPDA Jeffamine D-400

Figure 1. Chemical structures, names and abbreviations of materials used.

All of the above materials were used as received without further purification. The compositions of curable epoxy monomers/hardener/LC mixtures are listed in Table 1.

1.2 PDLC Preparation

In this study, the PDLC films were obtained by the PIPS process. The samples we prepared consisting of heat curable epoxy monomers/hardener and the less amount of nematic LC content (wt: 40%). At the beginning, they were mixed uniformly in a different proportions until they had been homogenized and then treated in different ways to investigate properties. In order to measure the electro-optical properties, the mixture was sandwiched between two pieces of indium-tin-oxide (ITO) coated glass substrates. The film thickness was controlled by $20.0 \pm 1.0 \mu m$ thick polyester spacers and then cured in an oven at different temperatures for 7 h. The composition ratios of the samples are listed in Table 1. It is calculated by $F_{av} = \sum \phi_i f_i$, where F_{av} is the average functionality of composite monomer, ϕ_i and f_i stand for the relative percentage and functionality respectively [10]. The theoretical reaction molar ratios of Monomer mixture^a (MM1)DGEBA/POPDA and Monomer mixture^b (MM2)TMGDE /POPDA are 2/1 and 1/1, respectively.

Table 1. The compositions of the samples A1-A7.

Sample	Monomers (Total 60 wt %)	SLC-	Curing
	MM1 ^a /MM2 ^b	1717 (wt%)	Temperature (K)
A1	30/30	40	344.2
A2	30/30	40	347.2
A3	30/30	40	350.2
A4	30/30	40	353.2
A5	30/30	40	356.2
A6	30/30	40	359.2
A7	30/30	40	362.2

2.3 Observation of the polymer network in the PDLC films

The morphology of the polymer network of the samples was observed by scanning electron microscopy (SEM, ZEISS, EVO18, Germany). The PDLC films were first separated and dipped into cyclohexane (C₆H₁₂) for four days at room temperature to extract the polymer network and then dried for 12 h under vacuum. After the films were sputtered with carbon, the microstructure of the polymer network was observed under SEM.

1.3 Electro-optical properties measurement

The electro-optical properties were measured by a liquid crystal device (LCD) parameters tester (LCT-5016C, Changchun Liancheng Instrument Co. Ltd.). A halogen laser beam (560 nm) was used as the incident light source and the incident wavelength (λ) through the samples were fixed with the help of wavelength (λ) filter (632.8nm). The transmittance of the PDLC systems was recorded by a photodiode, and the response of the photodiode was monitored by a digital storage oscilloscope. The active area of the detector was 0.36 cm². An electric field square wave (100 Hz) was applied, and the distance between the PDLC systems and photodiode was 300 mm. The transmittance of air was normalized as 100%.

III. RESULTS AND DISCUSSION

3.1 Morphology of Polymer Network of the samples

Figure 2 shows the morphology of the polymer networks of the samples A1 to A7 was observed by SEM to ascertain whether phase separation for the samples had taken place at different curing temperatures. It can be observed that the domain size of the LC is greatly affected due to the presence of the short chain length (TMGDE) and rigid chain segment containing curable monomer (DGEBA). As shown in Figure 2, the polymer networks of all samples have suitably distributed small holes in the PDLC films. As can be seen in figure 2, the domain size of the polymer network of samples A1-A7 proved that phase separation in the samples took place, and that with the raise of the curing temperature, the LC domain size of the polymer network decreased rapidly at first for the temperature from 344.2 K to 350.2 K, and then increased dramatically for the temperature from 350.2 K to 362.2 K. This variation was related to the competition between the diffusion of LC molecules and the polymerization rate of the epoxy monomers. In heat curing PIPS method the rate of diffusion of the LC domain size is directly proportional to the curing temperature, and it is given by the Fick's second law [11, 12].

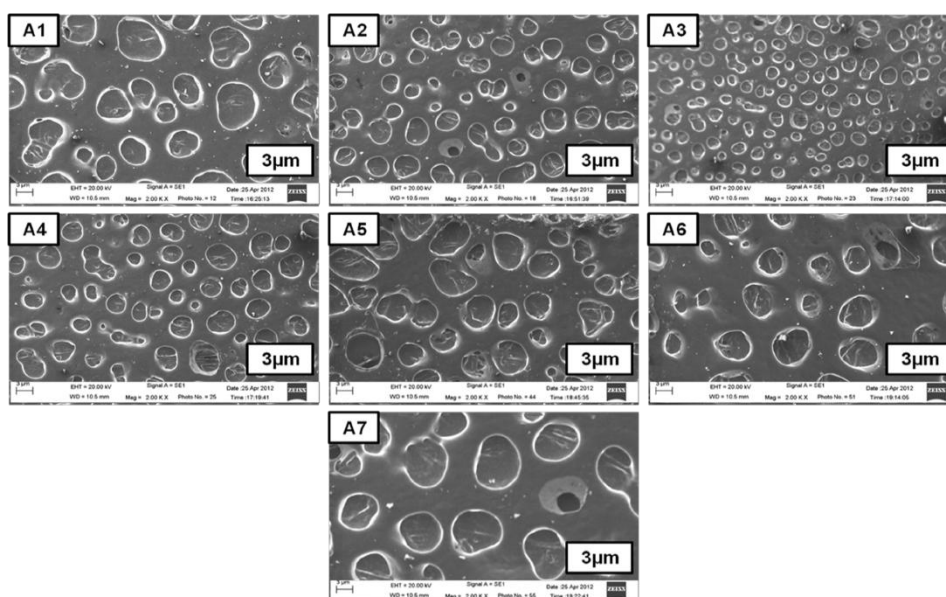


Figure 2. SEM micrographs of the polymer networks of the samples A1-A7.

$$D = D_0 \exp(-Q/RT) \quad (1)$$

Where D , D_0 , Q , T and R represent diffusion coefficient, diffusion coefficient constant, activation energy, absolute temperature and ideal gas constant of the LC, respectively.

Additionally, the initial increases of the curing temperature could particularly decrease the viscosity of the LC. The decrease of the viscosity of the LC was helpful to the diffusion of the LC, and then developed the accumulation of the LC and the growth of the domain size of LC. Although, the polymerization rate coefficient (k) of the epoxy heat curable monomers depends exponentially on temperature according to Arrhenius equation [13, 14, 15].

$$k = A \exp\left(\frac{-E_{act}}{RT}\right) \quad (2)$$

Where E_{act} is the activation energy, R is the ideal gas constant, A is the frequency (collisions) factor and T is the absolute temperature. Analysis of Equations (1) and (2) indicated the conclusion given below. When the epoxy curable monomers were cured from 344.2 K to 350.2 K, the increase in temperature could have significantly increased the solubility of the LC in the epoxy monomers, and then prevented the diffusion and the accumulation of the LC. For that reason, the LC domain size of the polymer network decreased in sequence in samples A1-A3. Though, when the polymerization the monomer occurred at above 350.2 K, the increase in the solubility of the LC in the epoxy monomers slowed down relatively. In other words, the diffusion rate of the LC molecules and the polymerization rate of the epoxy monomers depend exponentially on the heat curing polymerization at different temperatures and the 40 wt% of nematic LC also. It plays a vital role during the formation of the polymer networks and corresponds to the generation of macro-molecular polymer structures in all samples.

1.4 Electro-optical properties of the samples

The E-O properties are very elemental and significant in the evaluation of PDLC films. The transmittance applied voltage curves of sample A1-A7 are shown in figure 3. It can be seen that the transmittance of the all samples reached the saturation level T_{on} with the applied voltage increased. We observed that the transmittance curves were gentler for all samples.

Figure 4 shows the threshold voltage (V_{th}) and the saturation voltage (V_{sat}) of all samples A1-A7. The V_{th} and V_{sat} are defined as the electric voltage required for the transmittance to reach 10% and 90% of T_{on} respectively. As we can see that V_{th} and V_{sat} of samples A1-A7 increased at first and then decreased in sequence.

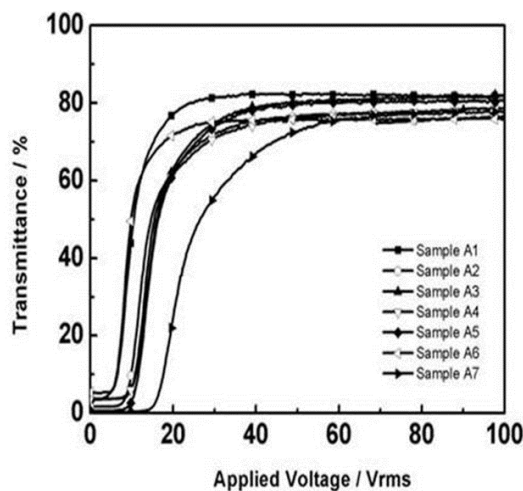


Figure3. The transmittance applied voltage curves of the samples A1-A7.

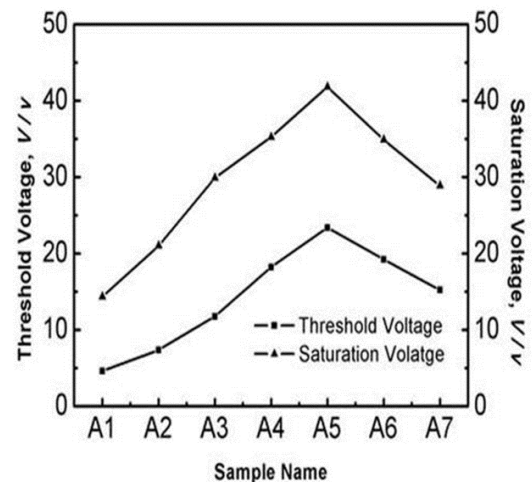


Figure 4. The threshold voltages and saturation voltages of the samples A1-A7.

It must be mentioned that, the size of the LC droplet has a strong association with E-O performance in a PDLC system. Usually, the V_{th} is inversely proportional to the radius of LC droplet (R) as shown below [16].

$$V_{th} = \frac{d}{3a} \times \left(\frac{\rho_p + 2}{\rho_{LC}} \right) \times \left(\frac{K(l^2 - 1)}{\Delta\epsilon \epsilon_o} \right)^{\frac{1}{2}} \quad (3)$$

Where d , l , ρ_p , ρ_{LC} , K , $\Delta\epsilon$ and ϵ_o thickness of the PDLC film, the ratio of the length of the semi-major axis, resistivity of the polymer, resistivity of the liquid crystal, elastic constant of liquid crystal, dielectric anisotropy of the liquid crystal and Vacuum permittivity of the LC, respectively.

Contrast ratio (CR) is a key measure of the electro-optical properties in a PDLC films. CR of PDLC films are used to characterize the difference in between a transparent and an opaque state. It is define as,

$$CR = \tau_R / \tau_D \quad (4)$$

Where τ_R and τ_D are transmittance in the on and off-state of PDLC film. A high value of CR can be

obtained when the microstructure of the PDLC film is appropriate. Figure 5 shows the off-state light transmittance (T_{off}) in fixing wavelength (632.8 nm) and the contrast ratio of all samples A1-A7. It can be seen that in samples A1-A4 the CR is continuously increased at first, then decreased in sequence increasing with altering the LC domain size and T_{off} also.

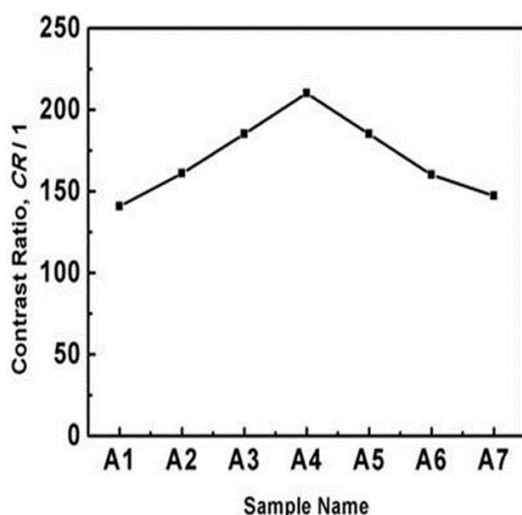


Figure 5. The contrast ratio (CR) of the samples A1-A7.

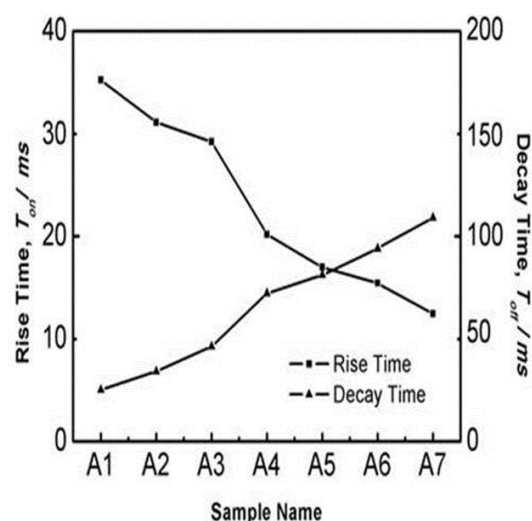


Figure 6. The rise time and decay time of the samples A1-A7.

Figure 6 shows about the response time of the PDLC films with applied voltage dependence of the *rise time* (τ_r) and *decay time* (τ_d) of samples A1-A7. *Rise time* is explained as the time which required to go from 10% to 90% of the maximum transmittance of the sample upon turning on and which required to go from 90% to 10% of the maximum transmittance of sample turning off is known as *decay time*. Usually, a competition between the applied electric field and the interface elastic forces anchoring the LC molecules governs the response time [17]. The τ_r of samples A1-A3 decreased slightly whereas their τ_d increased slightly at first, then the τ_r and τ_d of samples A4-A7 decreased rapidly and increased rapidly, respectively. This behavior was related to the competition between the applied field and the interface anchoring forces of the polymer network to the LC molecules of PDLC films. The smaller the LC droplet size, the stronger was the interface anchoring forces of the polymer network to the LC molecules. Thus, smaller LC droplets need more time to overcome more interface anchoring energy. When the applied electric field was detached, the LC molecules could revert quickly to the initial off-state due to the higher interface anchoring forces.

IV. CONCLUSION

We have investigated PDLC films by curable epoxy monomers structure using heat curing processes with different temperature, molecular structures and same weight%. The effects of short chain length and rigid chain segment containing monomers structure on the morphology and electro-optical properties have been studied. On the morphology, the LC droplet size in the PDLC films decreased at first and then increased with enhanced curing temperature; and existence of TMGDE and DGEBA monomers form suitably distributed small hole. Meanwhile, the variable E-O properties of the PDLC films depended strongly on the LC droplet size. The study also shows a special association between the epoxy curable monomers structure and the electro-optical properties of PDLC films with varying morphology. Furthermore, the results have been presented in this study also suggest that it is possible to regulate the LC domain size and optimize the electro-optic performance by adjusting the composition and weight ratio of heat curable epoxy monomers to obtain PDLC films which possess good electro-optical properties which is beneficial to decrease the total LC content in PDLC devices. The result in this paper brings significant advantages for manufacturing PDLC films and developing the PDLC market.

V. ACKNOWLEDGEMENTS

This work was supported by the Research Fund of the State Key Laboratory for Advanced Metals and Materials, the Open Research Fund of the State Key Laboratory of Bioelectronics (Southeast University) and the authors also thankful to the University of Science and technology Beijing for financial support from Chancellor Scholarship.

REFERENCES

- [1] Doane J. W., in Liquid Crystals -Applications and Uses,edited by B. Bahadur, World Scientific, book, Singapore vol. 1, p. 361-395,. 1990.
- [2] Doane J.W., Vaz N.A., Wu B.G., Zumer.S., Field controlled light scattering from nematic microdroplets. Applied Physics Letters, 48 , p.269-271,1986.
- [3] G.P. Crawford and S. Zumer, Liquid Crystals in Complex Geometries,Taylor Francis, London. Advanced Materials, 9 , p. 996-997,1996.
- [4] Kumar, P.; Raina, K.K. Morphological and electro-optical responses of dichroic polymer dispersed liquid crystal films. Current Applied Physics,7, p. 636-642,2007.
- [5] Cho, Y.H.; Kawakami,Y. High performance holographic polymer dispersed liquid crystal systems using multi-functional acrylates and siloxane-containing epoxides as matrix components .Applied Physics A-materials Science & Processing, 83, p. 365-375,2006.
- [6] Srivastava, J.K.; Singh, R.K.; Dhar, R.; Singh, S. Thermal and morphological studies of liquid crystalline materials dispersed in a polymer matrix. Liquid Crystals, 38,p. 849-859,2011.
- [7] Perju, E.; Marin, L .;Grigoras, V.C.; Bruma, M. Thermotropic and optical behaviour of new PDLC systems based on a polysulfone matrix and a cyanoazomethine liquid crystal. Liquid Crystals, 38 , p. 893-905,2011.
- [8] Dierking I, Kosbar L L, Lowe A C, Held A G. Polymer network structureand electro-optic performance of polymer stabilized cholesteric textures I.The influence of curing temperature [J]. Liquid Crystals, 24, p.387-395,1998.
- [9] PingSong, HuiCao, FeifeiWang, FangLiu, JingjingWang, MujtabaEllhi,FashengLi,HuaiYang. The UV polymerisation temperature dependence of polymer-dispersed liquid crystals based on epoxies/acrylates hybrid polymer matrix components. Liquid Crystals,39, p. 1131-1140,2012.
- [10] De Sarkar,M.;Gill, N.;Whitehead, J. B.;Crawford,G.P.Effect of Monomer Functionality on the Morphology and Performance of the Holographic Transmission Gratings Recorded on Polymer Dispersed Liquid Crystals, Macromolecules,36, p.630-638,2003.
- [11] Park, N.H.; Cho, S.A.;kim,J.Y.;Suh,K.D. Preparation of polymer-dispersed liquid crystal films containing a small amount of liquid crystalline polymer and their properties. Journal of Applied Polymer Science, 77, p. 3178-3188,2000.
- [12] Li, W.; Cao, H.; Kashima, M.;Liu,F.;Cheng,Z.; Yang, Z.; Zhu, S.; Yang, H. Control of the microstructure of polymer network and effects of the microstructures on light scattering properties of UV-cured polymer-dispersed liquid crystal films. Journal, 46, p. 2090-2099,2008.
- [13] Voytekunas, V.Y.; Ng, F.L.; Abadie, M.J.M. Kinetics study of the UV-initiated cationic polymerizationof cycloaliphatic diepoxide resins.European Polymer Journal, 44, p. 3640-3649,2008.
- [14] Cho, J.D.; Hong, J.W. Photo-curing kinetics for the UV-initiated cationic polymerization of a cycloaliphatic diepoxide system photosensitized by thioxanthone. European Polymer Journal ,41, p. 367-374,2005.
- [15] Boey, F.Y.C.; Qiang, W. Experimental modeling of the cure kinetics of an epoxy-hexaanhydro-4-methylphthalicanhydride (MHHPA) system. Polymer, 41, p. 2081-2094,2000.
- [16] West, J.H. Polymer- Dispersed Liquid Crystals, Liquid-Crystalline Polymers; ACS Symposium Series, Vol: 435, Chapter 32; American Chemical Society, Washington, DC, p. 475-495,1990.
- [17] Li, W. B.; Zhang, H. X.; Wang, L. P.; Ouyang, C.B.; Ding, X. K.; Cao, H.; Yang, H. Effect of a Chiral Dopant on the Electro-OpticalProperties of Polymer-Dispersed Liquid-Crystal Films. Journal of Applied Polymer Science, 105, p. 2185-2189,2007.

Advanced Linux Security

Ranjit Nimbalkar¹, Paras Patel², Dr. B. B. Meshram³

^{1,2,3}(Department of Computer Engg. & Information Technology, Veermata Jijabai Technological Institute, India)

Abstract : Using mandatory access control greatly increases the security of an operating system. SELinux, which is an implementation of Linux Security Modules (LSM), implements several measures to prevent unauthorized system usage. The security architecture used is named Flask, and provides a clean separation of security policy and enforcement. This paper is an overview of the Flask architecture and the implementation in Linux.

Keywords: Kernel, Linux, MAC, Security, SELinux.

I. INTRODUCTION

Security is a very broad concept, and so is the security of a system. All too often, people believe that a system is way more secure than it in practice is, but the biggest problems are still the human factor of the users; the possibility of careless or malicious users are commonly overlooked.

The standard “Unix way” of providing authentication and authorization is not very well suited for more complicated and dynamic environments. The available Discretionary Access Control mechanisms give the same rights to all users in a certain group, and all processes created by a user have exactly the same privileges. The acquired permissions can also be transferred to other subjects, and so a flaw in one software can lead to all the users’ data being compromised. Some system wide permission restrictions can be enforced by using several user groups, limiting the use of certain software to users belonging to that group, but each user process still has all the permissions of all the groups that the owning user belongs to [1]. Government agencies, among other similar organizations, need a more advanced way of defining system security policies. That is why the National Security Agency (NSA) began developing, for internal use, their own set of patches to the Linux kernel. These patches became known as Security-Enhanced Linux (SELinux) and was later released under the GPL and included in the main Linux kernel tree.

Nowadays SELinux is a security module for the Linux Security Modules framework. This paper is an overview of the SELinux features and how it changes the security configuration aspect of Linux. The architecture that SELinux implements, the Flask architecture, and its components are described in section 3.1. A brief description of the SELinux LSM module is given in section 3.2. Section 4 describes some of the other projects that aim to increase Linux security. This paper is intended as a brief overview of the technologies used, and thus does not contain very detailed information. There is plenty of in-depth documentation of the internals in the sources of this paper [2][3].

II. PROBLEM STATEMENT

Real security cannot be provided in user-space only. The need for security mechanisms in the operating system itself is evident as indicated in this section. The access control mechanisms used in most operating systems (usually Discretionary Access Control) are not capable of providing strong enough system security. One of the obstacles for creating really secure systems, is that there is not a single security architecture that could satisfy nearly all the different security needs.

Malicious code, that manages to bypass the application level security, will usually be executed with the same permissions the current user has. This means that all the users’ applications and data is compromised

at once, and in case the user is an administrator, the whole system is compromised. It is not possible to limit the resources different programs can access, so a web browser can access the files belonging to the mail program, and also all other, possibly sensitive, files the user has access to.

Malicious or careless users might also leak sensitive data unless the rules for handling such data are not enforced by the system. Even very experienced and careful users might be using flawed programs that could leak information [4]. From the system point of view, there is really no point in making a distinction between malicious or flawed programs and hostile users. Proper security mechanisms would handle them in a similar manner anyway.

2.1 Sandboxes and signatures

One attempt to minimize the effects of malicious code is run-ning code in a so called sandbox. The sandbox is a virtual environment set up by the code interpreter, such as the Java Virtual Machine, or Adobe Flash. This model relies entirely on the virtual machine implementation to be secure, and so a flaw in the virtual machine might grant the malicious code access to the host system with the privileges of the virtual machine; often administrative or even root.

Another way of trying to secure programs is to use code signing and allowing applications from trusted sources only. One problem with this solution is the cumbersomeness of getting even the smallest applets signed by a trusted party. Another problem is that the signed code might be getting way more privileges than actually needed or desired. The signature verification mechanisms and key storage must also be protected against tampering for this method to have any effect. For any of the solutions mentioned above to be effective, a secure operating system is needed to provide the basic prim-itives needed to secure them.

2.2 Data links

Data transmission between systems also needs to be secured. The current solutions such as IPSec and SSL only provide a partial solution, since they run in user space and therefore cannot provide a complete end-to-end secure channel. A compromise of the unsecured data on one of the endpoints renders the whole channel useless.

III. SELINUX

SELinux started as a security research project at NSA, together with Secure Computing Corporation and the University of Utah, to demonstrate the benefits of mandatory access control over the user/group schema. Today SELinux is included in the mainstream Linux kernel as a security module in the LSM framework. SELinux implements a flexible mandatory access control (MAC) architecture in the major subsystems of the kernel and provides a mechanism to en-force the separation of information based on confidentiality and integrity requirements [2].

2.3 Basic architecture

NSA tried to get their SELinux patches included in the 2.5 development branch kernel back in 2001, but Linus Torvalds rejected the proposal since there were other similar ongoing projects at the same time. A more general solution was needed so that the kernel would be able to support as many security architectures and implementations as possible, with-out sticking too much to the ideas of any specific implementation.

2.3.1 Linux security modules

To support various security models, an interface "Linux Security Module Interface" was proposed [3] by Crispin Cowan. The Linux Security Modules framework development got contributions from huge corporations, such as IBM and SGI, and naturally NSA.

In 2006, the only widely used LSM module included in the mainstream kernel was SELinux, but Torvalds still wanted to keep the door open for other implementations¹ and so SELinux was finally included in the mainstream 2.6 kernel as a security module in late 2003.

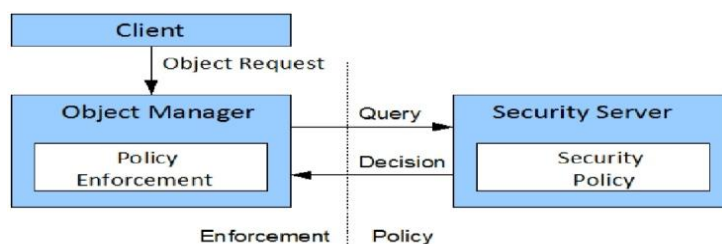


Figure 3.1 flask architecture

2.3.2 Flask architecture and concepts

The very flexible MAC architecture used in SELinux is Flask[6], which was derived from a micro-kernel based operating system named Fluke. Flask clearly separates the security policy from the enforcement mechanism (Fig. 3.1).

All subjects (processes) and objects (files, sockets, . . .) have a set of security attributes, referred to as the security context of the object. The attributes depend on the specific security policy in use, but generally contain the user id, a role and type enforcement domain.

Instead of working with the security context all the time, the security server maintains a mapping between security attribute sets and security identifiers (SIDs). When the object manager, the enforcing component, request labeling or access decisions, it typically passes a pair of SIDs to the security server, which looks up the related security contexts and makes the decision based on the policy in use.

Polyinstantiation is used when a certain resource needs to be shared by many clients. Such a resource could be the /tmp directory or the TCP port space. Filenames or port numbers might disclose some information about the owning process, and shared directories are subject to race-condition attacks. With polyinstantiation, each user can only see his or her own version of the resource based on username and/or security context.

The security server exists to provide policy decisions, map security contexts to SIDs, provide new SIDs and manage the Access Vector Caches (AVC), which is presented in section 3.2.1. It usually also provides means for loading policies and it keeps track of which subjects can access its services.

2.3.3 Type Enforcement

The SELinux Type Enforcement (TE) model differs slightly from traditional models; by using the security class information provided by the Flask architecture and using a single type attribute for both processes and objects. This effectively means that a single matrix is used to specify the access to and interaction between different types, and objects of the same type can be treated differently if their associated security classes differ. Users are not directly bound to security types, but instead RBAC, which is presented in section 3.1.4, is used.

Process transition rules are based on the current process domain, while types created through object transition rules are based on the creating process domain2 (the security type of the process identifier), the object security class and the type of the related object (e.g. parent directory for files). A process cannot change its domain during execution.

Transition rules and access vectors have default policies for cases where a rule is not explicitly defined; Allowed transitions are not audited unless defined by a audit allow rule, transitions are allowed only if explicitly allow rule and denied transitions are audited. All kinds of access vectors can have rules, including allow, audit allow, don't audit etc.

2.3.4 Role-Based Access Control

Role-based access control (RBAC) is used to define a set of roles that can be assigned to users. It is a more flexible model than standard DAC or MAC, and can simulate both of them using suitable rules. SELinux further extends the RBAC model to restrict roles to specified TE domains, and roles can be arranged in a priority hierarchy. Restricting roles to certain security domains allows most of the security decisions to be made through the TE configuration. The security context of a process contains a role attribute and also, while they are not actually applied, to objects. Role transitions are usually limited to a few TE domains to limit transitions to defined programs and users that need the ability, thus reducing the impact of malicious code being executed.

2.3.5 MLS

While type enforcement is the most important provider of mandatory access control, there might sometimes be a need for traditional multilevel security (MLS). SELinux optionally provides MLS abilities, which allows defining a hierarchical "sensitivity" level and categories to objects and subjects (processes). Subjects and objects can have a range of security levels (e.g. directories might contain files with different security levels and some "trusted processes" might need to downgrade information) defined when needed, but usually only one level is used. Any MLS defined constraints are enforced in addition to the TE policy, which means that checks must pass both of them for access to be granted.

2.3.6 User Identity

The "Unix" way of representing user identities using UIDs and GIDs is insufficient for SELinux, since changing a user role (e.g. su) involves changing the UID, which means that the actions following are actually performed as the other user and not just as the same user in another role. This makes auditing and accounting very difficult. SELinux user identity attribute is persistent in the security context, which is independent of the

current UID. This means that SELinux policies can be enforced without affecting compatibility with Linux DAC permissions.

Only a limited number of programs, like login, sshd and cron, need the ability to change the User Identity, so it is usually restricted to their respective TE domains. Depending on security configuration, the programs may or may not be able to change the user identity more than once. Allowing programs started from cron to change their user identity, for example, impacts accountability.

2.4 SELinux LSM Module

SELinux uses the LSM framework to accomplish its mission. The framework adds security fields to kernel data structures and calls to hook functions in critical points (kernel calls), to manage the security fields and perform access control. The most commonly used filesystems have been updated to support the file security attributes³. The hook calls are initialized to a dummy module that emulates traditional "Unix" superuser logic, and each security module, at load-time, registers the hooks it uses.

2.5 Internal Architecture

The SELinux module has six major components; the security server, the access vector cache, the network interface table, the netlink event notification code, the selinuxfs pseudo filesystem and the hook function implementations.

The default security server implements a combination of the Flask architecture components (TE, RBAC and optionally MLS), but it can be changed or replaced without affecting the rest of the SELinux module. The AVC provides caching of the decisions provided by the security server to minimize overhead in hook function calls and also provides an interface to the security server for managing the cache, like propagating policy updates. One of the drawbacks of the LSM framework is that it does not provide a security field for network devices, therefore a separate mapping to security contexts, the network interface table, is needed. Network interfaces are added and removed automatically, and there are callback functions defined for device configuration or policy changes. The netlink event notification code is used to keep the userspace AVC in sync with the kernel one, which enables the use of user-space enforcers, like security-enhanced X. The selinuxfs pseudo filesystem provides the security server API to processes and provides the low level support for policy manipulation calls. The hook functions are responsible for retrieving security information from the security server and AVC, and for enforcing the policies. They also maintain the security context of files. The SELinux module provides only rudimentary support for stacking with other LSM modules, but there is ongoing work to improve the stacking support.

2.6 What is new?

SELinux is constantly evolving and expanding. Some of the latest key extensions and feature improvements [8] are presented here.

- 1) SELinux Loadable policy modules: An attempt to ease policy maintenance, reduce resource requirements by removing the need for a policy development environment and allow for loosely coupled policies. Local customizations can be made to more generic or even 3rd party policies, and the policy source need not be available.
- 2) The Reference Policy [6] aims to be a baseline security policy, on which custom policies are easy to build. The policy is based on a single source and is clean and modular. It was originally based on the NSA example policy, which is somewhat difficult to comprehend without a good understanding of the underlying SELinux technologies, but has since evolved quite a bit.
- 3) Policy Management Interface: In addition to the Policy Modules, a new policy server is being developed. It facilitates fine-grained control over who can change the policy and how (currently any process that can change the policy, can change everything), User-space Object Managers to extend TE to user-space (e.g. the Security Enhanced X-Window system). Network wide deployment and management of security policies will also be possible through the use of security modules. A standard library for policy management (libsemanage) is introduced for policy tools to use.
- 4) Enhanced Audit Support: Syscall audit records have been extended with security contexts, audit records can be filtered based on security context and auditing of several SELinux specific events has been added.
- 5) Enhanced Multi Level Security Support (labeled networking, application integration), end-to-end network data labeling and traffic control (including policy-based packet filtering). Separation of network data labeling from enforcement; iptables is used for data labeling and SELinux for enforcing the policies.
- 6) Securing the desktop: The X Access Control Extension (XACE) framework is integrated into the Xorg server as of version 1.2. It is a general framework for X, much like the LSM kernel framework but for user-space. A Flask policy module, XSELinux, which will provide flexible MAC is also under development.

- 7) Troubleshooting and reporting has been improved, and several tools for security policy generation and manage- have been added or updated

IV. RELATED WORK

SELinux is not the only security project going on. This chapter aims to give a short introduction to related projects.

2.7 TrustedBSD

TrustedBSD consists of several branches; Access Control Lists, Event Auditing and OpenBSM, Extended Attributes and UFS2, Fine-Grained Capabilities, GEOM, Mandatory Access Control and OpenPAM[5]. The MAC Framework provides discretionary access control for all subjects and objects. Security-Enhanced BSD (SEBSD) is a port of the FLASK/TE implementation from SELinux that works as a module in the TrustedBSD MAC framework, but is not yet ready for production use due to lacking support in vital userspace applications.

The features included in the base FreeBSD distribution are Access Control Lists (basically an implementation of the POSIX.1eD17 draft specification), Security Event Auditing (based on Sun's Basic Security Module API), UFS2 (default file system which supports file tagging), GEOM (provides data transformation services between the kernel and I/O devices), OpenPAM (similar to Linux PAM, but more compatible with the Solaris PAM implementation).

2.8 AppArmor

AppArmor is a Linux Security Module, which relies on application profiles for decision making [1]. It provides Mandatory Access Control for file paths, instead of by inode. AppArmor was mostly maintained by Novell from 2005 to September 2007 as part of their SUSE distributions, but is now available under the GPL in other distributions also.

2.9 LIDS

The LIDS (Linux Intrusion Detection System) kernel patch version 1 was designed for Linux kernel version 2.2 and later 2.4. Version 2 will be turned into a module for the LSM framework, but is currently work in progress. LIDS includes several measures to minimize damage in case of a system compromise. Files can be marked as immutable, and changes to vital system configurations (like network setting and loaded modules) can be prevented. Even the root user cannot circumvent the protection without first stopping the LIDS system, which requires a password which is set at compile time.

2.10 Trusted Solaris

Solaris 10 has a component called Trusted Solaris Extensions, which is the successor of the former Trusted Solaris re-release. Trusted Solaris includes accounting, auditing, RBAC and Mandatory Access Control Labeling. MAC is enforced in every aspect of the OS by adding sensitivity labels to objects, allowing only explicitly authorized users or applications to access the objects.

2.11 GRSecurity

One major component of GRSecurity is PaX[2]. Memory page access is guarded by least privilege protection, the program memory is randomly arranged, and pages can be flagged as non-executable or non-writable. PaX reduces the impact of buffer overruns and other possible arbitrary code execution attacks to a mere Denial of Service attack, causing only the affected program to crash.

GRSecurity also provides a full Role-Based Access Control system, advanced auditing of specified user groups, and chroot jail hardening. Access to certain programs like dmesg and netstat is usually limited to root only, and Trusted Path Execution can optionally prohibit users from executing non-root owned binaries, effectively eliminating trojans and other malicious code from being run. Table captions appear centered above the table in upper and lower case letters. When referring to a table in the text, no abbreviation is used and "Table" is capitalized.

V. CONCLUSION

SELinux provides a much more fine-grained control over the security of a Linux system compared to the "Unix" standard. The baseline security configuration is almost usable for most environments, but some configuration is needed in most cases. The difficulty of configuration has maybe been the reason why most people have not taken SELinux in use, but the policy management tools are getting better.

Some people claim⁴ that the security framework provided by LSM is not extensive enough, that

several critical security hooks are missing and that SELinux security relies on the kernel being bug free. These claims are probably at least partially true, but the latest development in SELinux tries to address the remaining security issues (e.g. minimize the processed that can change the policy etc).

Complete system security is an utopia, but SELinux is one step in that direction. It is being included in most major Linux distributions, even though it might not be enabled by default. Installing or activating SELinux is pretty straight-forward, and no enforcement is being done until the user has checked the logfiles for possible problems and decides that the configuration is good enough.

REFERENCES

- [1]. P. A. Loscocco, S. D. Smalley, P. A. Muckelbauer, R. C. Taylor, S. J. Turner, and J. F. Farrell. The Inevitability of Failure: The Flawed Assumption of Security in Modern Computing Environments. In *21st National Information Systems Security Conference*, pages 303– 314. NSA, 1998.
- [2]. C. J. PeBenito, F. Mayer, and K. MacMillan. Reference Policy for Security Enhanced Linux. In *SELinux Symposium*, 2006.
- [3]. R. Spencer, S. Smalley, P. Loscocco, M. Hibler, D. Andersen, and J. Lepreau. The Flask Security Architecture: System Support for Diverse Security Policies. In *The Eighth USENIX Security Symposium*, pages 123– 139, August 1999.
- [4]. R. Spencer, S. Smalley, P. Loscocco, M. Hibler, D. Andersen, and J. Lepreau. The Flask Security Architecture: System Support for Diverse Security Policies. In *The Eighth USENIX Security Symposium*, pages 123– 139, August 1999.
- [5]. Nigel Edwards, Joubert Berger, and Tse Houn Choo. A Secure Linux Platform. In *Proceedings of the 5th Annual Linux Showcase and Conference*, November 2001
- [6]. Crispin Cowan, Steve Beattie, Calton Pu, PerryWagle, and Virgil Gligor. SubDomain: Parsimonious Server Security. In *USENIX 14th Systems Administration Conference (LISA)*, New Orleans, LA, December 2000.
- [7]. R. Wita and Y. Teng-Amnuay. Vulnerability profile for linux. In *Proceedings of the 19th International Conference on Advanced Information Networking and Applications*, pages 953–958. IEEE, 2005.
- [8]. Rhat enterprise linux 6 security guide (Red Hat Engineering Content Services).

Investigating Emission Values of a Passenger Vehicle in the Idle Mode and Comparison with Regulated Values

O.N Aduagba¹, J. D. Amine² and M.I. Oseni²

¹Raw Material Research and Development Council, Abuja, Nigeria

²University of Agriculture, Department of Mechanical Engineering, Markudi, Nigeria

Abstract: This paper presents an experimental study of emission values of a passenger vehicle in idle mode in comparison to regulated values. The results from the emission test conducted on the Golf 3 GTi Volkswagen 1996 model popularly used as “Taxi” in Nigeria were compared with emission value in Euro 2 to depict the year the car was manufactured. The devices used in the experimental work consist of a SV-5Q automobile exhaust gas analyzer and SV-1 engine tachometer. The measured emission results were 12.98, 1.43 and 1.58g/km for CO, HC and NO respectively. Generally, age and fatigue will produce a number of poor performances of engine such as break down in major operating variables that affect sparks ignition, engine performance, emission control (catalytic converter) if installed. This study showed high emission values in the aged vehicle and concluded that efforts to reduce the rate of emissions are necessary and to set standards for vehicular emission in the country using the accepted standards.

Keyword: Idle, RPM, Emissions, Standards

I. INTRODUCTION

Emission is the most common problem associated with vehicle idling in urban driving. The automobiles in Nigeria are mostly fairly used vehicles (high-mileage vehicles) yet with the growing fleet of vehicles and escalating amount of time spent in traffic by the drivers and passengers the emissions seem to increase. These vehicles usually consumed more fuel and emit more pollutants as a result of operational conditions. There is a hierarchy of emission estimation techniques (EETs), ranging broadly from the most accurate and site-specific to generic and least accurate, namely: direct emission measurement; indirect measurement; mass balance calculation; models and physicochemical relationships; emission factors; and engineering judgment. Vehicle characteristics such as engine size, power rating and weight are also factors influencing fuel consumption and emission rates. Generally, vehicles with large engine sizes (2.0L and above) emit more pollutants than vehicles with small engines, and large engine sizes are commonly accompanied with high maximum-horsepower. Ambient temperature is an important parameter affecting both exhaust and evaporative emissions. Previous studies, Kuhns [1] and Chan [2] commented that older vehicles emitted more pollutants than newer ones. Chan [2] also observed that the older trucks had higher CO emission factors but lower NOx emission factors due to poor engine combustion associated with their high usage rates and limited maintenance. For engine in idling mode the friction, the heat losses are greater than once fully warmed and the time required to reach steady-state operating temperature is longer. These factors contribute to a longer period of relatively poor combustion and consequent need for more fuel enrichment (operation with more fuel than required for stoichiometry). The combination of these factors results in higher exhaust concentration of unburned fuel in the form of hydrocarbon and carbon monoxide. Fossil fuels are the major contributors to urban air pollution and source of greenhouse gases. Due to unabated high emission rates, the ozone layer which plays a critical role in screening harmful ultra violet radiation is depletion thereby allowing the harmful radiation to reach the earth surface. Hence, it is highly desirable to reduce vehicular emissions more so as international concerns are being raised for control and restriction and strict environmental legislations.

II. MATERIALS AND METHODS

Materials

- a) SV-5Q Automobile Exhaust Gas Analyzer
- b) SV-1 Engine Tachometer
- c) SV Oil Temperature Profile
- d) Volkswagen (Golf GTi Model 1996)
- e) Black and Decker 400 (watt) Inverter
- f) Petrol (PMS) standard of with Research Octane Number (RON) 90
- g) HP Laptop with SV-5Q Gas Analyzer PC Contactor Interface Software System

Methods

The SV-5Q Automobile Exhaust Gas Analyzer is set for emission tests by connecting one side of sampling tube to the end of sampling while the other side is connected to the exit of fronted filter. Connect one side of short catheter with the front of fronted filter, while the other side is connected to sample gas vent of the analyzer. Every point is then checked to make sure they are firmly connected and no leakages.

Followed is separately connecting the power line, engine temperature measurement and speed tachometer, and temperature signal socket and speed signal socket. The analyzer is then powered and immediately goes into preheating for duration of 10 minutes for the analyzer to warm up. The tachometer was clipped to the high tension lines of engine's ignition distributor, and the undulation switch of the tachometer is set to number of strokes and cylinder of the engine under study, followed by inserting the temperature profile device into the lubricating oil rod vent of engine until it touches engine oil in the engine's bottom plate. Connected then is the device to the temperature measurement input port at the back of the gas analyzer. The results are displayed simultaneously as the analyzer reads emission values on Volkswagen (Golf GTi Model 1996) in the idle mode after the engine run for a time duration of 10 minutes from cold start. The readings were recorded at time duration of 30 seconds for every test conducted.



Plate 1: Conducting emission tests on the Golf 3 Volkswagen Vehicle in Abuja, Nigeria



Plate 2: Researcher carrying out exhaust emission tests on a 3-wheeler automobile in Hitec City, Hyderabad, India

III. RESULTS AND DISCUSSIONS

Table I: Result of Idle Tests at 1000 RPM

Time (sec)	Engine RPM	CO (%)	CO ₂ (%)	HC (ppm)	O ₂ (%)	NO (ppm)	□ (air/fuel equivalence ratio)	Engine Temp (°C)
30	1000	0.2	8.2	160	2.63	35	1.16	44.6
30	1000	0.12	8	162	2.48	34	1.17	47
30	1000	0.34	7.36	328	2.88	137	1.21	45.2
30	1000	0.42	8.9	120	4.03	142	1.22	56
30	1000	0.12	7.04	212	2.85	170	1.27	56.2
30	1000	0.1	7.22	206	3.08	130	1.26	57.3
30	1000	0.2	7.62	120	2.95	150	1.3	57.1
30	1000	0.38	9.5	116	3.47	165	1.22	48
30	1000	0.24	6.84	208	4.08	86	1.36	47.2
30	1000	0.26	6.84	286	5.04	81	1.41	49.8
30	1000	0.14	7.52	116	4.73	20	1.41	50.8
30	1000	0.12	7	214	4.62	20	1.44	51.8
30	1000	0.3	6.42	326	5.23	90	1.47	50.8
30	1000	0.3	7.12	174	5.83	168	1.5	51.1
	Total	3.24	105.58	2748	53.9	1428	18.4	712.9
	Mean	0.23	7.54	196.29	3.85	102.00	1.31	50.92

Results

Table II: Result of Idle Tests at 1500 RPM

Time (sec)	Engine RPM	CO (%)	CO ₂ (%)	HC (ppm)	O ₂ (%)	NO (ppm)	□ (air/fuel equivalence ratio)	Engine Temp (°C)
30	1500	0.26	8.42	176	2.42	36	1.14	47
30	1500	0.26	8.42	204	1.71	34	1.09	47.9
30	1500	0.38	8.04	322	2.24	244	1.14	46.2
30	1500	0.48	10.02	124	2.33	225	1.1	56.1
30	1500	0.14	7.52	204	1.71	195	1.11	57
30	1500	0.12	7.44	224	2	150	1.14	57.6
30	1500	0.28	7.9	166	2.31	170	1.16	58
30	1500	0.46	10.46	118	2.41	200	1.13	48.2
30	1500	0.38	7.04	214	2.52	214	1.19	47.9
30	1500	0.42	7.84	304	2.74	198	1.2	50.5
30	1500	0.24	7.78	122	2.87	51	1.23	50.9
30	1500	0.22	7.1	242	3.2	52	1.28	51.9
30	1500	0.32	7.12	296	2.74	179	1.2	50.9
30	1500	0.32	8.3	164	3.1	249	1.21	51.2
	Total	4.28	113.4	2880	34.3	2197	16.32	721.3
	Mean	0.31	8.10	205.71	2.45	156.93	1.17	51.52

Table III: Result of Idle Tests at 2000 RPM

Time (sec)	Engine RPM	CO (%)	CO ₂ (%)	HC (ppm)	O ₂ (%)	NO (ppm)	□ (air/fuel equivalence ratio)	Engine Temp (°C)
30	2000	0.3	8.48	172	0.83	170	1.03	47.2
30	2000	0.22	9.4	190	0.98	138	1.04	48
30	2000	0.36	8.02	296	2.05	265	1.12	46.4
30	2000	0.5	10.1	186	1.36	327	1.04	56.3
30	2000	0.18	8.12	202	1.36	230	1.03	57.1
30	2000	0.22	8.22	238	1	182	1.04	57.9
30	2000	0.3	8.86	164	1.22	340	1.04	58
30	2000	0.44	11.16	122	1.16	414	1.04	48.3
30	2000	0.32	7.06	198	1.25	377	1.07	48.3
30	2000	0.36	8.14	328	1.5	398	1.03	50.3
30	2000	0.28	8.7	120	1.5	137	1.09	50.9
30	2000	0.18	8.16	226	1.7	158	1.12	51.9
30	2000	0.34	8.02	328	1.27	370	1.1	50.95
30	2000	0.36	9.16	126	1.45	357	1.07	51.2
	Total	4.36	121.6	2896	18.63	3863	14.86	722.75
	Mean	0.31	8.69	206.86	1.33	275.93	1.06	51.63

Table IV: Result of Idle Tests at 2500 RPM

Time (sec)	Engine RPM	CO (%)	CO ₂ (%)	HC (ppm)	O ₂ (%)	NO (ppm)	□ (air/fuel equivalence ratio)	Engine Temp (°C)
30	2500	0.32	9.24	192	1.09	856	1.04	47.5
30	2500	0.32	9.46	270	0.7	317	1.01	48.2
30	2500	0.4	9.02	350	0.82	653	1.01	46.5
30	2500	0.52	10.84	154	0.92	367	1.01	56.6
30	2500	0.24	8.8	200	0.67	304	1.02	56.9
30	2500	0.34	7.76	306	1.02	860	1.04	58
30	2500	0.36	8.6	194	1	627	1.04	58.2
30	2500	0.48	11.1	124	1.01	633	1.03	50
30	2500	0.36	8.38	244	1.07	690	1.05	50
30	2500	0.38	8.3	318	1.21	740	1.05	50
30	2500	0.3	8.72	124	1.36	330	1.07	51
30	2500	0.26	8.36	288	1.22	367	1.06	52
30	2500	0.38	8.32	344	1.03	603	1.03	51
30	2500	0.4	9.7	228	1.21	697	1.05	51.3
	Total	5.06	126.6	3336	14.33	8044	14.51	727.2
	Mean	0.36	9.04	238.29	1.02	574.57	1.04	51.94

Table V: Result of Idle Tests at 3000RPM

Time (sec)	Engine RPM	CO (%)	CO ₂ (%)	HC (ppm)	O ₂ (%)	NO (ppm)	λ (air/fuel equivalence ratio)	Engine Temp (°C)
30	3000	0.4	9.18	250	1.03	783	1.03	48
30	3000	0.3	9.08	292	0.53	295	1	48.3
30	3000	0.38	9.12	330	0.75	793	1.01	47
30	3000	0.44	11.36	176	0.7	307	1.01	57
30	3000	0.23	8.54	244	0.58	457	1.01	57.1
30	3000	0.33	8.1	324	0.75	1000	1.02	58.1
30	3000	0.34	9	204	0.85	793	1.03	58.2
30	3000	0.46	10.42	126	0.93	798	1.02	53
30	3000	0.32	8.14	240	0.91	886	1.03	49.2
30	3000	0.32	8.26	304	1.03	935	1.04	49.2
30	3000	0.32	9.38	166	0.97	380	1.04	51
30	3000	0.28	8.68	252	1.07	327	1.05	52.5
30	3000	0.4	8.54	364	0.87	743	1.02	51.5
30	3000	0.42	9.72	200	0.92	770	1.03	51.8
	Total	4.94	127.52	3472	11.89	9267	14.34	731.9
	Mean	0.35	9.11	248.00	0.85	661.93	1.02	52.28

Table VI: Summary of Mean Values from the Results of the Idle Tests

S/N	Engine RPM	CO (%)	CO ₂ (%)	HC (ppm)	O ₂ (%)	NO (ppm)	λ (air/fuel equivalence ratio)	Engine Temp (°C)
1	1000	0.23	7.54	196.29	3.85	102	1.31	50.92
2	1500	0.31	8.1	205.71	2.45	156.93	1.17	51.52
3	2000	0.31	8.69	206.86	1.33	275.93	1.06	51.63
4	2500	0.36	9.04	238.29	1.02	574.57	1.04	51.94
5	3000	0.35	9.11	248	0.85	661.93	1.02	52.28
Total	10000	1.56	42.48	1095.15	9.5	1771.36	5.6	258.29
Mean	2000	0.312	8.496	219.03	1.9	354.272	1.12	51.658

Table VII: Measured values compared with Indian emission standards (4-wheel vehicles) for passenger cars

Type	Reference	Year	CO (g/km)	HC (g/km)	NO _x (g/km)	CO ₂ (not regulated)
Bharat Stage I	Euro 1	1992	4.5	0.60	0.49	-
Bharat Stage II	Euro 2	1996	3.28	0.34	0.25	-
Bharat Stage III	Euro 3	2000	2.30	0.20	0.15	-
Bharat Stage IV	Euro 4	2005	1.0	0.10	0.08	-
Average measured Values (g/km)	-	-	12.98	1.43	1.58	-

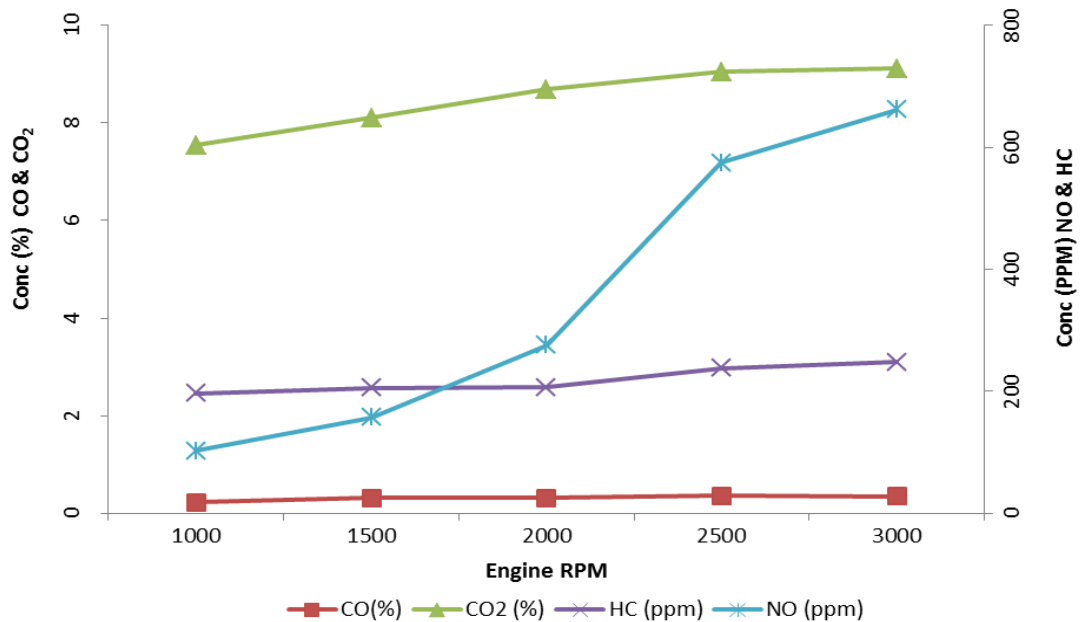


Figure 1 : Plot of emissions with engine RPM at Idle

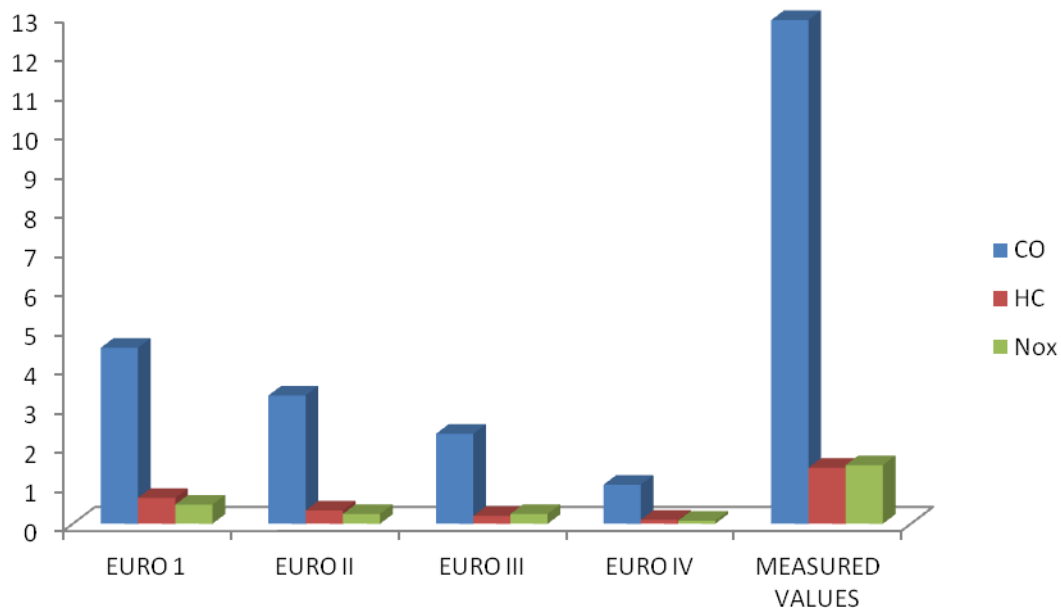


Figure 2: Plot of measured emission values with emission standard values

IV. DISCUSSIONS

Figure 1 shows the emission concentrations and the engine rpm of the vehicle under study, it was observed that the emission values of carbon monoxide (CO) concentration increase from 0.23% to 0.35%, carbon dioxide (CO₂) from 7.54% to 9.11%, Nitrogen Oxide (NO) from 102 to 661ppm and Hydrocarbon (HC) from 196 to 248 as the engine speed progressively moved from 1000 to 3000 rpm. The Idle test agrees with Vijayan [3] observations that emissions increase with engine speed (load), and that engine rpm is one of the most important variables affecting the concentrations of emissions. This is also substantiated by Roumegoux [4] that there is a correlation between emissions with engine speed.

Figure 2 shows the result of the mean idle emissions compared with the acceptable emission standards from Euro 1 to Euro 4 (and Bharat Stage I to IV for India standard). The results of the emission tests were analysed along with the Euro 2 indicating the year in which the vehicle under study was manufactured. The measured emission results were 12.98, 1.43 and 1.58g/km for CO, HC and NO respectively and compared with Euro 2 values of 3.28, 0.34 and 0.25 g/km for CO, HC and NO respectively. These measured high values cannot even stand comparable to Euro 4 (European standards by United Nations Economic Commission for Europe) and the proposed emission reduction of carbon monoxide by 23% , hydrocarbons by 6.5% reduction and oxides of nitrogen by 14% reduction in 2020, based on the Euro 4 values intended to limit average fuel consumption from new petrol passenger vehicles to 6.8L/100km as reported by Coffey [5]. The observed high values of emission vis-à-vis regulated standard is in agreement with Kuhns [1] that older vehicles emits more pollutants than new ones.

V. CONCLUSION

There is the need to work holistically and explore ways to reduce emissions from used vehicles found in Federal Capital Territory, Abuja Nigeria. The Government should set a high standard for the importation of used vehicles. Exhaust emission standards should be set by the relevant agencies and should be enforced with strict compliance. And as a matter of urgency, plans should be expedited to set standards for vehicular emission in the country using the accepted standard for vehicular emission which is the European standard adopted by most countries globally.

REFERENCES

- [1] Kuhns H., Etyemezian V. and Nikolich G (2004). Precision and Repeatability of the TRAKER Vehicle-based Paved road Dust Emission Measurement Desert Research Institute, Division of Atmospheric Sciences, 755 E. USA pp 95
- [2] Chan T.L., Ning Z., Leung C.W., Cheung C.S., Hung W.T. and Dong G. (2004). On- road Remote Sensing of Petrol Vehicle Emissions Measurement and Emission Factors Estimation in Hong Kong. Atmospheric Environment 38, pp205
- [3] Vijayan A. (2007) Characterization of Vehicular Exhaust Emissions and Indoor Air Quality of Public Transport Buses Operating on Alternative Diesel Fuels. Ph.D Dissertation
- [4] Roumegoux J.P. (1995). The Science of Total Environment 169, pp280
- [5] Coffey Geosciences(2006), Fuel Quality and Vehicle Emissions Standards Cost Benefit Analysis Prepared for MVEC Review of Vehicle and Fuel Standards Post pp 94

Comparison of Performance of Standard Concrete And Fibre Reinforced Standard Concrete Exposed To Elevated Temperatures

K.Srinivasa Rao, S.Rakesh kumar, A.Laxmi Narayana

Associate Professor, Department of Civil Engineering, Andhra University, Visakhapatnam.

Former PG Students (M.E Structures), Andhra University, Visakhapatnam.

Abstract: Concrete elements exposed to fire undergo temperature gradients and as a result, undergo physical changes or spalling which leads to expose steel reinforcement. This causes distress in concrete structures. The performance of concrete can be improved with the addition of steel fibres to concrete especially when it is exposed to heat. Therefore, this study has been carried out to generate experimental data on standard concrete of grade M45 and Fiber Reinforced Standard Concrete exposed to elevated temperatures.

For each type of concrete six sets of cubes, cylinders, and beams have been cast. Each set contains 5 specimens. A total of thirty cubes, thirty cylinders, and thirty beams of Standard Concrete and Fiber Reinforced Standard Concrete have been cast, out of which 5 sets of standard concrete and fiber reinforced standard concrete are exposed to elevated temperatures of 50°C, 100°C, 150°C, 200°C and 250°C for 3 hours and the sixth set is tested at room temperature as control concrete.

These specimens have been tested for compressive strength, split tensile strength, and flexural strength in hot condition immediately after taking out from oven. The results are analyzed and final conclusions are drawn.

I. INTRODUCTION

Concrete is a construction material composed of cement as well as other cementitious materials such as fly ash and slag content, aggregate (generally a coarse aggregate such as gravel, limestone, or granite, plus a fine aggregate such as river sand), water, and chemical admixtures. Apart from its excellent properties, concrete shows a rather low performance when subjected to tensile stress. Another rather recent development is steel fiber reinforced concrete (SFRC). The concept of using fibers as reinforcement is not new. Fibers have been used as reinforcement since ancient times.

Effect of fibers in concrete

Fibers are usually used in concrete to control plastic shrinkage cracking and drying shrinkage cracking. They also lower the permeability of concrete and thus reduce bleeding of water. Some types of fibers produce greater impact, abrasion and shatter resistance in concrete.

The amount of fibers added to a concrete mix is measured as a percentage of the total volume of the composite (concrete and fibers) termed volume fraction (V_f). V_f typically ranges from 0.1 to 3%. Aspect ratio (l/d) is calculated by dividing fiber length (l) by its diameter (d). Fibers with a non-circular cross section use an equivalent diameter for the calculation of aspect ratio. If the modulus of elasticity of the fiber is higher than that of the matrix (concrete or mortar binder), they help to carry the load by increasing the tensile strength of the material.

Some developments in fiber reinforced concrete

The newly developed FRC named as Engineered Cementitious Composite (ECC) is 500 times more resistant to cracking and 40 percent lighter than traditional concrete. ECC can sustain strain-hardening up to several percent strain, resulting in a material ductility of at least two orders of magnitude higher when compared to normal concrete or standard fiber reinforced concrete. ECC also has unique cracking behavior. When loaded

to beyond the elastic range, ECC maintains crack width to below 100 μm , even when deformed to several percent tensile strains.

Recent studies performed on a high-performance fiber-reinforced concrete in a bridge deck found that adding fibers provided residual strength and controlled cracking. By adding steel fibers while mixing the concrete, a so-called homogeneous reinforcement is created. This does not notably increase the mechanical properties before failure, but governs the post failure behavior. Thus, plain concrete, which is a quasi-brittle material, is turned to the pseudo ductile steel fiber reinforced concrete.

After matrix crack initiation, the stresses are absorbed by bridging fibers, and the bending moments are redistributed. The concrete element does not fail spontaneously when the matrix is cracked; the deformation energy is absorbed and the material becomes pseudo-ductile.

The steel fiber reinforcement not only improves the toughness of the material, the impact and the fatigue resistance of concrete, but it also increases the material resistance to cracking and, hence to water and chloride ingress with significant improvement in durability of concrete structures. Therefore, the use of SFRC in tunnel structures represents an attractive technical solution with respect to the conventional steel reinforcement, because it reduces both the labor costs (e.g. due to the placement of the conventional steel bars) and the construction costs (e.g. forming and storage of classical reinforcement frames, risks of spalling during transportation and laying). These preliminary SFRC examples exhibited reduced crack development and a lower risk of leakage and the falling off of concrete flakes, which often represents a concrete issue for tunnel road. Furthermore, the steel fiber reinforced details, such as the shear tooth of ring joints, was found to exhibit a higher ductility under localized force.

Due to the current lack of design rules for Steel Fibers Reinforced Concrete (SFRC) structures, engineers have usually designed SFRC tunnel lining segments by adopting the same rules that are valid for concrete with conventional reinforcement. However, the post-cracking behavior of SFRC structure is dramatically different from conventional RC structures. Steel fibre reinforced concrete (SFRC) has been successfully used in various types of construction due to the fact that adding steel fibers improves the durability and mechanical properties of hardened concrete, notably flexural strength, toughness, impact strength, resistance to fatigue, and vulnerability to cracking and spalling.

Fire resistance is a characteristic of a structure assembly, referring to the ability of the assembly to withstand the effects of fire. The expected performance of a fire-resistant assembly is either to restrict the spread of fire beyond the compartment of fire involvement or to support a load, despite exposure to a fire.

If the structure is not totally damaged or has suffered serious damage in one part only, an assessment needs to be made of fire severity so that the amount of damage may be quantified. One of the main differences between standard fire resistance test and fires in structure elements is that real fires do not have a uniform intensity throughout the structures and may have reached different peaks in different parts. Therefore it is necessary to divide the whole structure in different zones and make severity assessment for each zone. Fire reports usually prepared by the fire brigade indicate time of start and finish, efforts required to control the fire and any other problems experienced. It gives duration of fire and qualitative judgment whether it was a small or large, more or less damaging and whether particular areas had higher temperatures than others had. Examination of debris from different types of materials helps in judging the maximum temperatures achieved in different parts giving an idea about fire severity.

As per the existing practice, the comparison of standard concrete and standard fiber reinforced concrete exposed to different temperatures of standard fire has been dealt. This procedure is expensive as well as time consuming, since a large experimental research program is needed to cover all significant problem variables.

The study of behavior of concrete at elevated temperatures has achieved great importance in recent times because the accumulated annual loss of life and property due to fires is comparable to the loss caused by earthquakes and cyclones. This necessitates development of concrete mix of fire resisting.

Research Significance

The objective of this study is to generate experimental data base for compressive strength, flexural strength and split tensile strength of standard concrete and steel fiber reinforced standard concrete which are exposed to elevated temperatures of 50⁰C to 250⁰C for 3 hours. The tests have been conducted immediately on specimens in hot condition after taking out of oven.

Review of Literature

Nguyen Van Chanh¹ carried out investigations on mechanic properties, technologies, and applications of SFRC. As it is now well established that one of the important properties of steel fibre reinforced concrete (SFRC) is its superior resistance to cracking and crack propagation. As a result of this ability to arrest cracks, fibre composites possess increased extensibility and tensile strength, both at first crack and at ultimate, particular under flexural loading; and the fibres are able to hold the matrix together even after extensive

cracking. The net result of all these is to impart to the fibre composite pronounced post – cracking ductility which is unheard of in ordinary concrete. The transformation from a brittle to a ductile type of material would increase substantially the energy absorption characteristics of the fibre composite and its ability to withstand repeatedly applied, shock or impact loading.

Mehrdad Mahoutian et al² have proposed that adding of fibers into the concrete is an efficient method of increasing the mechanical properties of concrete. The most famous of fibers used in the concrete are steel, glass and polypropylene fibers. The addition of fibers significantly improves many of the engineering properties of mortar and concrete, notably impact strength and toughness. Tensile strength, flexural, failure strength and ability to spalling are also enhanced. Moreover addition of fibers makes the concrete more homogeneous and isotropic material.

Chih-Ta Tsai et al³ presents the way durability has been introduced to steel fiber reinforced concrete in Taiwan. It is generally acknowledged that steel fibers are added to improve the toughness, abrasion resistance, and impact strength of concrete. However, a locally developed mixture design method, the densified mixture design algorithm (DMDA), was applied to solve not only the entanglement or balling problem of steel fibers in concrete or to produce steel fiber reinforced self-consolidating concrete (SFRSCC) with excellent flow-ability, but also to increase the durability by reduction in the cement paste content. By dense packing of the aggregates and with the aid of pozzolanic material and superplasticizer (SP), concrete can flow honey-like with less entanglement of steel fibers. Such SFRSCC has already been successfully applied in several projects, such as construction of a low radiation waste container, bus station pavement, road deck panel, and two art statues.

S. P. Singh et al⁴ investigated to study the fatigue strength of steel fibre reinforced concrete (SFRC) containing fibres of mixed aspect ratio are presented. Approximately eighty one beam specimens of size 500 mm x 100 mm x 100 mm were tested under four-point flexural fatigue loading in order to obtain the fatigue lives of SFRC at different stress levels. About thirty six static flexural tests were also carried out to determine the static flexural strength of SFRC prior to fatigue testing. The specimens incorporated 1.0, 1.5 and 2.0% volume fraction of corrugated steel fibres. Each volume fraction incorporated fibres of two different sizes i.e. 2.0 mm x 0.6 mm x 25 mm and 2.0 mm x 0.6 mm x 50 mm by weight of the longer and shorter fibres in the ratio of 50% - 50%. Fatigue life data obtained has been analyzed in an attempt to determine the relationship among stress level, number of cycles to failure and probability of failure for SFRC. It was found that this relationship can be represented reasonably well graphically by a family of curves. The experimental coefficients of the fatigue equation have been obtained from the fatigue test data to represent the curves analytically.

L. Sorelli and F. Toutlemonde⁵ have focused on the application of SFRC in tunnel lining segments, as an alternative to conventional RC segments. Because of the structural applications of Steel Fiber Reinforced Concrete (SFRC) have recently been increasing due to the improvement of material properties, such as in the material toughness under tension and durability. However, because the behavior of such structures is fairly different from conventional Reinforced Concrete (RC) structures the classic design method should be critically reviewed considering the post-cracking resistant mechanism. Based on an accurate experimental investigation on full scale specimens, a smeared crack model, which implements the Hilleborg's criteria, was used. In order to assess the SFRC reliability, a wide population of tensile tests on cylinders drilled out from a reference full scale specimen was carried out. The tensile constitutive relation, which is the fundamental property for SFRC materials, was chosen on a probabilistic fashion accounting for the actual dispersions of fiber in the tunnel segment due to the casting procedure. According to the finite element analysis, the structural response of such structures was found to be very sensitive to the fiber dispersion. Finally, the AFREM recommendation for SFRC materials and the simplified 'struts and ties' model were evaluated by means of a parametric analysis.

K.Srinivasa Rao et al⁶ carried out studies for proper understanding of the effects of elevated temperatures on the properties of HSC. The paper reports results of laboratory investigations carried out to study the effects of elevated temperatures ranging from 50⁰C to 250⁰C on the compressive strength of HSC made with both ordinary Portland cement (OPC) and Portland pozzolana cement (PPC). The residual compressive strengths were evaluated at different ages. The results showed that at later ages HSC made with Portland pozzolana cement performed better by retaining more residual compressive strength compared to concrete made with ordinary Portland cement.

M.Potha Raju et al⁷ carried out a study aimed to study the effect of elevated temperatures ranging from 50 to 250⁰C on the compressive strength of high-strength concrete (HSC) of M60 grade made with ordinary Portland cement (OPC) and pozzolana Portland cement (PPC). Tests were conducted on 100 mm cube specimens. The specimens were heated to different temperatures of 50,100,150,200 and 250⁰C for three different exposure durations of 1, 2 and 3 h at each temperature. The rate of heating was maintained as per ISO-834 temperature-time curve for standard fire. After the heat treatment, the specimens were tested for compressive strengths. Test results were analysed and the effects of elevated temperatures on PPC concrete were compared with OPC concrete. The PPC concrete exhibited better performance than OPC concrete.

Experimental Programme
Table – 1: Total quantities used in present work

Ingredient	Quantity per m ³ of concrete	
	Standard Concrete	Standard Fiber Reinforced Concrete
Cement	256.328 kg	256.328 kg
Fine Aggregate	267.571 kg	267.571 kg
Coarse Aggregate	943.677 kg	943.677 kg
Fibers	-----	15.288 kg
SP 430	2.05 lts	2.05 lts
Water	103.3 lts	103.3 lts

Casting of test specimens

In the present work, the compressive strengths of Standard Concrete and Standard Fiber Reinforced Concrete were evaluated after exposing them to elevated temperatures for three hours duration and testing is made in hot condition immediately after taking out from the oven.

Work:

To produce Standard Concrete and Fiber Reinforced Standard Concrete, the major work involves designing an appropriate mix proportion and evaluating the properties of the concrete thus obtained. Modern concrete mix designs can be complex. The design of a concrete, or the way the weights of the components of a concrete is determined, is specified by the requirements of the project and the various local building codes and regulations.

The design begins by determining the "durability" requirements of the concrete. These requirements take into consideration the weather conditions that the concrete will be exposed to in service, and the required design strength. Many factors need to be taken into account, from the cost of the various additives and aggregates, to the tradeoffs between, the "slump" for easy mixing and placement and ultimate performance. In the present work standard concrete of 45 mix and w/b ratio of 0.5 is used. Compressive strength tests were conducted to know the strength properties of the mixes. Initially a simple mix design was followed and modifications were made accordingly while arriving at trial mixes to get an optimized mix which satisfies both fresh, hardened properties and economy. Finally a simple mix design for standard concrete have been developed according to IS 10262-1982⁸.

Strengths have been compared between standard concrete and fiber reinforced standard concrete exposed to fire. Exposures are made for 50°C, 100°C, 150°C, 200 °C, 250 °C for a time interval of 3 hours. Immediately after exposure compressive strength, flexural strength, and split tensile strengths have been determined in hot conditions.

Steel fibres of 0.41 w/b (aspect) ratios and straight fibers of 0.5 mm diameter and 50 mm length were added to the above mix.

Concrete: The mix proportion was 1: 1.04: 3.68 with water cement ratio of 0.41. The slump was found to be 80 mm. The cement used was Ordinary Portland Cement (OPC) conforming to IS 12269-1987⁹. The fine aggregate used was natural river sand conforming to zone IV of IS 383-1970¹⁰. The coarse aggregate used was crushed stone passing IS 20 mm sieve and retained on IS 4.75 mm sieve. Potable water of pH value 6.72 was used. The experimental program can be identified in two stages, first, to develop self standard concrete of M45 mix, which satisfy specifications given by Indian Standards. Then, in the second stage characteristics of compressive, bending and splitting tensile strengths exposed to different temperatures were studied by adding and without adding fibers.

The program consisted of arriving at mix proportions, weighing the ingredients of concrete accordingly, mixing them in a standard concrete mixer and then testing for the fresh properties of respective concrete. If fresh properties satisfy standard specifications, 9 Standard cubes of dimensions 150 mm x 150 mm x 150 mm were cast to check whether the target compressive strength is achieved at 7-days and 28- days curing. If either the fresh properties or the strength properties are not satisfied, the mix is modified accordingly. Standard cube moulds of 150 mm X 150 mm X 150 mm made of cast iron were used for casting standard cubes. The standards moulds were fitted such that there are no gaps between the plates of the moulds. The moulds then oiled and kept ready for casting. After 24 hours of casting, the specimen were demoulded and transferred to curing tank where in they were immersed in water for the desired period of curing.

For comparing strengths for M45 grade, standard concrete and fiber reinforced standard concrete, a total of 36 cubes, 36 cylinders and 36 beams were cast. Out of which, 18 cubes, 18 cylinders and 18 beams are tested for each type of concrete.

The concrete was mixed in a rotary mixer so as to ensure better mixing and to avoid any loss of materials. The mixer was hand-loaded with coarse aggregate first, then with fine aggregate and then with cement for Standard type of Concrete. And for the Fiber Reinforced Standard concrete the same is repeated with the inclusive of Fibers in the last. During the rotation of the mixer, first water was added to the ingredients inside and then with the required amount of super plasticizer. The rotation was continued up to 2 minutes. The mixer was tilted and the concrete was unloaded on a clean platform. Oil was applied to the inside faces of the moulds to avoid any sticking of concrete to the walls of the moulds.

Cubes

To study the compressive strength of concrete, 18 cubes of 150 mm size for each type of concrete were cast. 150 mm cube moulds were filled with concrete and placed on table vibrator and vibrated for 1 minute, after the compaction was completed, the surfaces of the cubes were leveled with a trowel and were marked for identification. These specimens were demoulded after 24 hours of casting.

Preparation of cylindrical specimens:

Cylindrical moulds (150mm diameter and 300 mm height) were used to determine the splitting tensile strength. Eighteen cylinders were cast of compacted for each batch of the mix. Specimens were removed from the moulds after 24 hrs and cured in water. Testing of specimens were carried out after 28 days of curing and then exposed to elevated temperatures.

Preparation of beam specimens:

Beam moulds (500 mm X 100 mm X 100 mm) were used to determine the flexural strength. Eighteen beams were cast and compacted for each batch of the mix. Specimens were removed from the moulds after 24 hrs and cured in water. Testing of specimens were carried out after 28 days of curing and then exposed to temperatures.

Curing of Specimens

After the specimens were demoulded, these were stored under water at room temperature until tested at an age of 28 days. The specimens were cured in a water tank for 28 days.

After 28 days of casting, all the specimens were taken out of curing tank and stored under laboratory air drying conditions until required for high temperature exposure or for any load test.

Testing of Specimens

After curing for 28 days, the specimens were tested for compressive strength and tensile strength of concrete in a 200-Ton compression testing machine and flexural strength in Universal Testing Machine according to IS 516-1959¹¹.

The cubes, cylinders and beams were tested immediately on removal from oven after exposing them to relevant temperatures.

The bearing surfaces of the compression testing machine were wiped clean. The cubes and cylinders to be tested were placed concentrically and in such a manner that the load was applied to the opposite sides of the cube as cast, that is, not on the top and bottom. Then the load was applied without shock and increased continuously at a rate of approximately 140 kg/sq cm/minute until the resistance of the cube to the increasing load broke down and no greater load could be sustained. The maximum load applied to the cube was then noted down. In the similar manner beams were tested under UTM for flexural strength.

Exposing Specimens to elevated temperatures and Testing

To determine the strength after exposed to elevated temperatures, the specimens were heated in oven. After exposing to specified temperatures for three hours, these specimens were tested for respective strengths in hot condition immediately after taking out of the oven.

Heating Specimens

The test specimens were subjected to temperatures from 50°C to 250°C at intervals of 50°C each for three hours duration. The specimens were heated to the specified target temperatures.

The specimens were placed on each tray of oven. The target temperatures was set in the control panel after the specimens were placed inside the oven. Initially the temperature inside the oven was 27°C. It took

some time for the oven to reach the target temperature depending upon the set temperature i.e., more time for higher temperatures.

Following attainment of the desired temperature, the exposure continued for three hours. Then the oven was switched off and the specimens were taken out of the oven and were tested in hot condition.

Discussions

II. COMPARISON OF SC AND FRSC FOR COMPRESSIVE STRENGTH

The compressive strength of SC (standard concrete) and FRSC (fibre reinforced standard concrete) specimens exposed to different elevated temperature is expressed as percentage of 28 days compressive strength of SC (standard concrete) at room temperature. The variation of compressive strength with temperature has been plotted as shown in Fig-1

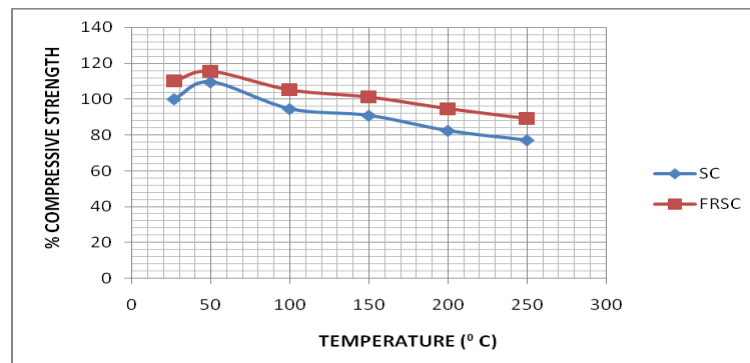


Fig. 1 Comparison of variation compressive strength with temperature for SC and FRSC.

From Fig 1, it can be observed that FRSC exhibits more compressive strength than the SC at the all temperatures. As the temperature is increased FRSC maintained low decreament profile than SC resulting in more percentage compressive strengths after 100°C. The difference between compressive strength of FRSC and SC varies in the range is 6-10 percentage.

III. COMPARISON OF SC AND FRSC FOR SPLIT TENSILE STRENGTH

The split tensile strength of SC (standard concrete) and FRSC (fibre reinforced standard concrete) specimens exposed to different elevated temperature is expressed as percentage of 28 days compressive strength of SC (standard concrete) at room temperature. The variation of compressive strength with temperature has been plotted as shown in Fig-2.

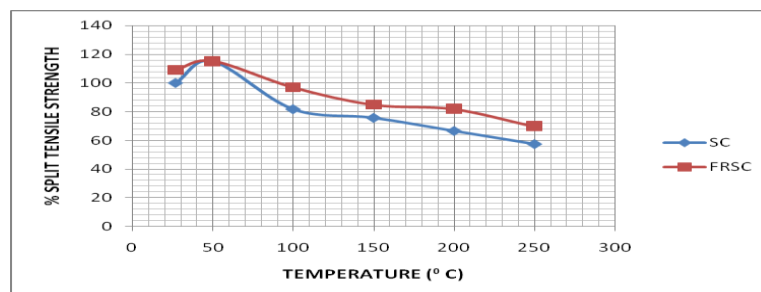


Fig. 2 Comparison of variation split tensile strength with temperature for SC and FRSC.

From Fig 2, it can be observed that FRSC exhibits more split tensile strength than the SC at the all temperatures. As the temperature is increased FRSC maintained low decreament profile than SC resulting in more percentage split tensile strengths after 100°C. The difference between split tensile strength of FRSC and SC varies in the range is 0-12 percentage.

IV. COMPARISON OF SC AND FRSC FOR FLEXURAL STRENGTH

The flexural strength of SC (standard concrete) and FRSC (fibre reinforced standard concrete) specimens exposed to different elevated temperature is expressed as percentage of 28 days compressive strength

of SC (standard concrete) at room temperature. The variation of compressive strength with temperature has been plotted as shown in Fig-3.

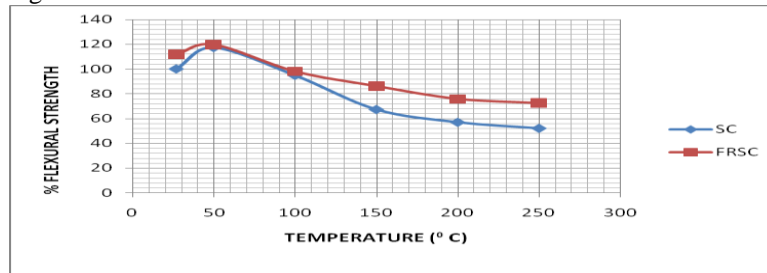


Fig. 3 Comparison of variation flexural strength with temperature for SC and FRSC.

From Fig 3, it can be observed that FRSC exhibits more flexural strength than the SC at the all temperatures. As the temperature is increased FRSC maintained low decreament profile than SC resulting in more percentage flexural strengths after 100°C. The difference between flexural strength of FRSC and SC varies in the range is 0-20 percentage.

V. CONCLUSIONS

- 1). An increase in compressive strength and tensile strength has been observed for both standard concrete and fiber reinforced standard concrete when exposed to a temperature of 50°C.
- 2). In the range of 50 to 80°C the split tensile strength of both standard concrete and fibre reinforced standard concrete is same.
- 3). Flexural strength of standard concrete is equal to that of the fibre reinforced standard concrete in range of 50°C-80°C.
- 4). Beyond 50°C, both standard concrete and fibre reinforced standard concrete are found to loose compressive strength gradually.
- 5). Fibre reinforced standard concrete is found to exhibit more compressive strength split tensile strength and flexural strength than standard concrete at all temperatures.
- 6). The difference between compressive strength of fibre reinforced standard concrete and standard concrete varies in the range of 6-10percentage.
- 7). The difference between split tensile strength of fibre reinforced standard concrete and standard concrete varies in the range of 0-12 percentage.
- 8). The difference between flexural strength of fibre reinforced standard concrete and standard concrete varies in the range of 0-20 percentage.

REFERENCES

- [1]. Nguyen Van Chanh "Steel Fiber Reinforced Concrete" Ho Chimin City University of Technology, pp 108 – 116.
- [2]. Mehrdad Mahoutian, Amir Bonakdar, Mahdi Bakhshi, Babak Ahmadi and Yaghoub Farnam "Fiber Reinforced Concrete, Improvement of mechanical properties of concrete" Construction Materials Institute, 2001, pp 1 - 2.
- [3]. Chih-Ta Tsai, Lung-Sheng Li, Chien-Chih Chang, and Chao-Lung Hwang "Durability design and application of Steel fiber reinforced concrete in Taiwan" The Arabian Journal For Science & Engineering Vol – 34, 2009, pp 57 - 79.
- [4]. S. P. Singh & B. R. Ambedkar, Y. Mohammadi, S. K Kaushik " Flexural fatigue strength prediction of steel fibre reinforced concrete beams" Electronic Journal Of Structural Engineering (8), 2008, pp 46 - 54.
- [5]. L. Sorelli, F. Toutlemonde "On the design of steel fiber reinforced concrete tunnel lining segments "Eleventh International Conference on Fracture, Turin (Italy), 2005, pp 20 -27.
- [6]. K.Srinivasa Rao, M.Potha Raju, P.S.N.Raju "Effect of elevated temperatures on compressive strength of HSE made with OPC and PPC" The Indian Concrete Journal, 2006, pp 1 - 6.
- [7]. M.Potha Raju, K.Srinivasa Rao, Prof. P.S.N.Raju "Compressive Strength Of Heated High-Strength Concrete" Magazine of Concrete Research, 2006, pp 1 – 7.
- [8]. IS 10262-1982. "Recommended Guidelines for Concrete Mix Design". Bureau of Indian Standards, New Delhi.
- [9]. IS 12269-1987. "Specification for 53 Grade Ordinary Portland Cement". Bureau of Indian Standards, New Delhi.
- [10]. IS 383-1970. "Specification for Coarse and Fine Aggregates from natural sources for concrete (second revision)". Bureau of Indian Standards, New Delhi.
- [11]. IS 516-1959. "Method of Test for Strength of Concrete". Bureau of Indian Standards, New Delhi.

Compressive Study on Importance of Wind Power in India

Dr. Srinivasa Rao Kasisomayajula

*Principal/Professor, Dept of Business Management, Vijaya P.G.College, Munaganoor, Hayathnagar, Hyderabad

**Res: H.No.3-2-112/3, Meena Nagar, Bhongir-508116,

Abstract: Wind power is the conversion of wind energy into a useful form of energy. The total amount of economically extractable power available from the wind is considerably more than present human power use from all sources. Since wind speed is not constant, a wind farm's annual energy production is never as much as the sum of the generator nameplate ratings multiplied by the total hours in a year.

I. INTRODUCTION:

Wind power is the conversion of wind energy into a useful form of energy. The construction of wind farms is not universally welcomed because of their visual impact, but any effects on the environment from wind power are generally less problematic than those of any other power source. The intermittency of wind seldom creates problems when using wind power to supply up to 20% of total electricity demand. Power management techniques such as exporting and importing power to neighboring areas or reducing demand when wind production is low, can mitigate these problems. Small wind facilities are used to provide electricity to isolated locations and utility companies increasingly buy back surplus electricity produced by small domestic wind turbines. Wind mills are typically installed in favourable windy locations. Humans have been using wind power for at least 5,500 years to propel sailboats and sailing ships. In July 1887, a Scottish academic, Professor James Blyth, undertook wind power experiments that culminated in a UK patent in 1891. The modern wind power industry began in 1979 with the serial production of wind turbines. These early turbines were small by today's standards, with capacities of 20–30 KW each. Since then, they have increased greatly in size, with the Enercon E-126 capable of delivering up to 7 MW, while wind turbine production has expanded to many countries.

The Earth is unevenly heated by the sun, such that the poles receive less energy from the sun than the equator; along with this, dry land heats up (and cools down) more quickly than the seas do. The differential heating drives a global atmospheric convection system reaching from the Earth's surface to the stratosphere which acts as a virtual ceiling. Most of the energy stored in these wind movements can be found at high altitudes where continuous wind speeds of over 160 km/h (99 mph) occur. Eventually, the wind energy is converted through friction into diffuse heat throughout the Earth's surface and the atmosphere. The total amount of economically extractable power available from the wind is considerably more than present human power use from all sources. The potential of wind power on land and near-shore is to be 72 TW, equivalent to 54,000 MToE (million tons of oil equivalents) per year, or over five times the world's current energy use in all forms. The potential takes into account only locations with mean annual wind speeds ≥ 6.9 m/s at 80 m. The study assumes six 1.5 megawatt, 77 m diameter turbines per square kilometer on roughly 13% of the total global land area.

II. OBJECTIVES

1. To compressive study on world wise wind power importance
2. Analytical study on wind power generation and utilization growth between countries
3. Cost Analysis of Wind power generation

Wind power usage countries:

In worldwide, many thousands of wind turbines are operating, with a total capacity of 1,94,400 MW. Europe accounted for 48% of the total in 2009. World wind generation capacity is more than doubling about every three years. In 2010, Spain became Europe's leading producer of wind energy, achieving 42,976 GWh. However, Germany holds the first place in Europe in terms of installed capacity, with a total of 27,215 MW at

December 31, 2010. Wind power accounts for approximately 21% of electricity use in Denmark, 18% in Portugal, 16% in Spain, 14% in the Republic of Ireland, and 9% in Germany (*Table 1*). According to Global Wind Energy Council (GWEC) figures in 2007 shows that an increase of installed capacity of 20 GW, taking the total installed wind energy capacity to 94 GW, up from 74 GW in 2006. Despite constraints facing supply chains for wind turbines, the annual market for wind continued to increase at an estimated rate of 37%, following 32% growth in 2006. In terms of economic value, the wind energy sector has become one of the important players in the energy markets, with the total value of new generating equipment installed in 2007 reaching US\$36 billion. Although the wind power industry was impacted by the global financial crisis in 2009 and 2010, a BTM Consult five year forecast up to 2013 projects substantial growth. Over the past five years the average growth in new installations has been 27.6 percent each year. In the forecast to 2013 the expected average annual growth rate is 15.7 percent. More than 200 GW of new wind power capacity could come on line before the end of 2013. Wind power market penetration is expected to reach 3.35 percent by 2013 and 8 percent by 2018.

Table-1 Top 10 Wind Power Usage Countries

Rank	Country	Wind Power Capacity (in MW)	Share in Total	Country	Electricity Generation EU countries (in GWh)	Share in Total
1	China	44,733	26%	Spain	42,976	33%
2	United States	40,180	24%	Germany	35,500	27%
3	Germany	27,215	15%	United Kingdom	11,440	9%
4	Spain	20,676	12%	France	9,600	7%
5	India	13,066	8%	Portugal	8,852	7%
6	Italy	5,797	4%	Denmark	7,808	6%
7	France	5,660	3%	Netherlands	3,972	3%
8	United Kingdom	5,204	3%	Sweden	3,500	3%
9	Canada	4,008	3%	Ireland	3,473	3%
10	Denmark	3,734	2%	Greece	2,200	2%
	Total	170,273	100%	Total	129,321	100%

Source: Global Wind Energy Council (GWEC) in March, 2011

Offshore wind power refers to the construction of wind farms in bodies of water to generate electricity from wind. Better wind speeds are available offshore compared to on land, so offshore wind power's contribution in terms of electricity supplied is higher. As of October 2010, 3.16 GW of offshore wind power capacity was operated, mainly in Northern Europe. According to BTM Consult, more than 16 GW of additional capacity will be installed before the end of 2014 and the UK and Germany will become the two leading markets. Offshore wind power capacity is expected to reach a total of 75 GW worldwide by 2020, with significant contributions from China and the US. In a wind farm, individual turbines are interconnected with a medium voltage (often 34.5 KV), power collection system and communications network. At a substation, this medium-voltage electric current is increased in voltage with a transformer for connection to the high voltage electric power transmission system. The surplus power produced by domestic micro generators can, in some jurisdictions, be fed into the network and sold to the utility company, producing a retail credit for the micro generators' owners to offset their energy costs.

Grid management

Induction generators, often used for wind power, require reactive power for excitation, so substations used in wind-power collection systems include substantial capacitor banks for power factor correction. Different types of wind turbine generators behave differently during transmission grid disturbances, so extensive modeling of the dynamic electromechanical characteristics of a new wind farm is required by transmission system operators to ensure predictable stable behavior during system faults. In particular, induction generators cannot support the system voltage during faults, unlike steam or hydro turbine-driven synchronous generators. Doubly-fed machines generally have more desirable properties for grid interconnection. Transmission systems operators will supply a wind farm developer with a grid code to specify the requirements for interconnection to the transmission grid. This will include power factor, constancy of frequency and dynamic behavior of the wind farm turbines during a system fault.

Capacity factor

Since wind speed is not constant, a wind farm's annual energy production is never as much as the sum of the generator nameplate ratings multiplied by the total hours in a year. The ratio of actual productivity in a year to this theoretical maximum is called the capacity factor. Typical capacity factors are 20–40%, with values

at the upper end of the range in particularly favourable sites. For example, a 1 MW turbine with a capacity factor of 35% will not produce 8,760 MWh in a year ($1 \times 24 \times 365$), but only ($1 \times 0.35 \times 24 \times 365$) produced 3,066 MWh, averaging to 0.35 MW. Online data is available for some locations and the capacity factor can be calculated from the yearly output. Unlike fueled generating plants, the capacity factor is affected by several parameters, including the variability of the wind at the site, but also the generator size- having a smaller generator would be cheaper and achieve higher capacity factor, but would make less electricity (and money) in high winds. Conversely a bigger generator would cost more and generate little extra power and, depending on the type, may stall out at low wind speed. Thus an optimum capacity factor can be used, which is usually around 20-35%. In a 2008 study released by the U.S. Department of Energy's Office of Energy Efficiency and Renewable Energy, the capacity factor achieved by the wind turbine fleet is shown to be increasing as the technology improves. The capacity factor achieved by new wind turbines in 2004 and 2005 reached 36%.

Penetration

Wind energy "penetration" refers to the fraction of energy produced by wind compared with the total available generation capacity. There is no generally accepted "maximum" level of wind penetration. The limit for a particular grid will depend on the existing generating plants, pricing mechanisms, capacity for storage or demand management, and other factors. An interconnected electricity grid will already include reserve generating and transmission capacity to allow for equipment failures; this reserve capacity can also serve to regulate for the varying power generation by wind plants. Studies have indicated that 20% of the total electrical energy consumption may be incorporated with minimal difficulty. These studies have been for locations with geographically dispersed wind farms, some degree of dispatchable energy, or hydropower with storage capacity, demand management, and interconnection to a large grid area export of electricity when needed. Beyond this level, there are few technical limits, but the economic implications become more significant. Electrical utilities continue to study the effects of large (20% or more) scale penetration of wind generation on system stability and economics. At present, a few grid systems have penetration of wind energy above 5%: Denmark (values over 19%), Spain and Portugal (values over 11%), Germany and the Republic of Ireland (values over 6%). But even with a modest level of penetration, there can be times where wind power provides a substantial percentage of the power on a grid. For example, in the morning hours of 8 November 2009, wind energy produced covered more than half the electricity demand in Spain, setting a new record.

Variability and intermittency

Electricity generated from wind power can be highly variable at several different timescales: from hour to hour, daily, and seasonally. Annual variation also exists, but is not as significant. Related to variability is the short-term (hourly or daily) predictability of wind plant output. Like other electricity sources, wind energy must be 'scheduled' and forecasting methods are used, but predictability of wind plant output remains low for short-term operation. Because instantaneous electrical generation and consumption must remain in balance to maintain grid stability, this variability can present substantial challenges to incorporating large amounts of wind power into a grid system. Intermittency and the non-dispatchable nature of wind energy production can raise costs for regulation, incremental operating reserve, and could require an increase in the already existing energy demand management, load shedding, or storage solutions or system interconnection with HVDC cables. At low levels of wind penetration, fluctuations in load and allowance for failure of large generating units require reserve capacity that can also regulate for variability of wind generation. Wind power can be replaced by other power stations during low wind periods. Transmission networks must already cope with outages of generation plant and daily changes in electrical demand. Systems with large wind capacity components may need more spinning reserve. Pumped-storage hydroelectricity or other forms of grid energy storage can store energy developed by high-wind periods and release it when needed. Stored energy increases the economic value of wind energy since it can be shifted to displace higher cost generation during peak demand periods. The potential revenue from this arbitrage can offset the cost and losses of storage; the cost of storage may add 25% to the cost of any wind energy stored, but it is not envisaged that this would apply to a large proportion of wind energy generated. In particular geographic regions, peak wind speeds may not coincide with peak demand for electrical power and hot days in summer may have low wind speed and high electrical demand due to air conditioning. Some utilities subsidize the purchase of geothermal heat pumps by their customers, to reduce electricity demand during the summer months by making air conditioning up to 70% more efficient.

A report on Denmark's wind power noted that their wind power network provided less than 1% of average demand 54 days during the year 2002. Wind power advocates argue that these periods of low wind can be dealt with by simply restarting existing power stations that have been held in readiness or interlinking with HVDC. Electrical grids with slow-responding thermal power plants and without ties to networks with hydroelectric generation may have to limit the use of wind power. Three reports on the wind variability in the

UK issued in 2009, generally agree that variability of wind needs to be taken into account, but it does not make the grid unmanageable; and the additional costs, which are modest, can be quantified. A 2006 International Energy Agency forum presented costs for managing intermittency as a function of wind-energy's share of total capacity for several countries, as shown in *Table 2*:

Table – 2 Increase in System Operation Costs (Euros per M.W)

Country	Germany	Denmark	Finland	Norway	Sweden
10% SOC Increase Wind Share	2.5	0.4	0.3	0.1	0.3
20% SOC Increase Wind Share	3.2	0.8	1.5	0.3	0.7
Variance	0.7	0.4	1.2	0.2	0.4
Change Percentage	28%	100%	400%	200%	133%

Capacity credit and fuel saving

Many commentators concentrate on whether or not wind has any "capacity credit" without defining what they mean by this and its relevance. Wind does have a capacity credit, using a widely accepted and meaningful definition, equal to about 20% of its rated output. This means that reserve capacity on a system equal in MW to 20% of added wind could be retired when such wind is added without affecting system security or robustness. But the precise value is irrelevant since the main value of wind is its fuel and CO₂ savings. According to a 2007 Stanford University study published in the *Journal of Applied Meteorology and Climatology*, interconnecting ten or more wind farms can allow an average of 33% of the total energy produced to be used as reliable, base load electric power, as long as minimum criteria are met for wind speed and turbine height.

Economics

Wind power has negligible fuel costs, but a high capital cost. The estimated average cost per unit incorporates the cost of construction of the turbine and transmission facilities, borrowed funds, return to investors, estimated annual production, and other components, averaged over the projected useful life of the equipment, which may be in excess of twenty years. Energy cost estimates are highly dependent on these assumptions so published cost figures can differ substantially. A British Wind Energy Association report gives an average generation cost of onshore wind power of around 3.2 pence per KW·h (2005). Cost per unit of energy produced was estimated in 2006 to be comparable to the cost of new generating capacity in the US for coal and natural gas: wind cost was estimated at \$55.80 per MW·h, coal at \$53.10/MW·h and natural gas at \$52.50. Other sources in various studies have estimated wind to be more expensive than other sources. In 2009 study on wind power in Spain by Gabriel Calzada Alvarez Universidad Rey Juan Carlos concluded that each installed MW of wind power led to the loss of 4.27 jobs, by raising energy costs and driving away electricity-intensive businesses. The U.S. Department of Energy found the study to be seriously flawed, and the conclusion unsupported. The presence of wind energy, even when subsidized, can reduce costs for consumers (€5 billion/yr in Germany) by reducing the marginal price by minimizing the use of expensive 'peaker plants'. The marginal cost of wind energy once a plant is constructed is usually less than 1 cent per KW·h. In 2004, wind energy cost a fifth of what it did in the 1980s, and some expected that downward trend to continue as larger multi-megawatt turbines were mass-produced. However, capital costs have increased. For example, in the United States, installed cost increased in 2009 to \$2,120 per kilowatt of nameplate capacity, compared with \$1,950 in 2008, a 9% increase. Not as many facilities can produce large modern turbines and their towers and foundations, so constraints develop in the supply of turbines resulting in higher costs.

III. INCENTIVES

More than 6,000 wind turbines in the Altamont Pass Wind Farm, in California, United States developed during a period of tax incentives in the 1980s, this wind farm has more turbines than any other in the US. Wind energy in many jurisdictions receives financial or other support to encourage its development. Wind energy benefits from subsidies in many jurisdictions, either to increase its attractiveness, or to compensate for subsidies received by other forms of production which have significant negative externalities. In the US, wind power receives a tax credit for each kW·h produced; at 1.9 cents per kW·h in 2006, the credit has a yearly inflationary adjustment. Another tax benefit is accelerated depreciation. Many American states also provide incentives, such as exemption from property tax, mandated purchases, and additional markets for "green credits". Canada and Germany also provide incentives for wind turbine construction, such as tax credits or minimum purchase prices for wind generation, with assured grid access. These feed-in tariffs are typically set well above average electricity prices. The Energy Improvement and Extension Act of 2008 contain extensions of credits for wind, including micro turbines. Secondary market forces also provide incentives for businesses to use wind-generated power, even if there is a premium price for the electricity.

IV. ENVIRONMENTAL EFFECTS

Compared to the environmental impact of traditional energy sources, the environmental impact of wind power is relatively minor. Wind power consumes no fuel, and emits no air pollution, unlike fossil fuel power sources. The energy consumed to manufacture and transport the materials used to build a wind power plant is equal to the new energy produced by the plant within a few months. While a wind farm may cover a large area of land, many land uses such as agriculture are compatible, with only small areas of turbine foundations and infrastructure made unavailable for use. There are reports of bird and bat mortality at wind turbines as there are around other artificial structures. The scale of the ecological impact may or may not be significant, depending on specific circumstances. Prevention and mitigation of wildlife fatalities, and protection of peat bogs, affect the siting and operation of wind turbines. There are anecdotal reports of negative effects from noise on people who live very close to wind turbines. Small-scale wind power is the name given to wind generation systems with the capacity to produce up to 50 kW of electrical power. Individuals may purchase these systems to reduce or eliminate their dependence on grid electricity for economic or other reasons, or to reduce their carbon footprint. Wind turbines have been used for household electricity generation in conjunction with battery storage over many decades in remote areas. A new Carbon Trust study into the potential of small-scale wind energy has found that small wind turbines could provide up to 1.5 terawatt hours (TW·h) per year of electricity (0.4% of total UK electricity consumption), saving 0.6 million tonnes of carbon dioxide (Mt CO₂) emission savings. This is based on the assumption that 10% of households would install turbines at costs competitive with grid electricity, around 12 pence (US 19 cents) a kW·h. Distributed generation from renewable resources is increasing as a consequence of the increased awareness of climate change. The electronic interfaces required to connect renewable generation units with the utility system can include additional functions, such as the active filtering to enhance the power quality.

V. WIND POWER SCENERIO AND POLICY IN INDIA

Since the 2003 Electricity Act, the wind sector has registered a compound annual growth rate of about 29.5%. The central government policies have provided policy support for both foreign and local investment in renewable energy technologies. The key financial incentives for spurring wind power development have been the possibility to claim accelerated depreciation of up to 80% of the project cost within the first year of operation and the income tax holiday on all earnings generated from the project for ten consecutive assessment years. In December 2009 the Ministry for New and Renewable Energy (MNRE) approved a Generation Based Incentive (GBI) scheme for wind power projects, which stipulated that an incentive tariff of Rs 0.50/kWh (EUR 0.8 cents/USD 1.1 cents) would be given to eligible projects for a (maximum) period of ten years. This scheme is currently valid for wind farms installed before 31 March 2012. However, the GBI and the accelerated depreciation are mutually exclusive and a developer can only claim concessions under one of them for the same project. Although the projected financial outlay for this scheme under the 11th Plan Period (2007-2012) is Rs 3.8 billion (EUR 61 million/USD 84 million), the uptake of the GBI has been slow due to the fact that at the current rate it is still less financially attractive than accelerated depreciation. Currently 18 of the 25 State Electricity Regulatory Commissions (SERCs) have issued feed-in tariffs for wind power. Around 17 SERCs have also specified state-wide Renewable Purchase Obligations (RPOs). Both of these measures have helped to create long-term policy certainty and investor confidence, which have had a positive impact on the wind energy capacity additions in those states.

Table-3 Total Installed Capacity in India

Year	2000	2001	2002	2003	2004	2005	2006	2007	2008	2009	2010
MWs	220	1,456	1,702	2,125	3,000	4,430	6,270	7,845	9,655	10,926	13,065
Trend%	100%	662%	774%	966%	1364	2014	2851	3566	4389	4966%	5939%

Table – 3 revealed that India had a record year for new wind energy installations in 2010, with 2,139 MW of new capacity added to reach a total of 13,065 MW at the end of the year. Renewable energy is now 10.9% of installed capacity, contributing about 4.13% to the electricity generation mix, and wind power accounts for 70% of this installed capacity. Currently the wind power potential estimated by the Centre for Wind Energy Technology (C-WET) is 49.1 GW, but the estimations of various industry associations and the World Institute for Sustainable Energy (WISE) and wind power producers are more optimistic, citing a potential in the range of 65- 100 GW. Historically, actual power generation capacity additions in the conventional power sector in India have been fallen significantly short of government targets. For the renewable energy sector, the opposite has been true, and it has shown a tendency towards exceeding the targets set in the five-year plans. This is largely due to the booming wind power sector. Given that renewable energy was about 2% of the energy mix

in 1995, this growth is a significant achievement even in comparison with most developed countries. This was mainly spurred by a range of regulatory and policy support measures for renewable energy development that were introduced through legislation and market based instruments over the past decade. The states with highest wind power concentration are Tamil Nadu, Maharashtra, Gujarat, Rajasthan, Karnataka, Madhya Pradesh and Andhra Pradesh. Today the Indian market is emerging as one of the major manufacturing hubs for wind turbines in Asia. Currently, seventeen manufacturers have an annual production capacity of 7,500 MW. According to the WISE, the annual wind turbine manufacturing capacity in India is likely to exceed 17,000 MW by 2013. The Indian market is expanding with the leading wind companies like Suzlon, Vestas, Enercon, RRB Energy and GE now being joined by new entrants like Gamesa, Siemens, and WinWinD, all vying for a greater market share. Suzlon, however, is still the market leader with a market share of over 50%. The Indian wind industry has not been significantly affected by the financial and economic crises. Even in the face of a global slowdown, the Indian annual wind power market has grown by almost 68%. However, it needs to be pointed out that the strong growth in 2010 might have been stimulated by developers taking advantage of the accelerated depreciation before this option is phased out.

The development of wind power in India began in the 1990s, and has significantly increased in the last few years. Although a relative newcomer to the wind industry compared with Denmark or the US, India has the *fifth* largest installed wind power capacity in the world. Table 4 reveals that as of 31st March 2010 the installed capacity of wind power in India was 11806.69 MW, mainly spread across Tamil Nadu (4906.74 MW). It is estimated that 6,000 MW of additional wind power capacity will be installed in India by 2012. Wind power accounts for 6% of India's total installed power capacity, and it generates 1.6% of the country's power. India is preparing wind atlas. India is the world's fifth largest wind power producer, with an annual power production of 11806.69MW. The worldwide installed capacity of wind power reached 157,899 MW by the end of 2009. USA (35,159 MW), Germany (25,777 MW), Spain (19,149 MW) and China (25,104 MW) are ahead of India in fifth position. The short gestation periods for installing wind turbines, and the increasing reliability and performance of wind energy machines has made wind power a favored choice for capacity addition in India. The essential requirements for establishment of a wind farm for optimal exploitation of the wind are High wind resource at particular site, adequate land availability, Suitable terrain and good soil condition, Proper approach to site, Suitable power grid nearby, Techno-economic selection of WEGs, Scientifically prepared layout.

Table-4 State-wise Wind Power Generation & Installed Capacity in India up to 31st March 2010

State	Wind Power Capacity (in MW)	Percentage to Total	Cumulative Generation (MU)	Percentage to Total	Cumulative Installed Capacity (MW)	Percentage to Total
Gujarat	4906.74	41%	8016	11%	1934.6	16%
Karnataka	2077.70	18%	9991	13%	1517.2	13%
Maharashtra	1863.64	16%	11790	15%	2108.1	17%
Tamil Nadu	1472.75	12%	41100	53%	5073.1	42%
Other States	1485.86	13%	6053	08%	1492.8	12%
Total	11806.69	100%	76950	100%	12125.8	100%

Source: WISE, January, 2011

Tamil Nadu (4132.72 MW): Tamil Nadu is the state with the most wind generating capacity: 4889.765 MW at the end of the March 2010. Not far from Aralvaimozhi, the Muppandal wind farm, the largest in the subcontinent, is located near the once impoverished village of Muppandal, supplying the villagers with electricity for work. The village had been selected as the showcase for India's \$2 billion clean energy program which provides foreign companies with tax breaks for establishing fields of wind turbines in the area. In february 2009, Shriram EPC bagged INR 700 million contract for setting up of 60 units of 250 KW (totaling 15 MW) wind turbines in Tirunelveli district by Cape Energy. Enercon is also playing a major role in development of wind energy in India. In Tamil Nadu, Coimbatore and Tiruppur Districts having more wind Mills from 2002 onwards, specially, Chittipalayam, Kethanoor, Gudimangalam, Poolavadi, Murungappatti (MGV Place), Sunkaramudaku, Kongal Nagaram, Gomangalam, Anthiur are the high wind power production places in the both districts.

Maharashtra (2077.70 MW)

Maharashtra is second only to Tamil Nadu in terms of generating capacity. Suzlon has been heavily involved. Suzlon operates what was once Asia's largest wind farm, the Vankusawade Wind Park (201 MW), near the Koyna reservoir in Satara district of Maharashtra.

Gujarat (1863.64 MW)

Samana in Rajkot district is set to host energy companies like China Light Power (CLP) and Tata Power have pledged to invest up to Rs.8.15 billion (\$189.5 million) in different projects in the area. CLP, through its India subsidiary CLP India, is investing close to Rs.5 billion for installing 126 wind turbines in Samana that will generate 100.8 MW power. Tata Power has installed wind turbines in the same area for generating 50 MW power at a cost of Rs.3.15 billion. Both projects are expected to become operational by early next year, according to government sources. The Gujarat government, which is banking heavily on wind power, has identified Samana as an ideal location for installation of 450 turbines that can generate a total of 360 MW. To encourage investment in wind energy development in the state, the government has introduced a raft of incentives including a higher wind energy tariff. Samana has a high tension transmission grid and electricity generated by wind turbines can be fed into it. For this purpose, a substation at Sadodar has been installed. Both projects are being executed by Enercon Ltd, a joint venture between Enercon of Germany and Mumbai-based Mehra group. ONGC Ltd has commissioned its first wind power project. The 51 MW project is located at Motisindholi in Kutch district of Gujarat. ONGC had placed the EPC order on Suzlon Energy in January 2008, for setting up the wind farm comprising 34 turbines of 1.5-mw each. Work on the project had begun in February 2008, and it is learnt that the first three turbines had begun production within 43 days of starting construction work. Power from this Rs 308 crore captive wind farm will be wheeled to the Gujarat state grid for onward use by ONGC at its Ankleshwar, Ahmedabad, Mehsana and Vadodara centres. ONGC has targeted to develop a captive wind power capacity of around 200 MW in the next two years.

Karnataka (1472.75 MW)

There are many small wind farms in Karnataka, making it one of the states in India which has a high number of wind mill farms. Chitradurga, Gadag are some of the districts where there are a large number of Windmills. Chitradurga alone has over 20000 wind turbines. The 13.2 MW Arasinagundi (ARA) and 16.5 MW Anaburu (ANA) wind farms are ACCIONA'S first in India. Located in the Davangere district (Karnataka State), they have a total installed capacity of 29.7 MW and comprise a total 18 Vestas 1.65MW wind turbines supplied by Vestas Wind Technology India Pvt. Ltd. The ARA wind farm was commissioned in June 2008 and the ANA wind farm, in September 2008. Each facility has signed a 20-year Power Purchase Agreement (PPA) with Bangalore Electricity Supply Company (BESCOM) for off-take of 100% of the output. ARA and ANA are Acciona's first wind farms eligible for CER credits under the Clean Development Mechanism (CDM). ACCIONA is in talks with the World Bank for The Spanish Carbon Fund which is assessing participation in the project as buyer for CERs likely to arise between 2010 and 2012. An environmental and social assessment has been conducted as part of the procedure and related documents have been provided. These are included below, consistent with the requirement of the World Bank's disclosure policy.

Rajasthan (1088.37 MW)

Gurgaon-headquartered Gujarat Fluorochemicals Ltd is in an advanced stage of commissioning a large wind farm in Jodhpur district of Rajasthan. A senior official told Projectmonitor that out of the total 31.5 mw capacity, 12 mw had been completed so far. The remaining capacity would come on line shortly, he added. For the INOX Group company, this would be the largest wind farm. In 2006-07, GFL commissioned a 23.1-mw wind power project at Gudhe village near Panchgani in Satara district of Maharashtra. Both the wind farms will be grid-connected and will earn carbon credits for the company, the official noted. In an independent development, cement major ACC Ltd has proposed to set up a new wind power project in Rajasthan with a capacity of around 11 mw. Expected to cost around Rs 60 crore, the wind farm will meet the power requirements of the company's Lakheri cement unit where capacity was raised from 0.9 million tpa to 1.5 million tpa through a modernisation plan. For ACC, this would be the second wind power project after the 9-mw farm at Udayathoor in Tirunelveli district of Tamil Nadu. Rajasthan is emerging as an important destination for new wind farms, although it is currently not amongst the top five states in terms of installed capacity. As of 2007 end, this northern state had a total of 496 mw, accounting for a 6.3 per cent share in India's total capacity.

Madhya Pradesh (229.39MW)

In consideration of unique concept, Govt. of Madhya Pradesh has sanctioned another 15 MW project to MPWL at Nagda Hills near Dewas. All the 25 WEGs have been commissioned on 31.03.2008 and under successful operation.

Kerala (27.75 MW)

The first wind farm of the state was set up at Kanjikode in Palakkad district. It has a generating capacity of 23.00 MW. A new wind farm project was launched with private participation at Ramakkalmedu in Idukki district. The project, which was inaugurated in April 2008, aims at generating 10.5 MW of electricity. The

Agency for Non-Conventional Energy and Rural Technology (ANERT), an autonomous body under the Department of Power, Government of Kerala, is setting up wind farms on private land in various parts of the state to generate a total of 600 mw of power. The agency has identified 16 sites for setting up wind farms through private developers. To start with, ANERT will establish a demonstration project to generate 2 mw of power at Ramakkalmedu in Idukki district in association with the Kerala State Electricity Board. The project is slated to cost Rs 21 crore. Other wind farm sites include Palakkad and Thiruvananthapuram districts. The contribution of non-conventional energy in the total 6,095 mw power potential is just 5.5 per cent, a share the Kerala government wants to increase by 30 per cent. ANERT is engaged in the field of development and promotion of renewable sources of energy in Kerala. It is also the nodal agency for implementing renewable energy programmes of the Union ministry of non-conventional energy sources.

West Bengal (1.10MW)

The total installation in West Bengal is just 1.10 MW as there was only 0.5 MW addition in 2006-2007 and none between 2007-2008 and 2008-2009. Bengal – Mega 50 MW wind energy project soon for country. Suzlon Energy Ltd plans to set up a large wind-power project in West Bengal. Suzlon Energy Ltd is planning to set up a large wind-power project in West Bengal, for which it is looking at coastal Midnapore and South 24-Parganas districts. According to SP Gon Chaudhuri, chairman of the West Bengal Renewable Energy Development Agency, the 50 MW project would supply grid-quality power. Gon Chaudhuri, who is also the principal secretary in the power department, said the project would be the biggest in West Bengal using wind energy. At present, Suzlon experts are looking for the best site. Suzlon aims to generate the power solely for commercial purpose and sell it to local power distribution outfits like the West Bengal State Electricity Board (WBSEB). Suzlon will invest around Rs 250 crore initially, without taking recourse to the funding available from the Indian Renewable Energy Development Agency (Ireda), said Gon Chaudhuri. He said there are five wind-power units in West Bengal, at Frazerganj, generating a total of around 1 MW. At Sagar Island, there is a composite wind-diesel plant generating 1 MW. In West Bengal, power companies are being encouraged to buy power generated by units based on renewable energy. The generating units are being offered special rates. S Banerjee, private secretary to the power minister, said this had encouraged the private sector companies to invest in this field.

VI. SUPPORT FRAMEWORK FOR WIND ENERGY

There has been a noticeable shift in Indian politics since the adoption of the Electricity Act in 2003 towards supporting research, development and innovation in the country's renewable energy sector. In 2010, the Indian government clearly recognized the role that renewable energy can play in reducing dependence on fossil fuels and combating climate change, and introduced a tax ("cess") of Rs.50 (~USD1.0) on every metric ton of coal produced or imported into India. This money will be used to contribute to a new Clean Energy Fund. In addition, the MNRE announced its intention to establish a Green Bank by leveraging the Rs 25 billion (EUR 400 million / USD 500 million) expected to be raised through the national Clean Energy Fund annually. The new entity would likely work in tandem with the Indian Renewable Energy Development Agency (IREDA), a government-owned non-banking financial company. In keeping with the recommendations of the National Action Plan on Climate Change (NAPCC) the MNRE and the Central Electricity Regulatory Commission (CERC) have evolved a framework for implementation of the Renewable Energy Certificate (REC) Mechanism for India.¹ This is likely to give renewable energy development a further push in the coming years, as it will enable those states that do not meet their RPOs through renewable energy installations to fill the gap through purchasing RECs.

VII. OBSTACLES FOR WIND ENERGY DEVELOPMENT

With the introduction of the Direct Tax Code², the government aims to modernize existing income tax laws. Starting from the fiscal year 2011-12, accelerated depreciation, the key instrument for boosting wind power development in India, may no longer be available. Another limitation to wind power growth in India is inadequate grid infrastructure, especially in those states with significant wind potential, which are already struggling to integrate the large amounts of wind electricity produced. As a result, the distribution utilities are hesitant to accept more wind power. This makes it imperative for CERC and SERCs to take immediate steps toward improved power evacuation system planning and providing better interface between regional grids. The announcement of India's Smart Grid Task Force by the Ministry of Power is a welcome first step in this direction.

Advantages:

The capital cost is comparable with conventional power plants. For a wind farm, the capital cost ranges between 4.5 crores to 6.85 crores per MW, depending up on the type of turbine, technology, size and location, Construction time is less, Fuel cost is zero, O & M cost is very low, Capacity addition can be in modular form, there is no adverse effect on global environment and the whole system is pollution free and environment friendly.

Limitation:

Wind machines must be located where strong, dependable winds are available most of the time, Because winds do not blow strongly enough to produce power all the time, energy from wind machines is considered “intermittent,” that is, it comes and goes. Wind towers and turbine blades are subject to damage from high winds and lightning. Rotating parts, which are located high off the ground can be difficult and expensive to repair, Electricity produced by wind power sometimes fluctuates in voltage and power factor, which can cause difficulties in linking its power to a utility system, The noise made by rotating wind machine blades can be annoying to nearby neighbors and People have complained about aesthetics of an avian mortality from wind machines.

Suggestions:

1. Despite growing worldwide demand for wind energy, present wind technology is not optimized and there are still significant challenges
2. The gains are seeking require new innovations in fluid dynamics, control, materials, manufacturing, structures, and electric power distribution, as well of new ways of engaging the public in appreciating and accepting this technology, the associated transmission infrastructure and its effects on reducing climate change. Design and analysis tools need to be developed.
3. Common computer codes need to be shared and refined in an open collegial way that cannot occur in industry. Researchers need to disseminate, debate, and share results openly, accelerating innovation in the subject.

REFERENCES

- [1] Compendium of Environment Statistics India, 2006, Central Statistical Organization, Ministry of Statistics and Programme Implementation, Govt. of India (Website: <http://www.mospi.gov.in>).
- [2] “Capacity of the Victorian Electricity Transmission Network to Integrate Wind Power.” Dec. 2007. Vencorp. 9 Feb. 2009 (www.vencorp.com.au)
- [3] El-Sayed, M. and Effat Moussa. “Effect of Large Scale Wind Farms On the Egyptian Power System Dynamics.” ICREPQ’09. 9 Feb. 2009 (www.icrepq.com)
- [4] India Ministry of Non-Conventional Energy Sources (MNES) <http://mnes.nic.in/>
- [5] The Energy & Resources Institute (TERI) <http://www.teriin.org/>
- [6] Akhtar, Mujeeb; and Asad Sarwar Qureshi, Tushaar Shah. (2003) ‘The Groundwater Economy of Pakistan’, Working Paper #64. International Water Management Institute: Battaramulla, Sri Lanka.
- [7] Akhtar, Mujeeb; and Asad Sarwar Qureshi. (2003) “Impact of Utilization Factor on the Estimation of Groundwater Pumpage” *Pakistan Journal of Water Resources*, Vol. 7, No. 1, pg. 17-27, January-June 2003.
- [8] Barnes, Douglas F. (2005) ‘Draft for Discussion: Meeting the Challenge of Rural Electrification in Developing Nations, The Experience of Successful Programs,’ *ESMAP*.
- [9] Batra, S.; and A. Singh (2003) “Evolving Proactive Power Supply Regime for Agricultural Power Supply,” *International Water Management Institute*: Anand, India.
- [10] Bhattacharyya, Subhes C. ‘Energy access problem of the poor in India: Is rural electrification a remedy?’ *Centre for Energy, Petroleum and Mineral Law and Policy*, University of Dundee, Scotland, UK.
- [11] Celeski, Elizabeth; and Moncef Aissa. (2004) ‘Low Cost Electricity and Multisector Development in Rural Tunisia.’ World Bank Energy Lecture Series: Washington DC.
- [12] ‘Electricity in India: Providing Power for the Millions’ (2002) International Energy Agency and Organization for Economic Co-operation and Development, *OECD/IEC*: Paris.
- [13] Gaunt, C. T. Meeting electrification's social objectives in South Africa, and implications for developing countries. *Energy Policy*, Volume 33, Issue 10, July 2005, Pages 1309-1317.
- [14] Government of India, (2002). Annual Report 2001-02, On the Working of State Electricity
- [15] Boards & Electricity Departments. New Delhi, Planning Commission.
- [16] Government of India, Ministry of Power (2005) Standing Committee on Energy APDRP Ninth Report: Delhi.
- [17] Iyer, R. Ramaswamy. (2003) ‘Water: Perspectives, Issues, Concerns.’ Sage publications: New Delhi.
- [18] Modi, Vijay; and Dominique Lallement, Susan McDade, Jamal Sagar. (2005) *Energy and the Millennium Development Goals*. Millennium Project Report, New York, 2005. Available from www.unmillenniumproject.org
- [19] Shah, Tushaar; and Christopher Scott, Avinash Kishore, and Abhishek Sharma. (2003) ‘Energy-Irrigation Nexus in South Asia: Improving Groundwater Conservation and Power Sector Viability.’ Research Report # 70. *International Water Management Institute*: Battaramulla, Sri Lanka.
- [20] World Bank (2003). ‘Why Are Power Sector Reforms Important for the Poor?’ The International Bank for Reconstruction and Development/The World Bank: New Delhi.

Rheological Behavior of Tomato Fruits Affected By Various Loads Under Storage Conditions

Nabil S. Albaloushi

Department of Agriculture Systems Engineering, College of Agricultural and Food Sciences, King Faisal University, P.O. Box 420, Al-Hassa 31982, Saudi Arabia.

Abstract: Rheological properties of fruits and vegetables are of interest to plant physiologists, horticulturalists, agricultural engineers and food engineers, due to different causes. the rheological properties are relevant to several aspects of the study of these materials, including the causes and extent of damage during harvesting, transport and storage; the human perception of product quality. The rheological constants of the four element Burgers model when tomatoes were subjected to various fixed loads (stresses) on the main dimensions of the fruits were investigated .The rheological constants, K_1 (instantaneous elasticity, N/mm), K_2 (retarded elasticity, N/mm), C_1 (free viscous element, N.min/mm and C_2 (retarded viscous element, N.min/mm) were decreased significantly with storage time.

Keywords: *rheological behavior, tomato, fixed load, burger model.*

I. INTRODUCTION

Texture is a quality attribute that is critical in determining the acceptability of fresh fruits. The handling and processing of fruits and vegetables involves special problems since the consumer has well-formed opinions and expectations regarding the proper texture of these products. Successful delivery of acceptable products requires care regarding texture changes, and this is most effectively applied when it is based on an understanding of the factors that influence texture. A better understanding of fruit texture and rheology and their relation to microscopic changes may lead to improvements in quality control and process design in the food industry and the marketplace. The rheological properties of foods are affected by their chemical composition which, in turn, affects the structural changes during handling and processing (Varela, P, et al., 2007).

Tomatoes are considering an agricultural biological material. Biological materials do not behave either as perfect elastic or perfect plastic materials. They exhibit both properties simultaneously. So, they are grouped under the definition of visco-elastic materials (Mohsenin, 1996, Faborode and Callaphan ,1989). In the same time, they show effects the dependent on time due to loading. The time dependent behavior of such viscoelastic materials may be described by constitutive equations whose variables are stress, deformation and time. These equations may be expressed by means of rheological models. Rheological models could describe and represent the behavior of biological materials. They help explain the stress, strain behavior of biological materials. The scope of the validity of such rheological models must be established by experiment. The most frequently applied quasistatic experimental methods, which can be utilized to determine viscoelastic properties of solid biological products like potatoes are creep and retardation and stress relaxation tests as well as increasing the stress or deformation under constant rate.

Storage of tomato in bulk is essential to ensure continuous supply of raw material for household consumption as well as for the tomato processing industry. However, tubers are living entities even after harvest and respire and transpire. These processes bring about physiological changes and water loss, which in turn affect the mechanical properties (Burton, 1989). Mechanical or rheological properties of potatoes have been frequently used as a measure of the textural characteristics (Laza, Scanlon, & Mazza, 2001; Scanlon, Day, & Povey, 1998; Thybo & Martens, 1999). Some rheological properties of tomatoes have been reported to be affected by storage time and temperature. However, information on the patterns of changes in the rheological properties during storage is lacking.

The increasing social and economic importance of food production, besides the technology complexity of producing, processing, handling and accepting these highly perishable and fragile food materials requires a more extensive knowledge of their physical properties; because of this, the rheological properties play an important role in

the handling and quality attributes of both minimally processed foods, such as fruits and vegetables. One of the important characteristic of rheological behaviour is the material properties dependence on temperature (Rao and Steffe, 1992).

The rheological properties of fruits and vegetables are of interest to plant physiologists, horticulturalists, agricultural engineers and food engineers, due to different causes. First, fruits and vegetables are increasing in importance in the contemporary human diet. Secondly, the rheological properties are relevant to several aspects of the study of these materials, including the causes and extent of damage during harvesting, transport and storage; the human perception of product quality; and the physiological changes that take place in the product during growth, maturation, ripening and storage after harvest (Rao and Steffe, 1992).

Several studies have indicated that the visco-elastic nature of agricultural and food materials can be analysed by rheological models (Bagley & Christianson, 1987; Bargale, Irudayaraj, & Marquis, 1994; Davis, McMahan, & Leung, 1983; Hamann, 1992; Pappas, Skinner, & Rao, 1988; Purkayastha, Peleg, Johnson, & Normand, 1985). Rheological characterization of fresh and cooked potatoes has been reported using creep tests (Alvarez & Canet, 1998; Alvarez, Canet, Cuesta, & Lamua, 1998; Purkayastha et al., 1985). However, the changes in the parameters of creep models with storage time and temperature were reported in these study.

The determined rheological parameters are a powerful tool in understanding changes in food structure during processing (Guerrero & Alzamora, 1998; Holdsworth, 1993). Considering the consumer demand for processed foods with high quality, there is a need to define changes in rheological properties of foods in processing operations that may affect their overall acceptability (Nindo. C. I, et al., 2007).

The knowledge of the rheological properties of fruit pulps is essential for processes and equipment development, quality evaluation, shelf-life control, and for understanding the structure and macromolecular conformation of pulp constituents (Barnes et al., 1989; Steffe, 1996). The rheological data are required for process engineering analyses (extrusion, pumping, mixing, agitation, heating, coating, process control), quality control and shelf-life estimation, texture evaluation, product development, and the development of constitutive equations for rheological characterization (Ofoli, 1990)

Models are mechanical analogues composed of element (springs and dashpots) where the ideal elastic behavior and the ideal viscous behavior are combined in different ways to model the actual behavior of the bio-materials. In stress relaxation test, the biological materials are deformed to a fixed strain and the strain is held constant. So the stress required to maintain this strain decreases with time. While in creep test, a constant load or stress is applied to the biological materials and the resulting (increasing) strain is measure with time. In fact this type of behavior is typical of fruits and vegetables. Besides it demonstrates the fact that the strain exhibited by the agricultural material under test is not independent of time (Mohsenin, 1996).

Pitt and Chen 1983 stated that this time dependent can have a significant effect on the accuracy of predicted damage levels in fruits and vegetables during harvesting, handling transportation and storage . Datta and Morrow. 1983, showed that the generalized kelven model (a series of kelven bodies) in series with Maxwell model must best represents the creep data obtained from apples, potatoes, and cheese. In this direction numerical attempts to fined a rheological model to represent the flesh of apples, potatoes, pear and other fruit as well as low, methoxyle pectingel preparations under condition of static creep have yielded the Burgers model (Mohsenin , 1996). It can be seen in figure (1). The creep curves of apples (Skinner 1983), tomatoes (Abdel Maksoud , 1992) and grain dust (Chang and Martin ,1983) showed behavior identical to that of the four element Burgers model. In addition , (Mohsenin, 1996) shows the behavior of the four elements Burger model as shown in figer (1) and added that the rheological equation biased on the model in creep and recovery test is given as follows:-

$$\varepsilon(t) = \sigma_0 \left[\frac{1}{E_0} + \frac{1}{E_r} (1 - e^{-t/T_{ret}}) + \frac{t}{\eta_v} \right]$$

Where:

ε = Strain;

t = time, min;

σ_0 = stress, MPa;

E_0 = instantaneous modulus or modulus at zero time;

η = viscosity coefficient of the liquid in the dashpot, Mpa.min;

η_v = Viscosity, Mpa.min; and $T_{ret} = \eta / E_r$ The time of relaxation.

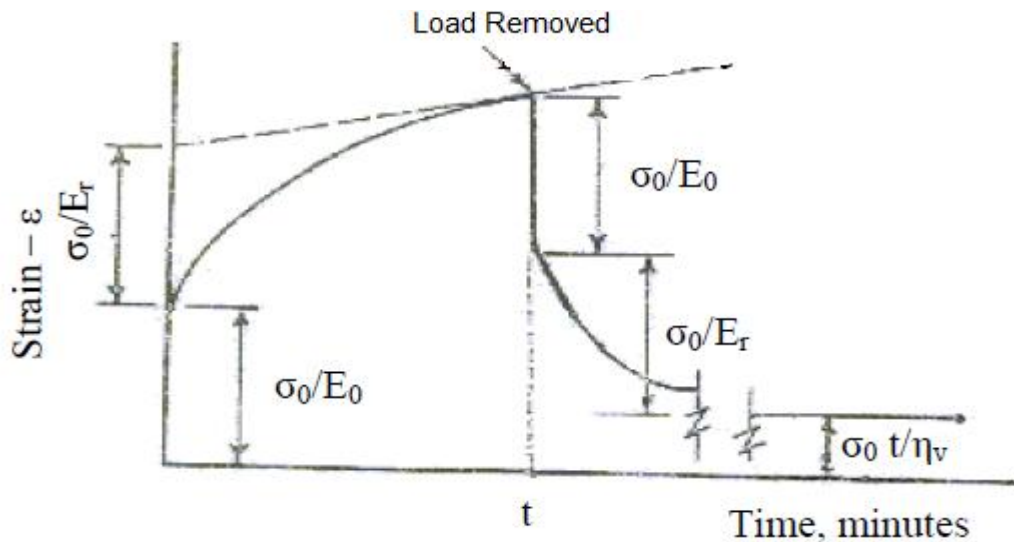


Figure. 1. Typical creep and recovery curve in a viscoelastic material exhibiting instantaneous elasticity, retarded elasticity and viscous flow.

This equation is based on the model consists of a Kelvin model connected in series to a spring and a dashpot element. Mohsenin, 1996, illustrated a typical curve for creep and recovery test of Mackintosh apple as a relationship between deformation in inches and time in minutes as shown in figure (2).

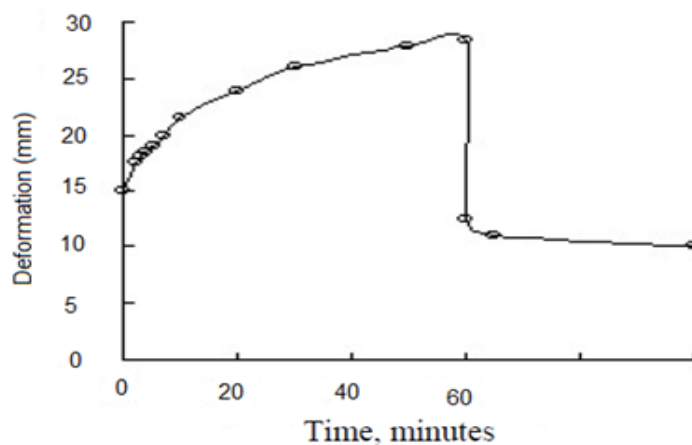


Figure. 2. Distortion of McIntosh apple under dead load of 210 N determined by axial creep and recovery test with 60 mm rigid plunger.

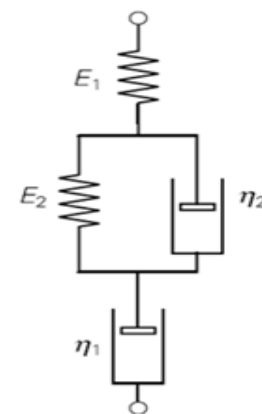


Fig. 3. Creep of the Four-element model (Burgers' model).

Similarly, Abd el Maksoud, 1992, Sabbah et al. 1994 used the four element Burgers model and the following equation as illustrated in figure (3) to determine the rheological constants of the model (K_1 , K_2 , C_1 , C_2) and their relations with fruit (tomatoes) parameters. Ayman Eissa et al., 2012, used the four element Burgers model and the following equation as illustrated in figure (3) to determine the rheological constants of the model (K_1 , K_2 , C_1 , C_2) and their relations with fruit (pears) parameters.

$$\varepsilon = \sigma \left[\frac{1}{E_1} + \frac{1}{E_2} (1 - e^{-t/\tau}) + \frac{t}{\eta_1} \right]$$

Where:

ε = The total deformation at any time t ; mm;

E_1 = Instantaneous elasticity, N/mm;

η_1 = Free viscous element, N. min/mm;

$\tau = \eta_2 / E_2$ the time of retardation.

σ = Constant load, N;

E_2 = Retarded elasticity, N/mm;

η_2 = Retarded viscous element, N. min/mm; and

Sabbah et al., 1994 reported that the deformation increases with increasing of loading level and stage of maturity. Generally, it was inversely proportional with fruit size under the same loading. Meanwhile, they observed considerable variations throughout creep tests on individual fruits due to the non homogenous nature of tomatoes and the stress concentration set up by its irregular shape surface.

Knowledge of the rheological model constants by creep test experiments helps in describing the behavior of the biological material under the static load applied. These are essential for the designer of harvesting and handling equipment to estimate and even predict the amount of material damaged an applied load or deformation. The specific objectives addressed by this investigation are:

- 1- Using the creep and recovery test to determine the viscoelastic properties of tomatoes through the constants of the rheological Burgers model.
- 2- Studying the effect of the storage time under different temperatures on the rheological constants of the model.

II. MATERIAL AND METHODS

100 for creep and recovery test experiments including, three load levels (10, 14 and 18N) and two loading positions (L – longitudinal, D – diameter axis). The procedure to conduct the creep test was run by using the creep test device. It was constructed specifically according to the creep test device used by (Ayman Eissa et al., 2012) as shown in figure (4). Experiments were run by placing the tomato between two parallel plates. The tomato was placed on the base of the apparatus in the considered position while, the crosshead was just touching its surface at zero loading condition. The tomato was then loaded by the concerned fixed load. The instantaneous deformation with time was indicated by the dial micrometer and then recorded. The total time of every test was one hour. It divided into 30 minutes loading period and 30 minutes unloading period (retardation). The obtained data from tests of this investigation were used for plotting creep curves for calculating the constants of the rheological Burgers model (E_1 , E_2 , η_1 , η_2) for tomatoes.

Then tomato was loaded by a specific load, and the experiments were conducted at three levels of temperature (5, 15, 25 °C) the instantaneous deformation was indicated by dial micrometer, and the reading of micrometer was continuously read as samples was deformed. The total test time was one-hour and distributed to two parts during the first half hour the fruit loaded and reading of micrometer was continuously read (creep period), while during the second half hour period the load lifted for fruit (retardation period), and then the test was finished.

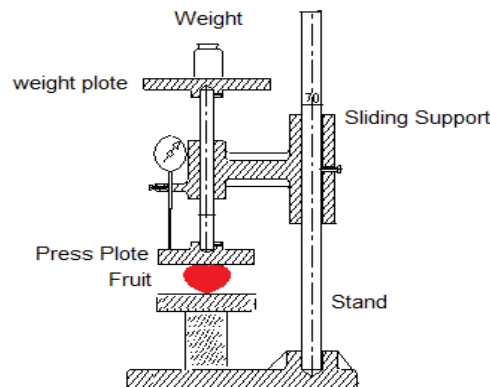


Fig. 4. Creep test apparatus.

III. RHEOLOGICAL PROPERTIES EXPERIMENTS:

Fig.(5), show typical creep test curves and the rheological constants of Burgers model for tomato using 10 N static load at the tomato harvesting day. Considerable variations were obtained throughout the results of the creep tests on individual tomato. Two reasons for this are the nonhomogenous nature of the tomato sample and the stress concentration set up by its irregular shape or surface. The latter is considered to be an important factor is apparent through comparing the results of tomatoes tested at longitudinal and diameter axis position. The mean creep data which obtained from testes were analyzed by Four-elements model (Burgers model) to determine the model constants (k_1 = Instantaneous elasticity, N/mm; K_2 = Retarded elasticity, N/mm; C_1 = Free viscous element, N.min/mm; and C_2 = Retarded viscous element, N.min/mm) as the following:

3.1. Instantaneous elasticity (k_1), N/mm:

Figures. (6); and (7), show the instantaneous elasticity (k_1) decreased during storage time for tomato at three levels of temperature. The instantaneous elasticity (k_1) values increased as the temperature increased, its values increased as the static load increased from 10 N to 18 N.

Significant differences between the instantaneous elasticity (k_1) values for the three levels temperature were observed for all samples. The instantaneous deformation of tested samples specimens when subjected to the constant step load increased with increasing the storage time under all levels of temperature. This increase in deformation led to a significant reduction in the values of (k_1).

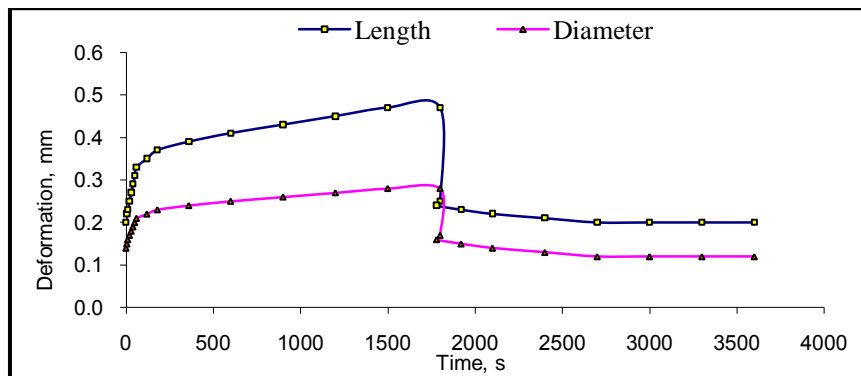


Fig.5. Typical curve of creep retardation test for fresh tomato at load 10N at 5 °C temperature.

The average of the obtained Burger model constants for tomato.				
ITEM	K_1 N/mm	K_2 N/mm	C_1 N.min/mm	C_2 N.min/mm
L position	47.62	50	1500	609.75
D position	71.43	76.92	2500	821.21

The fresh tomato exhibited a straight-line relationship, which is typical of elastic materials, whereas the stored tomato showed a curve linear relationship below that of fresh tomato indicating the loss of firmness. It has been reported that these changes in the mechanical properties of tomatoes during storage are due to loss of turgor pressure and other biochemical reactions and returned to change in room temperature which affect the cell wall and middle lamella of the tissue. And it has been found that the values of k_1 determined at different storage time decreased with increase in compression levels. From these data, in general, the instantaneous elasticity (k_1) is inversely proportional with storage time,

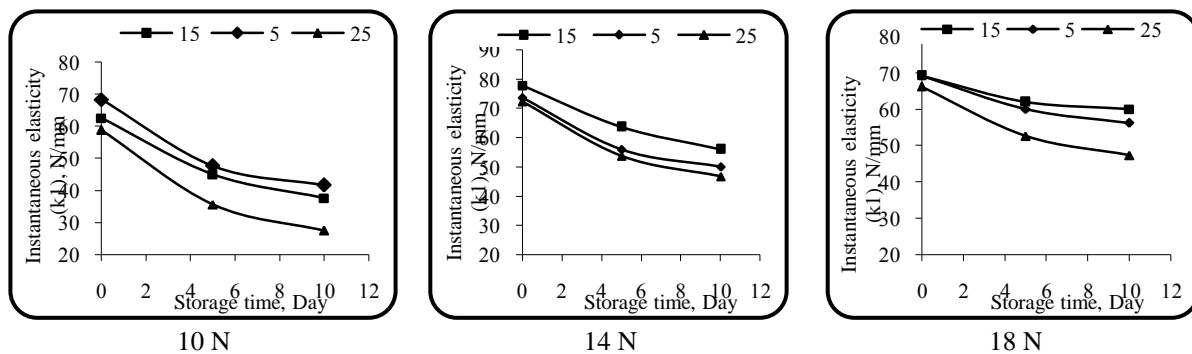


Fig.6. Relationship between instantaneous elasticity with storage time for tomato at longitudinal loading position and different levels of static load, temperature.

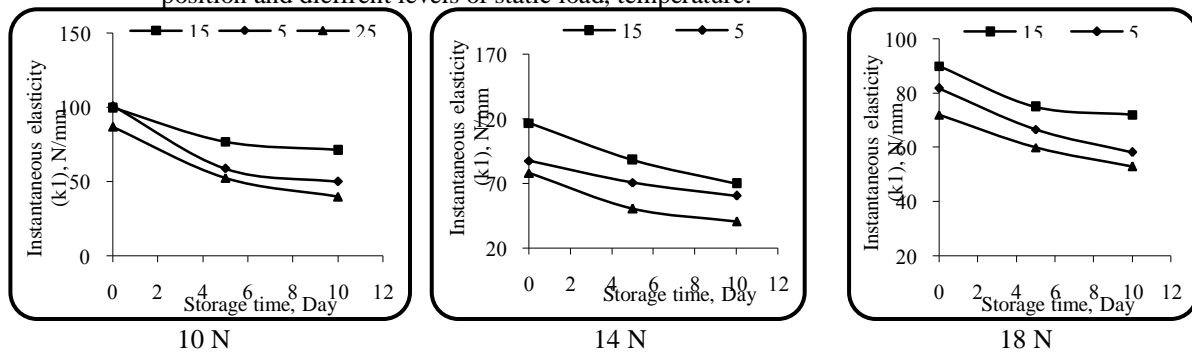


Fig.7. Relationship between instantaneous elasticity with storage time for tomato at diameter loading position and different levels of static load, temperature.

3.2. Retarded Elasticity (K_2), N/mm:

The results of the retarded elasticity (K_2) are presented in Figs. (8); (9). The results show that retarded elasticity (K_2) was decreased by increasing storage time at temperature levels. Its values increased as increasing temperature, its values increased as the static load increased from 10 N to 18 N. Significant differences between the retarded elasticity (K_2) values for all three levels of temperature were observed for all samples, and differences retarded elasticity as well as their interaction were significant in three loaded positions of fruit. In the same time, there were significant differences when using the three levels of load as affected by storage time. From these data, in general, the retarded elasticity (k_2) is inversely proportional with storage time.

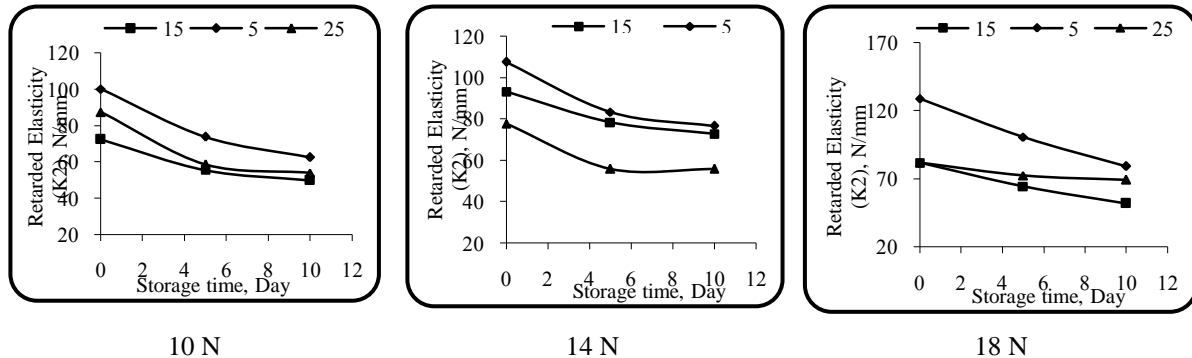


Fig.(8) Relationship between retarded elasticity, with storage time for tomato at longitudinal loading position and different levels of static load, temperature.

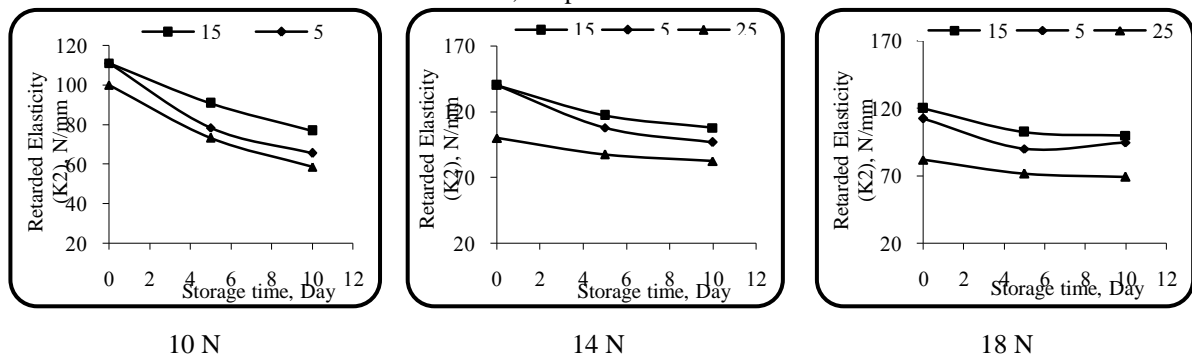


Fig.9. Relationship between retarded elasticity with storage time for tomato at diameter loading position and different levels of static load, temperature.

3.3. Free viscous element (C_1), N.min/mm:

The results of the free viscous element (C_1) are presented in Figs. (10); and (11). The results show that free viscous element (C_1) decreased by increasing storage time for tomato tested at levels of temperature. The free viscous element (C_1) values increased as increasing temperature, its values increased as the static load increased from 10 N to 18 N. Significant differences between free viscous element (C_1) values for all different temperature levels were shown for all fruits. Significant differences between free viscous element and the three positions of sample load. From these data, in general, the Free viscous element (C_1) is inversely proportional with storage time.

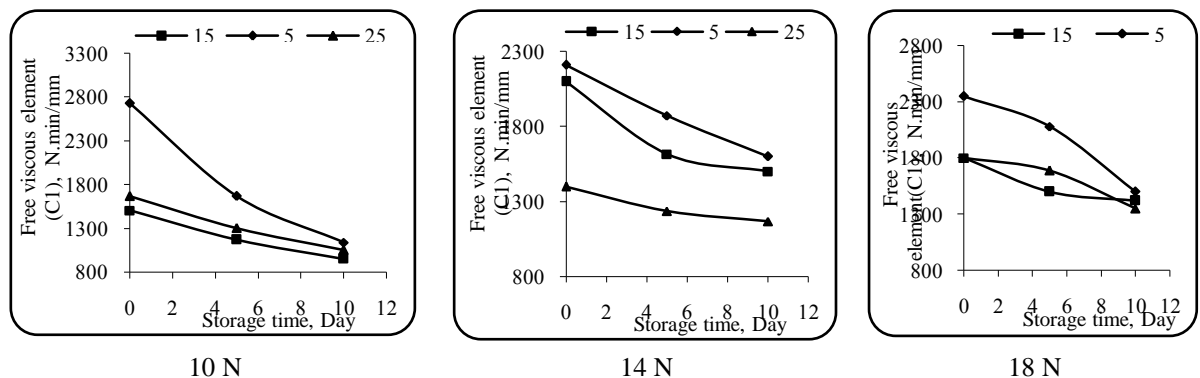


Fig.10. Relationship between Free viscous element with storage time for tomato at longitudinal loading position and different levels of static load, temperature.

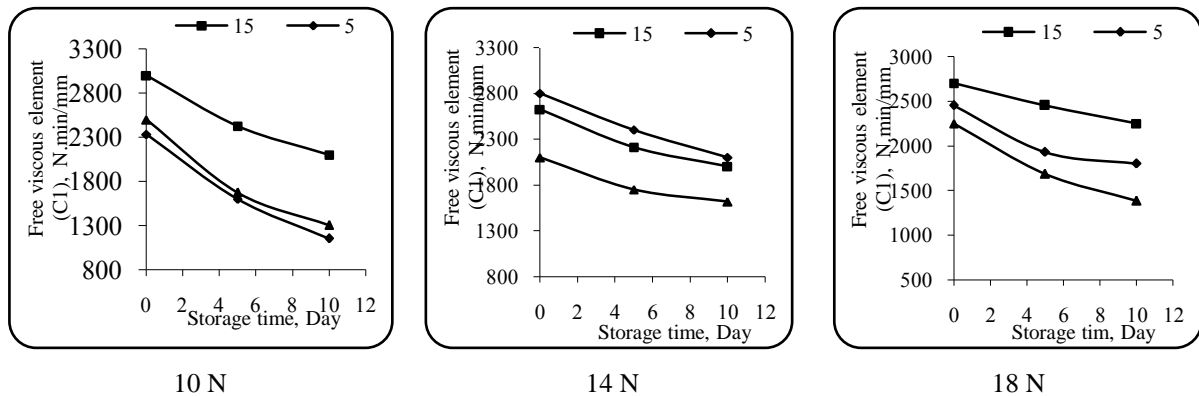


Fig.11. Relationship between Free viscous element with storage time for tomato at diameter loading position and different levels of static load, temperature.

3.4. Retarded Viscous Element (C_2), N.min/mm:

The results of the retarded viscous element (C_2) are presented in Figs. (12) and (13). It is cleared that retarded viscous element (C_2) decreased by increasing storage time at temperature levels. The retarded viscous element at room temperature are highly than low room temperature than high room temperature. The retarded viscous element magnitudes increased by increasing the static load from 10 N to 18 N. Significant differences were shown among different at room temperature levels for all fruits. And differences in retarded viscous element as well as their interaction were significant in three loaded positions of fruit. From these data, in general, the retarded viscous element (C_2) is inversely proportional with storage time.

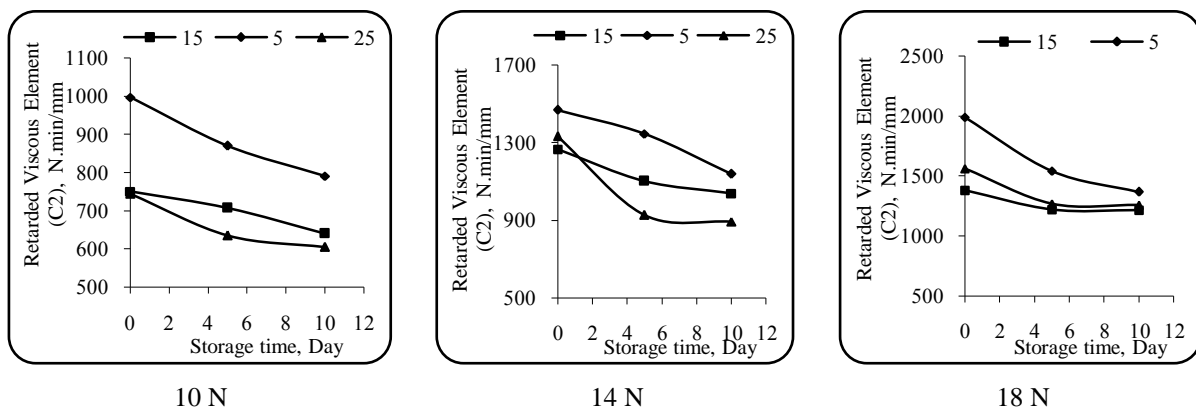


Fig.12. Relationship between retarded viscous element with storage time for tomato at longitudinal loading position and different levels of static load, temperature.

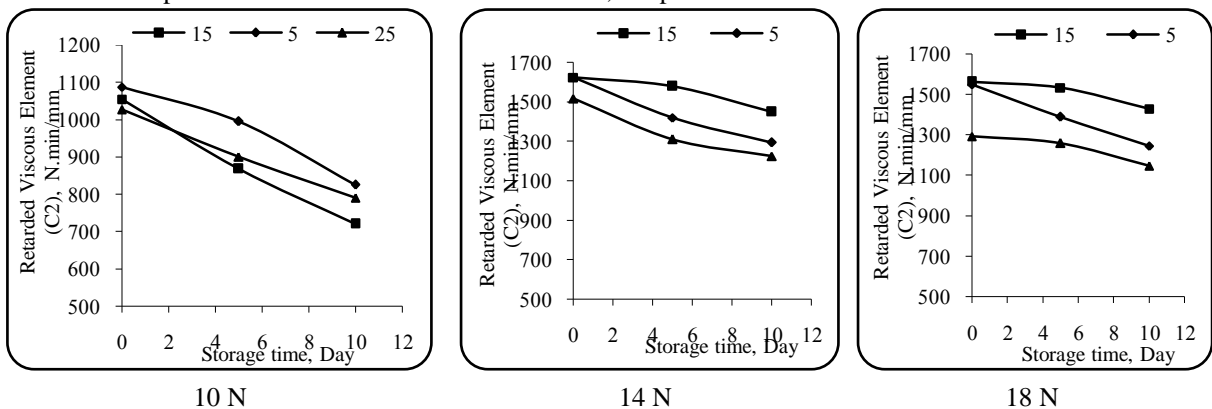


Fig.13. Relationship between retarded viscous element with storage time for tomato at diameter loading position and different levels of static load, temperature.

IV. CONCLUSIONS

A modified exponential model successfully represented the changes in the rheological properties of tomatoes due to storage under constant condition using creep tests. The changes in the rheological properties of tomatoes under fluctuating storage condition could be adequately described as a storage time. It is recommended to put the tomatoes in the packages on longitudinal position (L) so that it leads to less deformation under loads. Concerning temperature, the mean values of the rheological model constants were higher in magnitude when storing tomatoes in higher storage temperature than lower storage temperature. It was observed from the creep and retardation test for tomatoes that, the instantaneous deformation of the tested tomatoes when subjected to the constant load increased with time and also with storage time under all storage conditions in the investigation. When the tomato unloaded, the deflection happened due to the effect of the static load divided to two portions. One is not recoverable due to the fluid which has moved out of the cells. The other is recoverable which is probably due to the elasticity of the cell walls of the tomato.

REFERENCES

- [1] Abdelmaksoud, M.A., 1992. Rheological properties of tomatoes and their dependence on maturity. M.Sc. thesis. Ag. Eng. Dept.; Fac. of Ag., Alexandria Univ.
- [2] Ayman H. Amer Eissa; Abdul Rahman O. Alghannam and Mostafa M. Azam, 2012. Mathematical Evaluation Changes in Rheological and Mechanical Properties of Pears during Storage under Variable Conditions. *Journal of Food Science and Engineering*. (2); 564-575.
- [3] Bagley, E. B., & Christianson, D. D. (1987). Measurement and interpretation of rheological properties of foods. *Food Technology*, 41(3), 96-99.
- [4] Bargale, P. C., Irudayaraj, J. M., & Marquis, B. (1994). Some mechanical and stress relaxation characteristics of lentils. *Canadian Agricultural Engineering*, 36(4), 247-254.
- [5] Barnes, H.A., Hutton, J.F., Walters, K., 1989. *An Introduction to Rheology*, first ed. Elsevier Science Publisher, Amsterdam. 212p.
- [6] Burton, W. G. (1989). *The potato*. UK: Longman Scientific and Technical.
- [7] Chang, C.S. and C.R. Martin, 1983. Rheological properties of grain dust, *Trans. Of the ASAE*. 1249:1256.
- [8] Davis, D. C., McMahan, P. F., & Leung, K. H. (1983). Rheological modeling of cooked potatoes. *Transactions of American Society of Agricultural Engineers*, 26, 630-634.
- [9] Faborode, M. O. and J.R., O Calla ghan (1989). A rheological model for the compaction of fibrous agricultural material. *J.agric.Engn.Res.* 42: 165 – 178.
- [10] Guerrero, S. N., & Alzamora, S. M. (1998). Effect of pH, temperature and glucose addition on flow behavior of fruit purees: II. Peach, papaya, and mango purees. *Journal of Food Engineering*, 33, 239-256.
- [11] Hamann, D. D. (1992). Visco-elastic properties of surimi seafood products. In M. A. Rao, & J. F. Steffe (Eds.), *Visco-elastic properties of foods* (pp. 157-171). Barking Essex, UK: Elsevier Science Publishing Inc.
- [12] Holdsworth, S. D. (1993). Rheological models used for the prediction of the flow properties of food products: A literature review. *Transactions of the Institution of Chemical Engineers*, 71C, 139-179.
- [13] Laza, M., Scanlon, M. G., & Mazza, G. (2001). The effect of tuber preheating, temperature and storage time on the mechanical properties of potatoes. *Food Research International*, 34, 659-667.
- [14] Mohsenin, N.N. 1996. *Physical properties of plant and animal materials*. Gordon and Breach science publishers, New York, 498.
- [15] Nindo. C. I, Tang. J, Powers. J. R, Takhar. P. S., 2007. Rheological properties of blueberry puree for processing applications. *LWT* (40): 292-299.
- [16] Ofoli, R. Y. (1990). Interrelationships of rheology, kinetics, and transport phenomena in food processing. In H. Faridi & J. M. Faubion (Eds.), *Dough Rheology and Baked Product Texture*. New York. AVI.
- [17] Pappas, G., Skinner, G., & Rao, V. N. M. (1988). Effect of imposed strain and moisture content on some viscoelastic characteristics of cowpeas. *Journal of Agricultural Engineering Research*, 39, 209-219.
- [18] Pitt, R.E. and Chen, H. L. (1983). Time – dependent aspects of strength and rheological of vegetative tissue. *Trans. Of the ASAE* 26(5):1275 – 1280.
- [19] Purkayastha, S., Peleg, M., Johnson, E. A., & Normand, M. D. (1985). A computer aided characterization of the compressive creep behavior of potato and cheddar cheese. *Journal of Food Science*, 50, 45-50, 55.
- [20] Rao, M. A., & Steffe, J. F. (1992). *Viscoelastic Properties of Foods*. London: Elsevier Applied Science.
- [21] Sabbah, M.A.; Soliman S.N. and M.A. Abdelmaksoud, 1994. Creep properties of tomatoes and their dependence on maturity. *Mist.J. Ag. Eng.*, 11(1).
- [22] Scanlon, M. G., Day, J. A., & Povey, J. W. M. (1998). Shear stiffness and density in potato parenchyma. *International Journal of Food Science and Technology*, 33, 461-464.
- [23] Steffe, J.F., 1996. *Rheological Methods in Food Process Engineering*, second ed. Freeman Press, Michigan. 418p.
- [24] Thybo, A. K., & Martens, M. (1999). Instrumental and sensory characterization of cooked potato texture. *Journal of Texture Studies*, 30, 259-278.
- [25] Varela. P; Ana Salvador and Susana Fiszman, 2007. Changes in apple tissue with storage time: Rheological, textural and microstructural analyses. *Journal of Food Engineering* 78 (2007) 622-629

Dwt - Based Feature Extraction from ecg Signal

V.K.Srivastava¹, Dr. Devendra Prasad²

¹Research Scholar, Deptt. of Electronics & Comm. Engg., JJT University, Jhunjhunu, Rajasthan, India

²Associate Professor, Deptt. of Computer Sc.& Engg., M.M. University, Ambala, Haryana, India

Abstract: Electrocardiogram is used to measure the rate and regularity of heartbeats to detect any irregularity to the heart. An ECG translates the heart electrical activity into wave-line on paper or screen. For the feature extraction and classification task we will be using discrete wavelet transform (DWT) as wavelet transform is a two-dimensional timescale processing method, so it is suitable for the non-stationary ECG signals (due to adequate scale values and shifting in time). Then the data will be analyzed and classified using neuro-fuzzy which is a hybrid of artificial neural networks and fuzzy logic.

Keyword: Electrocardiogram (ECG), DWT, Neuro Fuzzy.

I. INTRODUCTION

To attain a progressive sustainable development in all regions of the world, attention should be diverted to the health of a population. All sciences contribute to the maintenance of human health and the practice of medicine. Medical physicists and biomedical engineers are the professionals who develop and support the effective utilization of this medical science and technology as their responsibilities to enhance human health care with the new development of the medical tools such as electrocardiogram (ECG). Heart disease is a broad term that includes several more specific heart conditions which are Coronary Heart Disease, Heart Attack, Acute Coronary Syndrome, Aortic Aneurysm and Dissection, Ischemia, Arrhythmias, Cardiomyopathy, Congenital Heart Disease, Peripheral Arterial Disease (PAD). The most common heart condition is coronary heart disease, which can lead to heart attack and other serious conditions [22] and the Myocardial Ischemia is the most common cause of death in the industrialized countries [9].

The electrocardiogram (ECG) is a noninvasive and the record of variation of the biopotential signal of the human heartbeats. The noninvasive technique meaning that this signal can be measured without entering the body at all. Electrodes are placed on the users skin to detect the bioelectric potentials given off by the heart that reach the skins surface. The ECG detection which shows the information of the heart and cardiovascular condition is essential to enhance the patient living quality and appropriate treatment. It is valuable and an important tool in the diagnosing the condition of the heart diseases.

In recent year, numerous research and algorithm have been developed for the work of analyzing and classifying the ECG signal. The classifying method which have been proposed during the last decade and under evaluation includes digital signal analysis, Fuzzy Logic methods, Artificial Neural Network, Hidden Markov Model, Genetic Algorithm, Support Vector Machines, Self-Organizing Map, Bayesian and other method with each approach exhibiting its own advantages and disadvantages.

The ECG features can be extracted in time domain [5][4] or in frequency domain [8][9]. Some of the features extraction methods implemented in previous research includes Discrete Wavelet Transform [4], Karhunen-Loeve Transform [11], Hermitian Basis and other methods [10].

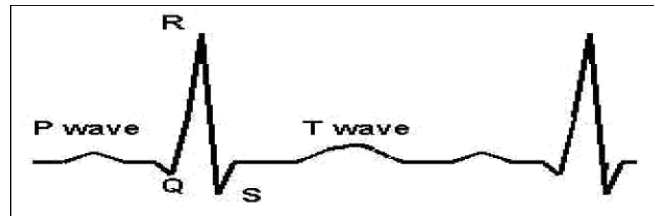


Figure 1: An example of normal ECG trace

All of the ECG waveforms pattern and variability must be determine accurately to get the better diagnostic result that will shown the correct heart disease of the patient. Figure 1 shows the normal ECG traces which consist of P wave, QRS complex and T wave. The P wave is the electrical signature of the current that causes atrial contraction, the QRS complex corresponds to the current that causes contraction of the left and right ventricles and the T wave represents the repolarization of the ventricles.

This research is mainly aimed to extract important parameters from the ECG signal through the DWT technique. By applying this signal analysis technique, the most important parameter of the ECG signal can be taken as the analysis data. Then, the data will be used as an input to the classifier to identify the heart disease. The idea of the ECG analysis and classification using Neuro Fuzzy has been start around 1990, yet it remains one of the most important indicators of proper heart disease classification today.

The most difficult problem faced by an automatic ECG analysis is the large variation in the morphologies of ECG waveforms, it happen not only for different patients or patient groups but also within the same patient. So the Neuro Fuzzy is the most suitable technique because it is more tolerance to morphological variations of the ECG waveforms. This project is useful for the medical application enhancement such as in hospital, clinic which can automatically help to increase the patient health care.

II. RELATED RESEARCH

The Wavelet transform is a two-dimensional timescale processing method for non-stationary signals with adequate scale values and shifting in time [17]. The wavelet transform is capable of representing signals in different resolutions by dilating and compressing its basis functions [18]. The researcher Cuiwei Li et al [4] use the Wavelet transforms method [19][20][21] because the results indicated that the DWT-based feature extraction technique yields superior performance. Neuro-fuzzy is a hybrid of artificial neural networks and fuzzy logic [1]. Fuzzy Neural Network as in the literature [1] incorporates the human-like reasoning style of fuzzy systems through the use of fuzzy sets and a linguistic model consisting of a set of IF-THEN fuzzy rules. The learning process of FNN consists of three phases which are fuzzy membership, fuzzy rule identification and supervised fine-tuning.

Neuro-Fuzzy approach consist of a five-layer neural network called input linguistic layer, condition layer, rule layer, consequent layer, output linguistic layer. The fuzzification of the inputs and the defuzzification of the outputs are performed in the input linguistic stage and output linguistic layers performed by the fuzzy rule identification.

The performance enhancement using proposed method in Neuro-Fuzzy using autoregressive model coefficients, higher-order cumulant and wavelet transform variances as features had been used by Mehmet Engin [15]. It used self-organizing layer which responsible for the clusterization of the input data which is feature vector and the outputs of the membership values form the input vector to the second sub-network (MLP).

This research use the output of DWT technique as features vector and Neuro-Fuzzy as the classifier for the ECG analysis, because based on the previous research, the accuracy rates achieved by the combined neural network model presented for classification of the ECG beats were to be higher than stand alone classifier model.

III. PROPOSED SYSTEM

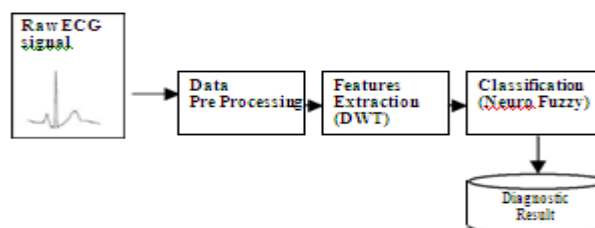


Figure 2: Block diagram of the system

Various methodologies of automated diagnosis have been done. The ECG data analysis techniques are reviewed in and evaluate proposed methods of the classification methods. In our proposed, the process of ECG analysis can be generally subdivided into a number of disjoint processing modules have been identified which are:

1. Data acquisition
2. Pre-processing beat detection
3. Feature Extraction
4. Classification

A. Data acquisition

1. Data Collection

The heart sound using ECG will record simultaneously from patients. The ECG Database in PhysioBank also being used as a data of ECG input signal for features extraction part processing.

2. Preparation of Data

Partitioning the ECG signal into cardiac cycles, and detection of the main events and intervals in each cycle. Major features such as the QRS amplitude, R-R intervals, waves slope of ECG signal can be used as features to create the mapping structure.

B. Preprocessing

The first step of signal pre processing is filtering the ECG signal because as any other measured signal, ECG is also contaminated with high frequency noise. The unwanted noise of the heart biopotential signal must be removing. ECG were filtered using a bandpass filter between 0.05Hz-100Hz to eliminate the motion artifact, baseline wander and 50Hz notch filter to eliminate power line noise.

C. Features Extraction using DWT

The Wavelet Transform (WT) is designed to address the problem of non-stationary ECG signals. It derived from a single generating function called the mother wavelet by translation and dilation operations. The main advantage of the WT is that it has a varying window size, being broad at low frequencies and narrow at high frequencies, thus leading to an optimal time-frequency resolution in all frequency ranges.

The WT of a signal is the decomposition of the signal over a set of functions obtained after dilation and translation of an analyzing wavelet [13]. The ECG signals which consisting of many data points, can be compressed into a few features by performing spectral analysis of the signals with the WT. These features characterize the behavior of the ECG signals. Using a smaller number of features to represent the ECG signals is particularly important for recognition and diagnostic purposes [14].

The ECG signals were decomposed into time-frequency representations using Discrete Wavelet Transform (DWT). The DWT technique has been widely used in signal processing tasks in recent years. The major advantage of the DWT is that it provides good time resolution. Good resolution at high frequency and good frequency resolution at low frequency. Because of its great time and frequency localization ability, the DWT can reveal the local characteristics of the input signal.

The DWT represents a 1-Decomposition signal $s(t)$ in terms of shifted versions of a low pass scaling function $\phi(t)$ and shifted and dilated versions of a prototype bandpass wavelet function $\psi(t)$.

$$\Psi_{j,k}(t) = 2^{(-j/2)} \psi(2^{-j}t - k) \quad (1)$$

$$\phi_{j,k}(t) = 2^{-j} \phi(2^{-j}t - k) \quad (2)$$

where: j controls the dilation or translation

k denotes the position of the wavelet function

Discrete Wavelet Transform is also referred to as decomposition by wavelet filter banks. This is because DWT uses two filters, a low pass filter (LPF) and a high pass filter (HPF) to decompose the signal into different scales. The output coefficients of the LPF are called approximations while the output coefficients of the HPF are called details. The approximations of the signal are what define its identity while the details only imparts nuance.

The DWT can be calculated at different resolutions using Mallat-algorithm to utilize successive lowpass and highpass filters to compute DWT.

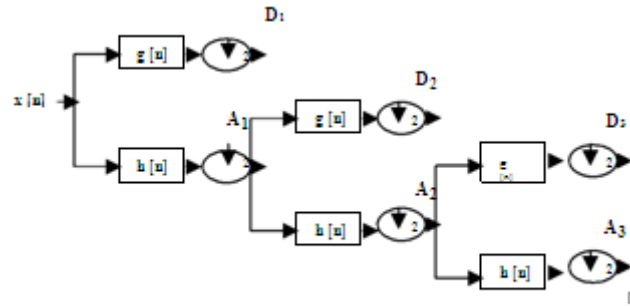


Figure 3: Decomposition of DWT

The procedure of DWT decomposition of a input signal $x[n]$ is schematically shown in the Figure 3 above. Each stage consists of two digital filters and two downsamplers by 2 to produce the digitized signal. The first filter, $g[n]$ is the discrete mother wavelet, which is high-pass filter, and the second, $h[n]$ is low-pass filter. The downsampled outputs of first high pass filters and low-pass filters provide the detail, $D1$ and the approximation, A . The first approximation, $A1$ is decomposed again and this process is continued. The decomposition of the signal into different frequency bands is simply obtained by successive highpass and lowpass filtering of the time domain signal. The signal decomposition can mathematically be expressed as follows:

$$y_{hi}[k] = \sum x[n].g[2k - n] \quad (3)$$

$$y_{lo}[k] = \sum x[n].h[2k - n] \quad (4)$$

D. ECG Classification using Neuro Fuzzy

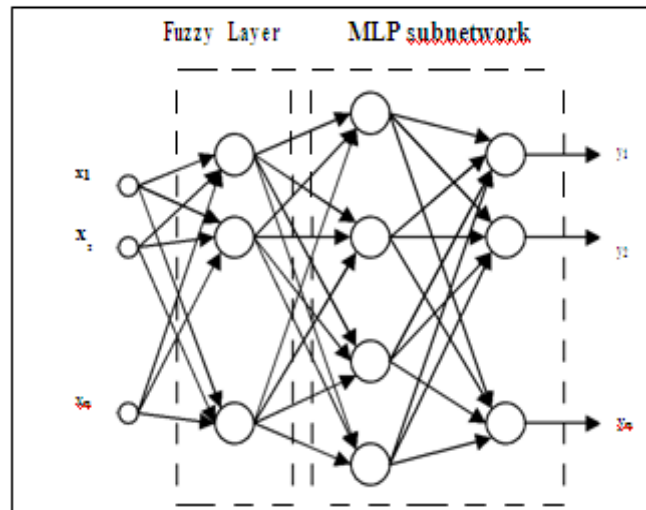


Figure 4: Structure of the Neuro Fuzzy adapted from [2]

In the classifier stage, the idea to apply fuzzy hybrid neural network which composed of two subnetworks connected in cascade. The cascading of the fuzzy self-organizing layer performing the pre classification task and the Multilayer Perceptron (MLP) of Neural Network working as the final classifier which is the fuzzy rules are modeled by artificial neural networks (ANNs)

In the fuzzy self-organizing layer, it is responsible to analyze the distribution of data and group the data into the different membership values. This membership value is applied as the input vector to the MLP Neural Network classifier. The membership value also representing the parameter of each heart beat class. The used of Fuzzy neural network has a number of advantages when compared to ordinary learning of neural networks class. The fuzzy neural network is more tolerant to the noise and less sensitive to the morphological changes of the ECG characteristics.

E. Neuro Fuzzy Model

A Neuro Fuzzy model contains three main components, which are fuzzification stage, the rule base and the defuzzification stage.

1. The first layer represents the direct input layer. Each node represents one ECG feature and sends this input variables from the features extraction to next layer directly.
2. The second layer is the fuzzification layer. In this layer, each extracted ECG feature is fed to fuzzy nodes. These nodes perform to transform the crisp values of the input variables into fuzzy membership values. It represent the membership degree of the input ECG feature to its linguistic description.
3. The third layer represents the fuzzy rules stage. Each node in this layer represents one fuzzy if-then rule.
4. The last layer is the neural network connecting layer. The

linguistic description will shows the ECG classification result of each lead group. Based on the Mamdani model [16], the fuzzy system by existing knowledge described as:

Rule i , R^i : IF x_1 is A_1^i and x_2 is A_2^i ...and x_n is A_n^i ,
THEN y^i is C^i (5)

Where R^i ($i=1,2,\dots,n$) denotes the i th fuzzy rules. $x=(x_1,x_2,\dots,x_n)$ is the input vector,
 y^i is the output of the fuzzy rule R^i
 A_j^i ($j=1,2,\dots,n$) are fuzzy membership function (linguistic description)

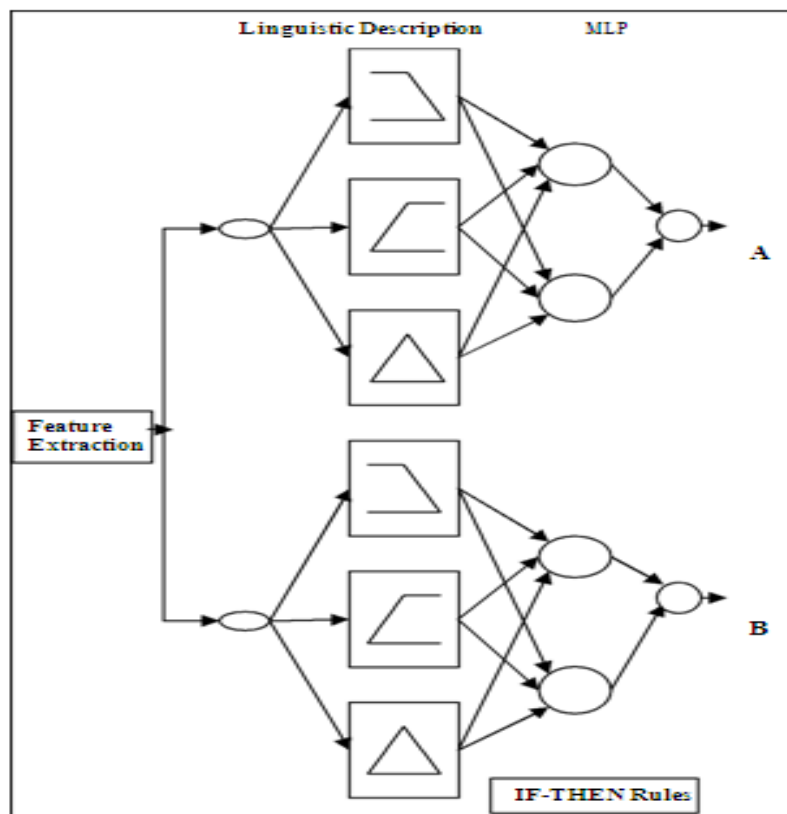


Figure 5: Feedforward Neuro-Fuzzy

The performance measures used to evaluate the performance of the classifiers were accuracy, sensitivity, specificity.

- (i) Specificity = $\frac{\text{number of correct classified normal}}{\text{Number of total normal beats}}$
- (ii) Sensitivity = $\frac{\text{number of correct classified heart disease}}{\text{Number of total heart disease}}$
- (iii) Accuracy = $\frac{\text{Number of beats correctly classified}}{\text{Total number of beats tested}}$

IV. RESULT

The experiment result of ECG analysis using MATLAB programming has been done to show the preprocessing of biosignal analysis before the features extraction process. The ECG Database from Holy Hospital has been used for ECG input signal of the preprocessing stage.

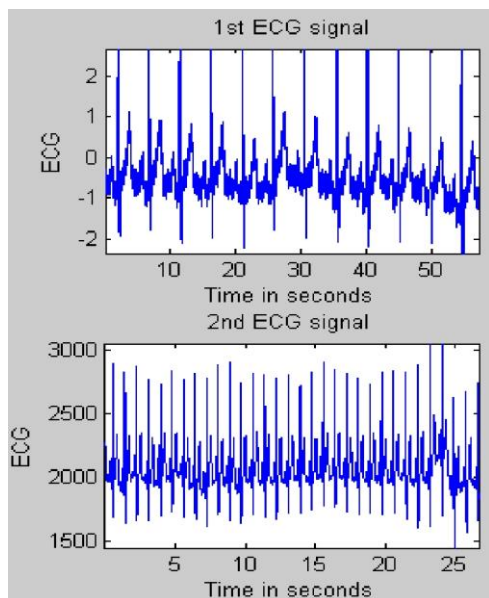


Figure 6: Original ECG signal

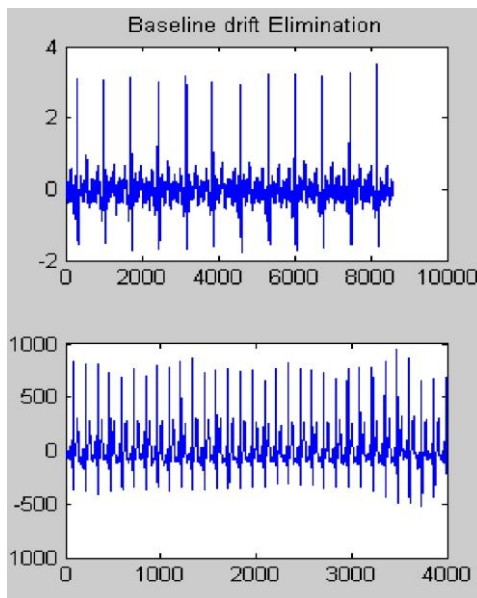


Figure 7: Baseline Elimination of ECG signal

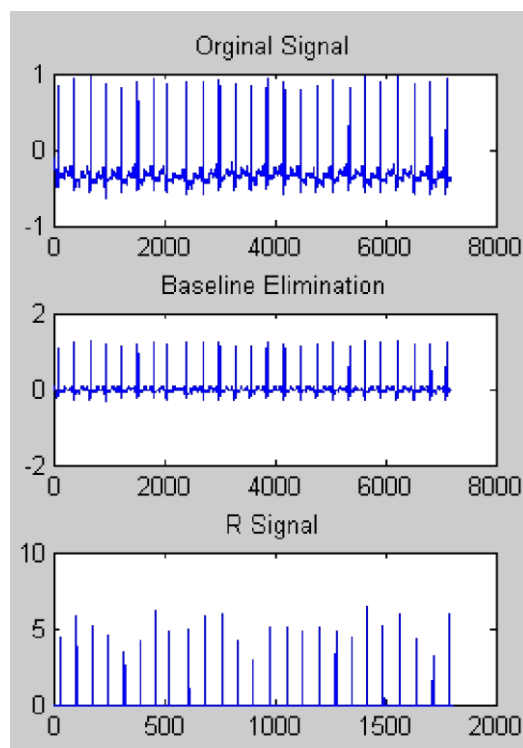


Figure 8: Flow of ECG signal process

V. CONCLUSION

This paper has presented the system which based on the application of Neuro Fuzzy network for reliable heartbeat classification on the basis of the ECG waveform. The DWT characterization will delivers the stable features to the morphology variations of the ECG waveforms. The potential of accuracy rate for Neuro Fuzzy system as ECG diagnostic decision aid is very high.

REFERENCES

- [1]. Yuksel Ozbaya, Rahime Ceylan, Bekir Karlik, "A Fuzzy Clustering Neural Network Architecture For classification Of ECG Arrhythmias", Department of Electrical & Electronics Engineering, Selcuk University, Konya, Turkey, Computers in Biology and Medicine 376–388, 2006.
- [2]. Stanislaw Osowski and Tran Hoai Linh, "ECG Beat Recognition Using Fuzzy Hybrid Neural Network", IEEE Transactions on Biomedical Engineering, Vol. 48, No. 11, November 2001.
- [3]. Tran Hoai Linh, Stanislaw Osowski and Maciej Stodolski, "On-Line Heart Beat Recognition Using Hermite Polynomials and Neuro-Fuzzy Network", Warsaw University of Technology, 2003.
- [4]. Cuiwei Li, Chongxun Zheng, Changfeng Tai, "Detection of ECG Characteristic Points Using Wavelet Transforms", IEEE Transactions on Biomedical Engineering, Vol. 42, No. 1, January 1995.
- [5]. Hu, Y.H., Palreddy, S., Tompkins, W., "A Patient Adaptable ECG Beat Classifier Using A Mixture Of Experts Approach", IEEE Trans. Biomed. Eng. (44), 891–900, 1997.
- [6]. De Chazal, P., Reilly, R.B., "Automatic Classification of ECG Beats Using Waveform Shape And Heart Beat Interval Features", In Proceedings of the IEEE International Conference on Acoustic, Speech and Signal Processing (ICASSP'03), Hong Kong, China, 2003.
- [7]. Minami, K., Nakajima, H., Toyoshima, T., "Real-Time Discrimination of Ventricular Tachyarrhythmia with Fourier-Transform Neural Network", IEEE Trans. Biomed. Eng. (46), 1999.
- [8]. Moraes, J.C.T.B., Seixas, M.O., Vilani, F.N., Costa, E.V., "A Real Time QRS Complex Classification Method Using Mahalanobis Distance" Comput. Cardiol., 2002.
- [9]. De Chazal, P., Reilly, R.B., "Automatic Classification of ECG Beats Using Waveform Shape And Heart Beat Interval Features", In Proceedings of the IEEE International Conference on Acoustic, Speech and Signal Processing (ICASSP'03), Hong Kong, China, 2003.
- [10]. Minami, K., Nakajima, H., Toyoshima, T., "Real-Time Discrimination of Ventricular Tachyarrhythmia with Fourier-Transform Neural Network", IEEE Trans. Biomed. Eng. (46), 1999.
- [11]. Moraes, J.C.T.B., Seixas, M.O., Vilani, F.N., Costa, E.V., "A Real Time QRS Complex Classification Method Using Mahalanobis Distance" Comput. Cardiol., 2002.
- [12]. Costas Papaloukas, Dimitrios I. Fotiadis, Aristidis Likas, Lampros K. Michalis, "Automated Methods for Ischemia Detection in Long Duration ECGs", 2003.
- [13]. David Cuesta-Frau, Juan C. Perez-Cortes, Gabriela Andrea Garcia, Daniel Navak, " Feature Extraction Methods Applied to the Clustering of Electrocardiographic Signals. A Comparative Study", Czech Technical University In IEEE Proceeding, 2002.
- [14]. Franc Jager, "Feature Extraction and Shape Representation of Ambulatory Electrocardiogram Using the Karhunen-Loève Transform" Electrotechnical Review, Ljubljana, Slovenija, 2002.
- [15]. Inan Gulera, Elif Derya Ubey, "Ecgbeat Classifier Designed By Combined Neural Network Model", Pattern Recognition, 199 – 208, 2005.
- [16]. I. Daubechies, "The Wavelet Transform, Time-Frequency Localization and Signal Analysis, IEEE Trans. Inform. Theory, 961–1005, 1990.
- [17]. Z. Dokur and T. Olmez, "ECG Beat Classification By A Novel Hybrid Neural Network, Comput. Meth. Prog. Biomed, 167–181, 2001.
- [18]. Mehmet Engin, "Ecg Beat Classification Using Neuro-Fuzzy Network", Pattern Recognition Letters 25, 1715–1722, 2004.
- [19]. E. H. Mamdani and S. Assilian, "An Experiment In Linguistic Synthesis With A Fuzzy Logic Controller," Int.J. Man-Mach Stud., vol. 7, pp. 1–13, 1975.
- [20]. Thakor, N.V., "Multiresolution Wavelet Analysis Of Evoked Potentials", In IEEE Trans. Biomedical. Eng. 40 (11), 1993.
- [21]. Clark, I, " Multiresolution Decomposition Of Non-Stationary EEG Signal; A preliminary study", Computer Bio.Medical. 25 (4), 1995.
- [22]. S. Z. Mahmoodabadi, A. Ahmadian, D. Abolhasani, M. Eslami, J. H. Bidgoli, "ECG Feature Extraction Based on Multiresolution Wavelet Transform", In Proceedings of the 2005 IEEE Engineering in Medicine and Biology 27th Annual Conference Shanghai, China, September 1-4, 2005.
- [23]. Louis C Pretorius and Cobus Nel, "Feature Extraction From ECG for Classification By Artificial Neural Network", University of Pretoria, In IEEE Proceeding, 2002.
- [24]. Ming-Yao Yang, Wei-Chih Hu and Liang-Yu Shyu, "ECG Events Detection and Classification Using Wavelet and Neural Networks", In IEEE Proceedings 19th International Conference, Oct to Nov, 1997.
- [25]. Joe-Air Jiang, Chih-Feng Chao, Ming-Jang Chiu, Ren- Guey Leec, Chwan-Lu Tsengd, Robert Lin, "An Automatic Analysis Method For Detecting And Eliminating ECG Artifacts In EEG", Computers in Biology and Medicine, January 2006.

Spatiotemporal Pattern of Crime Using Geographic Information System (GIS) Approach in Dala L.G.A of Kano State, Nigeria

M. Ahmed and R. S. Salihu

Department of Geography Bayero University, Kano.

Abstract: This study explores the use of Geographic Information Systems (GIS) and spatial database of crime characteristics which helps in the determination of hotspots in Dala LGA of Kano State and also it identifies the challenges facing police departments that seek to implement computerized crime mapping systems. Different data sources were used, data from the Nigerian Police Force (Dala and Jakara Division) of 2008 – 2010. For this study, the crime was divided into four categories: offence against person, offence against property, offence against authority and offence against local act. The spatiotemporal distributions of the crimes from the three years were analyzed. ArcGIS version 9.3 was used for the analysis and results reveal that crime rate is higher outside the city wall while the rate increased from time to time especially in the year 2010. There are more hotspots outside the city wall. It also shows that crime doesn't occur closer to police stations, but seldom occur around outpost police stations. The buffer zones of 2Kms were used and it analyzed that places like kurna, Gobirawa and YanMata are in need of Police Stations.

Keywords: Crime, GIS, Police station, Spatial, Temporal

I. INTRODUCTION

Crime is a phenomenon which is universal in its varying forms in all cultures and societies, at all stages of organization. The alarming increase in the rate of criminal activities in Nigeria, as reported daily in the local news and media is perhaps a reflection of the nature of every society where goals are used to measure individuals status in society. The Nigerian Police are not equipped with modern automated information system. This is one of the basic problems militating against the effective prevention, detection and control of crime (Rilwani and Eguabor, 2000). Even though, there are so many police stations and their outpost distributed around without enough equipment Musa (2005) explained that Police cannot perform their noble role effectively and efficiently except when provided with adequate funding, equipment, infrastructural facilities, social amenities, and manpower. The level of effectiveness of the police in any country depends mainly on the level of manpower and equipment provided. The level of violent crimes in Nigeria is on the increase looking at the state of the nation.

Yusuf (2010) describe the distribution of Police stations and Manpower in Kano Metropolis which shows Dala LGA had 2 police station, 4 police outpost, 8 senior officers, 123 junior officers with the population of 418,759 (2006 census) and is the least area with senior police officers, even though is the second most populous local government in the Kano Metropolis. He further explained that the distribution of the police station and manpower in Kano Metropolis are uneven. The population ratio of the police according to United Nations should be 1:450 recommended standards (Luivei Times Kenya Sept. 2, 2010). However, Dambazau (2007) explained that there is a general belief that the Nigerian Police has been with a strength of personnel that is far below the capacity required to police the estimated Nigerian population of approximately 120 million, considering the minimum United Nations standard. That is why the study focuses on seeing how GIS would be useful for the Nigerian Police in crime detection, analysis and mapping.

II. GEOGRAPHIC INFORMATION SYSTEM AND THE POLICE FORCE

Today, with the rapid advancement of technology, a computer-based technique for exploring, visualizing, and examining the occurrences of criminal activity is essential. GIS is one of the most influential

tools for facilitating and exploration of the spatial distribution of crime. The fundamental strength of GIS over traditional crime analytical tools and methods is the ability to visualize, analyze and explain the criminal activity in a spatial context. Certain environmental factors, such as the physical layout of the area, proximity to various services and land use are likely to influence criminal behavior and it is necessary to take them into account when analyzing the crime data. Burrough, (1998) described GIS as a powerful set of tools for collecting, storing, retrieving at will, transforming and displaying spatial data from the real world for a particular set of purposes. Smith *et al* (1987) lamented that GIS is a database system in which most of the data are spatially indexed and upon which a set of procedures operated in order to answer queries about spatial entities in the database. It is a decision support system that involves the integration of spatially referenced data in a problem solving environment. Environmental Systems Research Institute, (ESRI) California (1990), defined GIS as an organized collection of computer hardware, software and personnel to efficiently capture, store, update, manipulate, analyze and display all forms of geographically referenced information. Consequently, modern GIS software allows law enforcement agencies to produce more versatile electronic maps by combining their crime databases of reported crime locations with digitized maps of the target areas (Sahu and Peeyush2011).

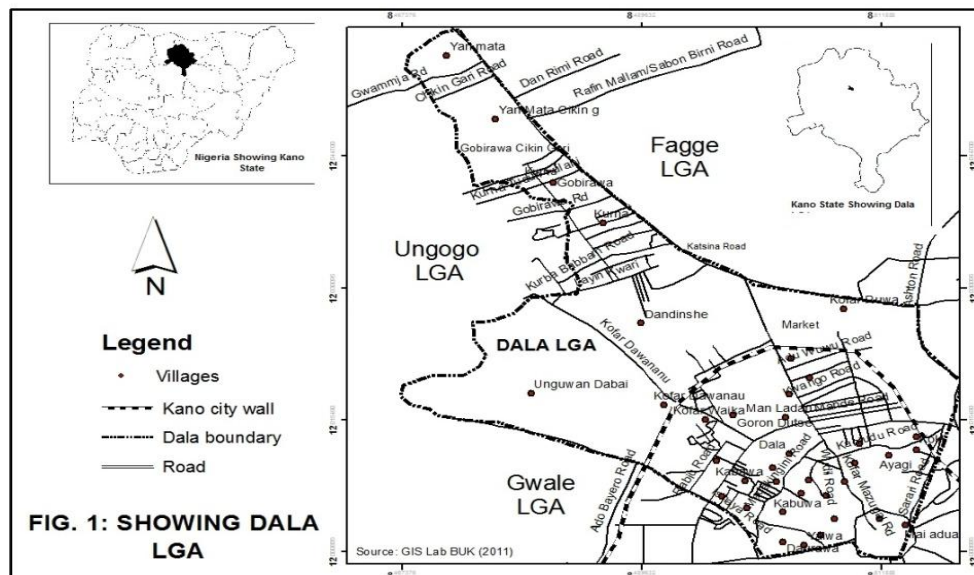
Crime mapping is used by analyst in law enforcement agencies to map, visualize, and analyze crime incident patterns. In addition it enabled them to identify crime hot spots along with other trends and patterns (Soneye, 2002). It was established that a large proportion of the men of the Nigerian Police Force hardly ascertain the areas under the jurisdiction of their stations or define the shortest route from their stations to specific crime areas. As discovered by Soneye, the police stations in Ikeja Local Government Area, Lagos State are far from being distributed according to geographical spread, population characteristics or crime incidences (*ibid*).

Among its wider applications, GIS is used to support operations; aid in command and control decisions; assist in crime and other investigations; complement community problem oriented policing activities; target crime prevention programs; conduct cross-jurisdictional analysis and enhance collaboration with courts and corrections (Source). The ability to map locations of events by their characteristics is an invaluable tool for police officers. Access to this tool is one of the biggest decisions that police departments face when implementing a GIS. Even though desktop mapping programs have become relatively user friendly, none are simple enough to use without extensive training. GIS is also used to answer the question, Where are the highest concentrations of crimes? Several algorithms are available to calculate the areas of highest density in a point distribution (Elizabeth *et al* 1998). In addition the use of maps by the police using GIS and remotely sensed data allows analysts to identify hot spots, along with other trends and patterns. GIS also allows analysts to overlay other datasets such as census demographics, locations of police station, dispatching to emergencies, banks, filling station, schools etc., to better understand the underlying causes of crime and help law enforcement administrators to devise strategies to deal with the problem.

Potential uses for the technology are limited only by the imaginations of individuals in the field. This study will provides an overview of how law enforcement agencies are to use GIS to support a wide variety of activities. This study may contribute to a better management and allocation of police resources, once the occurrences and their associated patterns have been located. The identification of relations between certain types of crime and it distributions may help in the combating and prevention. (This study focuses on the three years data (2008, 2009 and 2010) data collected from the two Police Units at Dala and Jakara Division). The aim of this study is to show the usefulness of GIS technology in crime pattern analysis in Dala LGA of Kano State. The objectives in specific terms are to explain the spatiotemporal pattern of crimes from 2008 – 2010 and to analyze how accessible the police stations are in the area.

III. STUDY AREA

Dala LGA (Figure 1) is among the eight (8) Metropolitan local government areas of Kano state. Is located at latitude $12^{\circ} 00' 00''\text{N}$ to $12^{\circ} 03' 21''\text{N}$ and longitude $8^{\circ} 27' 30''\text{E}$ to $8^{\circ} 31' 40''\text{E}$. Its population was 418,759 (NPC 2006) with total land area of about 1481 Km^2 . It is bounded by in west by Ungogo in the southwest by Gwale, southeast by Municipal, Nassarawa by the east and Fagge by the north.



IV. MATERIAL AND METHODS

Data Acquisition

Crime mapping refers to the process of conducting spatial analysis within the range of activities of crime analysis (Boba, 2005). Relevant administrative records from Nigerian Police Force Dala and Jakara Divisions of Dala local government, supplementary and attribute data were collected through field work interactive use of Global Positioning System (GPS) which provided the co-ordinates of all the police stations in the area. Data were sourced from documentary sources including textbooks, journals, newspapers, magazines and field survey which involve personal interviews and also the map of Kano Metropolis produced by Ministry of Land and Survey Kano State 1978 and a Street guide map produced by ministry of lands and physical planning Kano State 2008.

Spatial, Attribute and Geo-referencing Data

The study was based on spatial database creation and analysis in a computer based GIS environment. The data were created in an excel file (window 2007) in the form of text and later imported and transformed in to a shape file in the GIS environment, during geo-referencing, certain identified abnormalities such as projection and symbolization errors, which are quite common of such convectional maps were rectified before adopted for the study. ArcGIS 9.3 was used for the mapping and the analysis.

Mapping Method

Mapping method for visualizing the spatial distribution of crime based on the boundaries of neighborhood was interpolated. There are three methods for interpolation; Inverse Distance Weighted (IDW), Spline, Kriging. All of them were performed for neighborhoods, but the best result was obtained from Inverse Distance Weighted method

V. RESULT AND DISCUSSION

The criterion for categorization of crimes in this study was based on the Nigerian Police Abstract of Statistics (NPACS). Dambazau (1997) offences are categorized into four main categories: *Offences against person*: These includes Murder, Attempted murder, Manslaughter, Suicide, gravior harm / Wounding, assault, Child stealing, Slave dealing, Rape / Indecent assault, kidnapping, Unnatural offences, Other offences. *Offences against property*: Armed robbery, Demand with menace, Thief/Stealing, Burglary, House Breaking, Store breaking, False Pretence/Cheating, Receiving Stolen Property, Unlawful Possession (Drugs/Guns), Arson, Other offences. *Offences against lawful authority*: Forgery of currency notes, Coining offences, Gambling, Breach of Peace, Perjury, Bribery and Corruption, Escape from Custody, Other offences. *Offences against local act*: Traffic offences, Township offences, Liquor offences, Dog act, Firearms Act, Narcotics, Other Offences.

Temporal Distribution of Crime

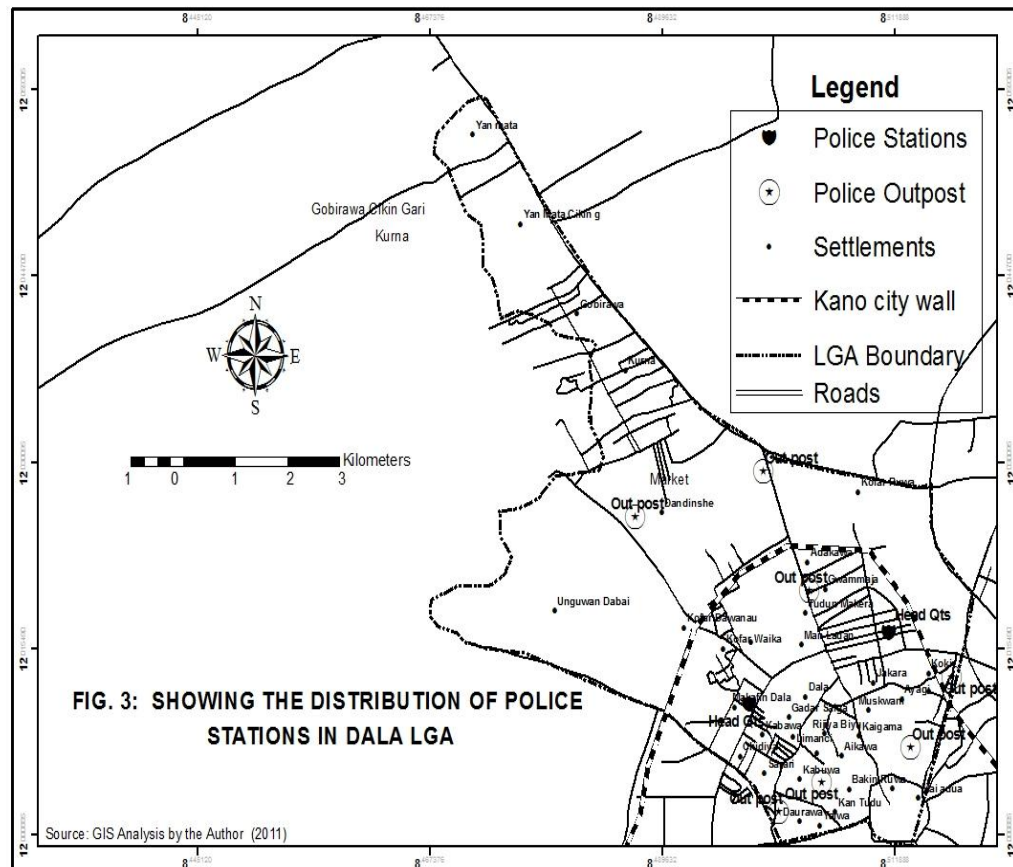
Figure 2 shows the analysis of the crime record collected from the Police units of Dala and Jakara Divisions for the years 2008 – 2010. In the year 2008 offence against local act having the highest crimes recorded with 23 and about 28% of the total crimes recorded, this has to do with the town ship offences and other drug activities especially the youths that venture into the selling and buying of the *Indian hemp*. However, crime against property having the total record of 18 about 29.5% of the total crime, this included the robberies that took place in area around Dandinshe and others are shop breaking and theft. Offence against person was having the record of 17 and taking about 27.9% of the total record and this has to do with some of these crimes like indecent assault, wounding and even the grievous harm or injury which are the most common crime in the area. Offences against authority were having the least record of 3 only in that year of about 5% of the total record, this means that less record of crime that is related to traffic offence, corruption, forgery and others were observed during this year but there is one record of somebody trying to escape from prison (Custody).

FIG. 2: SHOWING THE TEMPORAL DISTRIBUTION OF CRIME IN DALA LGA

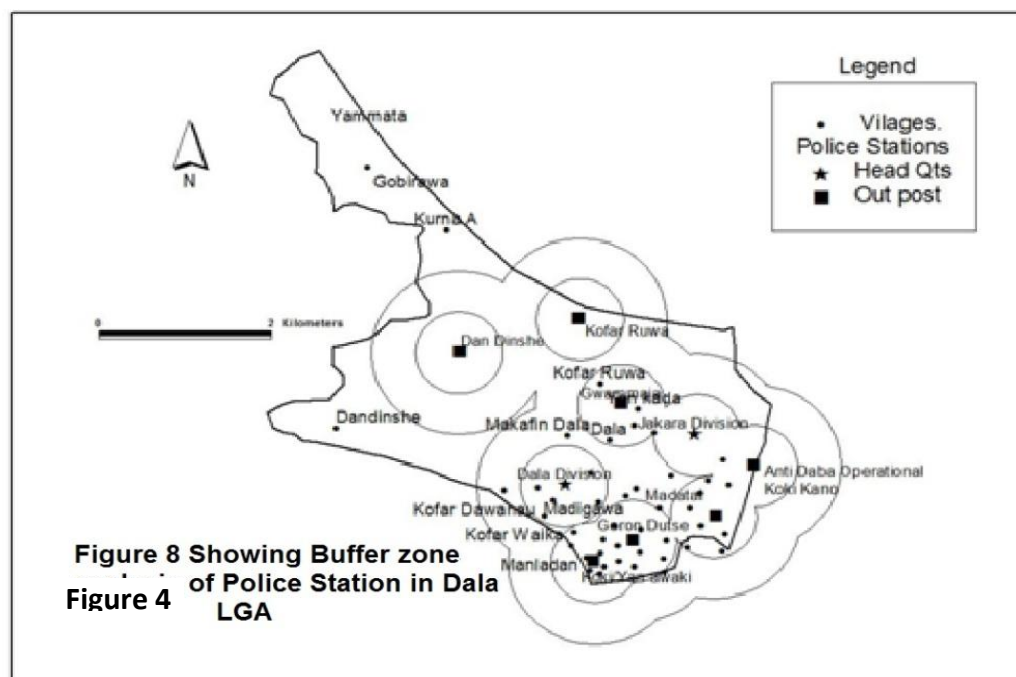
In the year 2009, offences against person recorded of 27 and about 42.2% of the total crime at that year which is the highest and this has to do with gravious harm, wounding and unnertural offence are most common among them, followed by offences against property with 17 in the record and about 26.6% of the total crime recorded and this has to do with stealing, house breaking and receiving stolling property. Also offences against local act have record of 17 which is 26.6% of the total recorded cases in the year, and these was attached with cases that involved township offences and the use of *Indian hemp* by the youth in the area. The least one was the offences against authority with record of 3 cases which takes 4.7% of the total crime recorded. This shows that less record was observed on the crime that is related to currupction and bribery because many can confess involvement and is a crime that is very difficult to establish some facts agaist committers. In the year 2010, the highest recorded cases of crime that were related to offences against property was 40 and with 37% of the total record and this was attached to some cases that has to do with car theft, cheating, house and shop breaking. Also cases with the total record of 34 is offences against person with 31.5% some of these cases were insult, gravoious hurt and unnertural offences. Offences against local act was having 27 and about 25% of the total record in the year and this has to do with local crimes and mostly by the youths of the area, some of these cases were the use of narcotics and township offenses.

Distribution of Police Station

Figure 3 show that the area has a total number of nine (9) police stations. Among which the city wall (*cikingari*)hasseven (7) police stations and two are Divisions (Jakara and Dala), while the remaining four (4) are outpost stations and the remaining two are outpost sited outside the city wall (Dandinshe and KofarRuwa station). According to Yusuf (2010) the total population of police personnel in Dala LGA shows 152 and these should take the population of more than 418,759 persons (census 2006). Table 2 shows that Madatai, Gwammaja, Koki, Dandinshe, KofarRuwa, Yan Awaki and GoronDutse all have the police outpost, while Dala and Jakara are the Head Quarters.



The buffer zone analysis, (Fig. 4) showing the first radius with 1000 meters (1Km) while the second having 2000m. The distance of 2000 meters (2Km) radius has been selected for the purpose of this study to analyse the accessibility to a Police stations and it shows that a person has to travel to some certain distance before reaching to a police station or an outpost station. The first circle shows areas of neglect, places like Makafin Dala, Kofar Dawanau. While the second circle of the 2000m show areas around Kurna, Gobirawa, and U/Dabai.



Spatial Distribution of Crime

A crime hotspot is generally defined as an area containing dense clusters of criminal incidents (<http://www.geospatialworld.net>). Identifications of hotspots help public safety institutions to allocate resources for crime prevention activities. This geographical analysis was made based on crime recorded by the Police of Dala and Jakara Unit of crime events of three years (2008, 2009 and 2010).

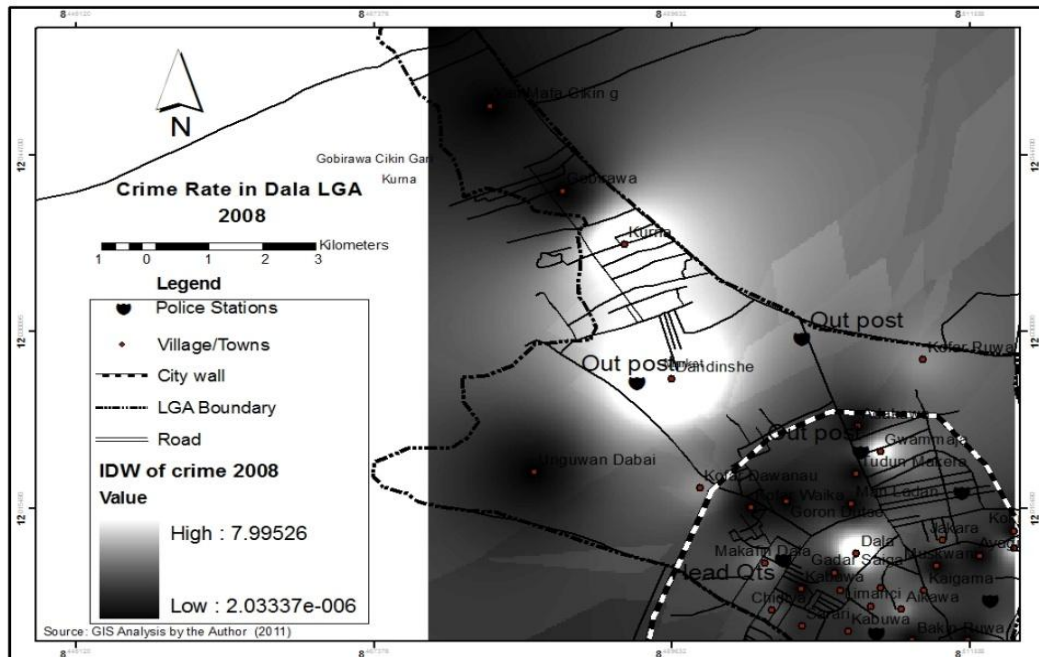


FIG.5: SHOWING THE CRIME HOTSPOTS FOR 2008

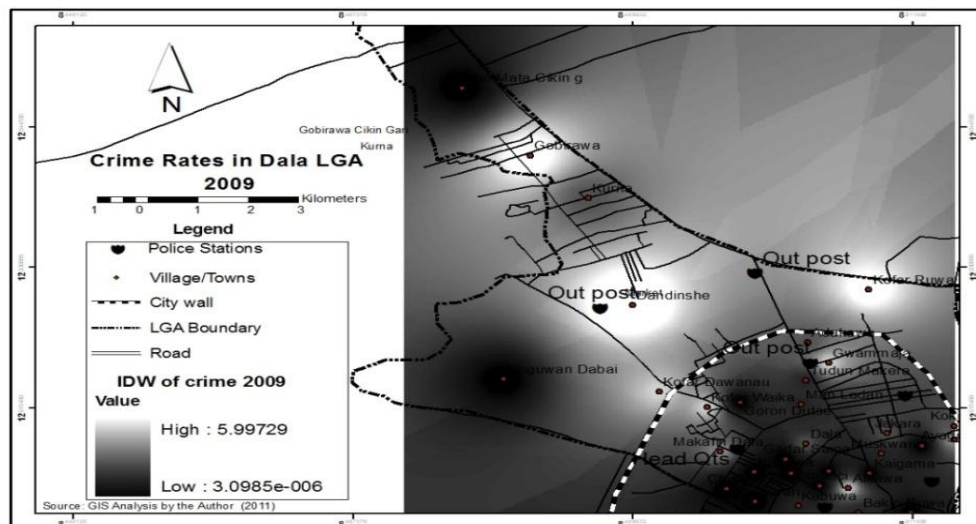


FIG.6: SHOWING THE CRIME HOTSPOTS FOR 2009

Figure 5 analysed the 2008 distribution of crime and hotspots areas, it shows that in the city wall (*cikingari*) have less distribution, but areas around Gwammaja, Dala and some part of Kofar Mazugal and Goro Duste. Other areas outside the city have clustering hotspot, places like Dandinshe and Kurna, while areas around Gobirawa and UnguwanDabai have no record of case. In 2009 figure 6 showing the hotspots within the city, that shows a fair distribution of crime, while places like Jakara, Kofar Dawanau, Makafin-Dala, Gwammaja and some pat of Yalwa are having fewer cases. However, spots outside the city wall were observed, palaces like

Dandinshe, Gobirawa and KofarRuwa and some areas around kofar Dawanau, while U/Dabai areas around Yan Mata have no record of case.

In 2010, figure 7 showing the analysis of the recorded cases reported in this year the rate of crime increased, but this time around it clustered within the city wall (*cikingari*) areas around Dala, Gwammaja, Waika, Dawanau, Bakinruwa and Kofar Mazugal, however it was in this year that the city experienced a tremendous record of cases. Outside the city wall smaller patches of cases were recorded around Dandinshe, Kurna and Gobirawa but Kofar Ruwa was the hottest spot outside the city while U/Dabai and Yan Mata had no record of cases.

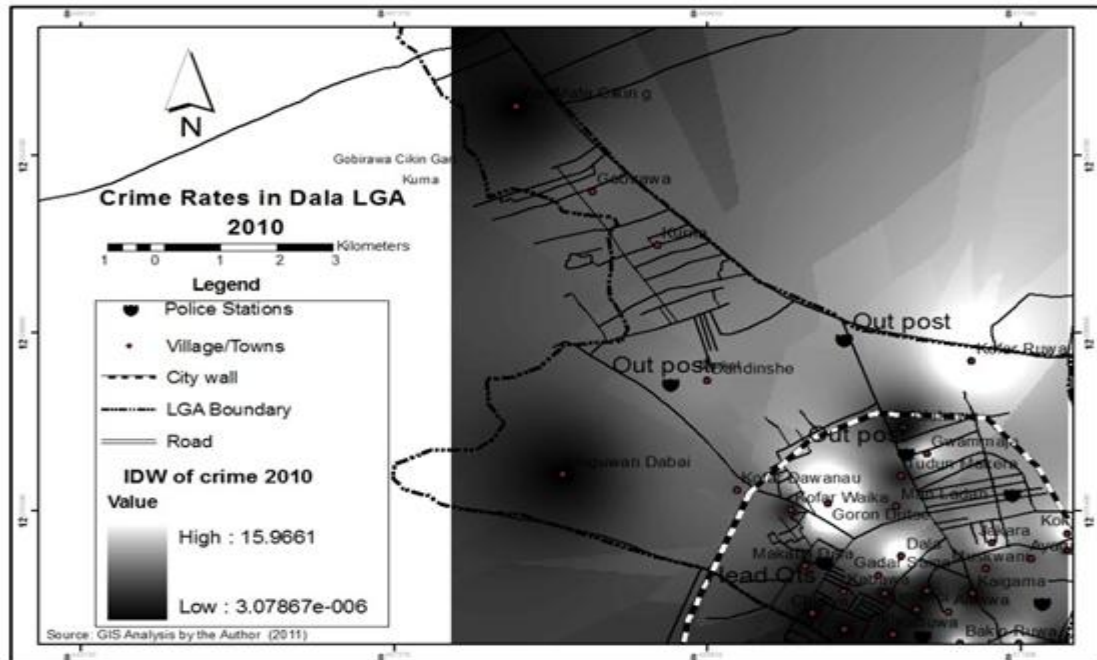


FIG.7: SHOWING THE CRIME HOTSPOTS FOR 2009

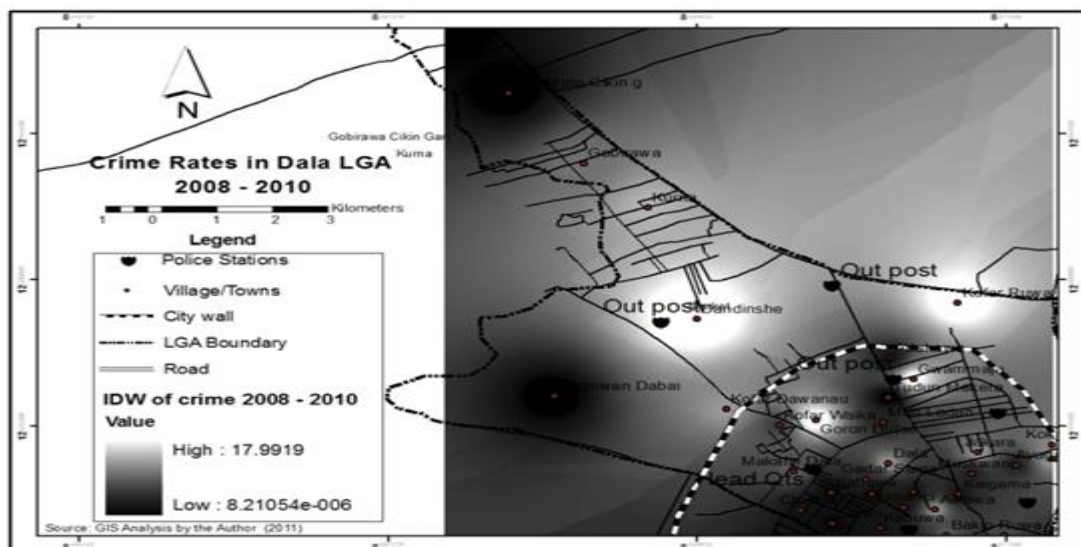


FIG.8 SHOWING THE COMBINATIONS OF CRIME HOTSPOTS FOR 2008, 2009 AND 2010

Figure 8 shows the combinations of the reported cases of 2008, 2009 and 2010 (layers). The hottest spots in the three years are Dandinshe and Kofar Ruwa which all outside the city wall, while in the city wall some patches of spots were experienced to mention few are Kofar Waika and Gwammaja.

VI. CONCLUSION

The findings of this study shows that the spatial pattern of crimes tended to be clustered outside the city wall, areas around Dandinshe, Kofar Ruwa and Kurna, this could be as the result of absence of Police Stations, even though, there are Police outpost but this cannot have enough Manpower and facilities/equipment for policing activities. The study revealed that using GIS is a much more compatible means of crime pattern analysis, because of its geographic referencing capabilities. The three basic categories of GIS functions (database management, spatial analysis and visualization) in a single computer-based system created an environment that is better than the present method of analysis by the law enforcement agencies.

Not only can GIS applications benefit law enforcement agencies in their efforts to analyze crime patterns, but it also has the potential to help the public target high crime areas with preventative measures. Through GIS, communities could be provided with better information on crime in their immediate areas and work with law enforcement officials to determine the best means to reduce the crime rate in their neighborhoods, other public agencies could benefit from GIS in determining the allocation of resources and initiating new programs. Many organizations have a need for an improved system of data manipulation and analysis that can link information to its geographic location, and GIS is an alternative that could aid in this area and result in improvements in the decision-making process.

REFERENCES

- [1]. Boba R (2005) Crime analysis and crime mapping, *Sage publications*, London
- [2]. Burrough, P.A. (1998) *Principles of Geographic Information System*. New York, Oxford University
- [3]. Dambazau A. B (2007) *The Nigerian Police and Crime Prevention : Criminology and Criminal Justice Nigerian Defense Academy Press*, Kaduna. Ch 5, pp221
- [4]. E. Akpinar, N. Usul(2006) *Geographic Information Systems Technologies in Crime Analysis and Crime Mapping*
- [5]. ESRI (1990) *ARC News* Vol. 23, September (Environmental Systems Research Institute, Inc., Redlands, CA, www.esri.com)
<http://www.geospatialworld.net> Accessed 8/18/2011
- [6]. *Luivei Times* (2010) Kenya Magazine Sept. 2, 2010
- [7]. Musa B. A. (2005) Measuring Police Effectiveness in Nigeria. An Evaluation of Input and Output Crime and Policing in Nigeria: Challenges and Options. Edited by Etannibi E.O. Alemika& Innocent C. Chukwuma *CLEEN FOUNDATION* 2004 ISBN: 978-35160 -9-4
- [8]. Rilwani M.I and Eguabor D.O (2000). The need for GIS and Crime Prevention, Detection and Control: A case study of Edo State Police Command *Nigerian Journal of Cartography and GIS* Vol.1. No.1 pp. 86.
- [9]. **Sahu and Peeyush** (2011) *Effective crime control using GIS* gisdevelopment.net.
- [10]. Smith T.R., Menon, S., Starr, J.E., (1987). Requirement and Principles for the implementation and construction of large scale geographic information system. *International Journal of Geographic Information System*.
- [11]. Yusuf. (2011) *Spatial Distribution of Police Stations in Kano Metropolis* An Under graduate Theses submitted to the Department of Geography Bayero University, Kano.

Quality of Irrigation Water and Soil Characteristics of Watari Irrigation Project

Adamu G.K

Department Of Geography And Regional Planning, Federal University Dutsin-Ma Pmb 5001 Katsina State, Nigeria

Abstract: This research was carried out in Watari River Irrigation Project, located on the slopes of Watari River valley in Bagwai local government of Kano state with aim of assessing soil properties and quality of irrigation water. A total of 32 representative soil samples were randomly collected from the eight sectors. Seven water samples were also collected from the sectors and the dam. The samples were treated and analyzed for physical, chemical and fertility related indices. Typically, the quality of irrigation water is assessed based on the salt and salt inducing contents, the presence and abundance of micro and macro nutrients, trace elements, alkalinity, acidity, hardness and the amount of suspended solids. The results are grouped into general quality parameters which included salinity and salt inducing cations and anions and pollutants. The Findings indicated that the mean pH ranged from 7.10 to 7.50, while the mean EC values across the sectors ranged from 50 to 60 μ S/m. The mean metal cations in the water ranged from 15.00 to 20.07; 5.41 to 16.22; 3.29 to 6.57; 14.83 to 15.00cmol/l for Na, Ca, Mg and K respectively. The SAR ranged from 6.87 to 10.17, while the range of TDS values was from 31.00 to 36.00mg/l. The mean carbonates concentration detected in the irrigation water was from 4.00 to 12.00cmol/l, while the mean bicarbonate content ranged from 22.00 to 55.00cmol/l. The ranges for chloride and nitrate were 9.87 to 31.58 and 1.00 to 1.65mg/kg respectively. The residual sodium carbonate (RSC) ranged from 8.00 to 30.69. There was no detectable NH_4 in the irrigation water. The results have shown that all the eight sectors had sand dominated texture. The mean pH in the soil ranged from 5.50 to 5.95. The EC ranged between 0.49 to 1.30cmol/kg, the Cl^- ranged between 0.29 to 1.07cmol/kg and SAR ranged between 0.13 to 0.72. The mean soil organic carbon across the sectors ranged between 0.62 to 1.49%. The total nitrogen ranged between 0.0043 to 0.084% while NH_4^+ and NO_3^- Forms of nitrogen ranged between 0.0043 to 0.0065cmol/kg and 0.0025 to 0.0065mg/kg respectively. The CEC ranged between 9.04 to 12.68cmol/kg. The exchangeable bases ranged from 3.13 to 4.25; 1.06 to 1.73 and 1.28 to 2.08cmol/kg for Ca, Mg and K respectively. The boron content in the soil across the sectors ranged between 4.09 to 6.34mg/kg. It was recommended that adequate drainage with emphasis on surface drainage should be provided and salt and sodium build up should be monitored regularly.

Key words: Irrigation water, Watari, Physico-chemical properties, Quality, Assessment, Soil properties and, Fertility.

I. INTRODUCTION

The primary goal of water analysis is to examine the effect of the water on the soil, and ultimately on the plants grown on the soil. As such, much of the interpretation of the water analysis is based on a prediction of the consequences for the soil. Typically, the quality of irrigation water is assessed based on the salt and salt inducing contents, the presence and abundance of micro and macro nutrients, trace elements, alkalinity, acidity, hardness and the amount of suspended solids (U.S. Salinity Laboratory Staff, 1954; Ajayi et al. 1990).

Poor quality of irrigation water affects both soil quality and crop production adversely (Bello, 2001). Regardless of its source, Irrigation water contains some dissolved salts (Michael, 1985). The amount and characteristics of these dissolved salts depend on the source and chemical composition. The most ordinarily dissolved ions in water are sodium, magnesium, calcium (Ca^{2+}), sulphate (SO_4^{2-}), nitrate (NO_3^-), chloride (Cl^-), boron (Br), carbonate (CO_3^{2-}) and bicarbonates (HCO_3^-). The concentration and proportion of these dissolved ions among other things determine the suitability of water for irrigation (Ajayi et al., 1990).

The function of soil is generally threatened by the increasing and very often conflicting demands of a constantly growing human population and its activities (such as irrigation), as well as by land use and climate change. This leads to a number of physical and chemical degradation processes that affect the sustainable functioning of soils (EEA/UNEP, 2000). Soil degradation can be defined as human-induced deterioration of its quality, which means the partial or entire loss of one or more functions of soil (Blum, 1988). Soil quality then should be related to the potential socioeconomically and ecological soil functions. Irrigation is helpful for sustaining agricultural production in any place; therefore, it is imperative that good quality water should be used so as to sustain the soils. However, continuous use of soil for irrigation may pose some adverse effects on both soil and water quality. Adequate management of soil is required to achieve the Millennium Development Goals of the United Nations of food security by the year 2015. One of such efforts by government to develop land for food production is in the area irrigation scheme.

This paper assessed soil and water conditions in the Watari Irrigation Scheme with a view to making proper recommendations on the implications of the current trend of land use in the irrigation scheme. The results are grouped into general quality parameters which included salinity and salt inducing cations and anions and pollutants.

II. STUDY AREA

Watari Irrigation Scheme is a medium scale irrigation project located on the slopes of the Watari River valley in Bagwai Local Government, which is about 18km from Bichi. It is located at the Northwestern part of Kano between latitudes $12^{\circ}6'54.54''N$ and $12^{\circ}9'17.8''N$ and longitudes $08^{\circ}11'50.62''E$ and $08^{\circ}16'28.05''E$.

The main canal is about 10km long, while the command area consists of 5 sectors that are completed, numbered 1 through 4 and sector 8 the kanyu pilot farm. The net irrigable land area in rounded figure per sector is as follows:

Table: 1 The Area of Irrigable Land in Watari River Irrigation Scheme

SECTOR	HECTARE
1	160
2	170
3	216
4	72
8	72
TOTAL	690

Source: KNARDA, 2011

III. METHODOLOGY

A total of 4 soil samples were randomly collected from each of the 8 sectors from a depth of 0-20cm thereby making a total of 32 representative samples which were treated and analyzed for physical chemical and fertility related indices.

Seven water samples were collected and analysed for physiochemical and salinity related parameters. One sample was collected from the Dam water which is the main source of water in the scheme. Six other samples were collected from the sectors: one, two, three, four, five and eight

Particle size distribution was determined using bouyouscos (1957) method. Textural triangle was also used for determining textural classes. Organic carbon was determined using the Walkley-Black (1934) method. Phosphorus (P) content determination was done using the colorimeter method using sodium hydrogen carbonate extract (Adepetu et al, 2000). Exchangeable bases were extracted by the ammonium acetate extraction technique and determined by flame photometry (Adepetu et al, 2000). The CEC was determined using ammonium acetate saturation method as described by Hesse (1971). The total nitrogen was determined using Kjeldal method while pH was determined using 1:2.5 $CaCl_2$ dilution method (Adepetu et al, 2000)

The water samples were analysed according to American public health association standards method for examination of water and waste water (1985). Digital pH meter was used for determining Ph of the samples. Conductivity was determined by using conductivity cell containing platinised electrodes. The Nessler's method was used to determine ammonia. Nitrates were determined by the phenoldisulphoric acid method. Turbidity was determined by spectrophotometric method. Colorimetric method using molybdate was used for determining phosphate and atomic absorption spectrometer was used for the metal analyses. SAR was computed using the appropriate formula.

IV. RESULTS AND DISCUSSION

General Water Quality of the Watari Irrigation Scheme

Part 2: Salinity and Cations

The general quality of the irrigation water in terms of salinity and cations is assessed based on the parameters shown in Table 2. The values are shown for both samples taken from the dam and the water flowing in the canals serving the sectors. The mean pH ranged from 7.10 to 7.50, while the mean EC values across the sectors ranged from 50 to 60 $\mu\text{S}/\text{m}$. The mean metal cations in the water ranged from 15.00 to 20.07; 5.41 to 16.22; 3.29 to 6.57; 14.83 to 15.00 cmol/l for Na, Ca, Mg and K respectively. There was no detectable NH_4 in the irrigation water. The SAR ranged from 6.87 to 10.17, while the range of TDS values was from 31.00 to 36.00 mg/l .

Interpretation

Generally pH values for normal irrigation should be between 6.00 and 7.00, while values above 7.00 are considered as of increasing hazard (Singh et al. 1996, Danko, 1997). The pH is logarithmic, meaning that a change of 1.0 unit is a ten-fold change in either acidity or basicity. Therefore, changes of even less than 1.0 unit may be significant. This characteristic of the water has a significant influence on other characteristics or reactions in the soil and water, as well as the way plants perform.

The concentration of total salt content in irrigation waters is estimated in terms of EC and it may be the most important parameter for assessing the suitability of irrigation waters (Belan, 1985, Ajayi et al., 1990). It gives an estimate of the total amounts of dissolved salts in the water and the total amount and kinds of salts determine the suitability of the water for irrigation use (Belan, 1985). Generally, the ranges considered for irrigation water suitability are 20 to 70, 70 to 300 and $>300 \mu\text{S}/\text{cm}$ being normal, increasingly severe and severe with respect to salinity hazards (Schoeneberger, 1998). From this perspective, none of the sectors could be described as under any immediate threat, as even the highest mean recorded at sector 3 was still within the normal range. These low EC values further corroborates the values in the soil which also falls much lower than the ranges described as critical for salinity as shown in Table 2.

The amount of Na ions in the water predicts the sodicity danger of the water (Singh, 2000). Sodium ions are important criteria for irrigation water quality because of its effect on soil permeability and water infiltration (Ajayi, 1990). Sodium also contributes directly to the total salinity of the water and may be toxic to sensitive crops such as fruit trees (cite). Sodium ions cause deflocculation of particles and subsequent sealing of soil pores thereby preventing water passage into the soil (cite). Sodic water causes excess Na to be adsorbed to exchange complex and in the process causes dispersion of aggregates and thereby blocking pores in the soil and preventing or reducing infiltration of applied water. Generally, values greater than 9.0 cmol/l in terms of Na concentrations are regarded as posing increasing severity of sodicity especially in soils high in clay content (Davis & Dewest, 1966). The values recorded across all the sectors may therefore be interpreted as posing severe risk factor of sodium toxicity to the soil. The apparent lack of effect as shown by the EC values may be as a result of the fact that the soil is also low in clay content which is the principal particle that deflocculates in the presence of excess sodium. Sodium toxicity to sensitive crops may however not be ruled out with increasing application. Of greater importance in terms of irrigation water quality evaluation than the Na content is the sodium absorption ratio (SAR). The SAR relates the relative concentration of Na to the combined concentrations of Ca and Mg ions (Landon, 1991). Increasing sodicity hazards may be associated with values exceeding 6. As SAR is a factor of sodium against calcium and magnesium, the high values recorded may not be a surprise as the sodium values are also relatively high. These further elaborate the risk factor associated with this irrigation water.

The normal range of Ca^{2+} in irrigation water should be 0 – 20 cmol/l , while that of Mg^{2+} should be between 0 – 5 cmol/l (Christenson et al. 1977). By these criteria the calcium content within the sectors could be described as within safe limit. This also applies to the magnesium content except at sectors 3, 4, 5 and 8 where the values exceed the recommended mean. The relatively lower amounts of magnesium compared to the calcium may be good because Mg deteriorates soil structure particularly where waters are sodium-dominated (as is the case with most of the sectors assessed here) and highly saline. The reason for this structural degradation is that high level of Mg usually promotes a higher development of exchangeable Na in irrigated soils and the negative effect of high sodium content in soil is as described above. The Magnesium content of water is also considered as important qualitative criteria in determining the quality of water for irrigation because more magnesium in water will adversely affect crop yields, as the soils become more alkaline. Generally, calcium and magnesium maintain a state of equilibrium in most waters (Christenson et al., 1977). The combined effect of these two ions is in their countering the negative effect of the sodium by lowering the SAR as shown above. Their cumulative lower value than sodium has contributed significantly to the higher SAR value recorded across the sectors.

The presence of potassium ions in excessive amounts does not constitute any risk and may even supplement crops' needs as only values exceeding 50 cmol/l may be considered as posing any serious risk factor with irrigation water.

One of the miscellaneous ions assessed for evaluation of irrigation water quality is the level of ammonium nitrogen ($\text{NH}_4\text{-N}$). Values that exceed 30mg/l are regarded as increasingly posing a risk factor in irrigation water (Christenson et al., 1977). By this standard therefore the sectors may be regarded as critically lacking in this form of ion as each of them records 0.0mg/l. This does not however mean the water is unsafe for irrigation and may even be good especially with the slightly acidic nature of the soil. However its presence may compliment crops' supply.

TDS is also another criterion for the assessment of salt content in the water as salts constitute important part of TDS (FAO,1985). Water used for irrigation can vary greatly in quality depending upon type and quantity of dissolved salts. Salts are present in irrigation water in relatively small but significant amounts (Michael, 1985). They originate from dissolution or weathering of the rocks and soil, including dissolution of lime, gypsum and other slowly dissolved soil minerals (Belan, 1985). These salts are carried with the water to sites of use. In the case of irrigation, the salts are applied with the water and remain behind in the soil as water evaporates or is used by the crop.

Irrigation water with total dissolved solids (TDS) less than 450mg/l is considered good, and that with greater than 2000 mg/l is unsuitable for irrigation purpose(FAO,1985). By this therefore, the waters in all the sectors could be considered as falling within the safe limit for irrigation.

Management implication

The results here reveal water that may have the potential to be hazardous to the soil as well as to the crop grown, because the two most important parameters used in assessing the safety of irrigation; namely, Sodium ions and the associated SAR are within the unsafe limits. This is notwithstanding the fact that some other factors of salinity are within safe limit. The implication of these high values is that there is the tendency for the soil to be saline and therefore what are recommended here may be measures aimed at mitigating the development of saline or sodic soil. The following measures are worthy of note and implementation singly or in combination.

1. Provision of adequate drainage with emphasis on surface drainage, as the textural property of the soil indicates soil with potency for good internal drainage. If however, barriers restrict movement of water through the root zone especially in those sectors with appreciable clay content (Table 1) additional emphasis should be given to internal drainage.
2. Although the soil has not as yet indicated clear symptoms of salts development, provision should be made for use of clean water to meet the necessary leaching requirement over-irrigation. This is necessary to avoid build-up of salts in the soil solution to levels that will limit crop yields. Effective rainfall can be considered part of the leaching requirement.
3. The soil should be maintained at high available moisture level (always moist and not soaked) and should not be allowed to become more than moderately dry, since the crop cannot remove all the normally available water due to the higher salt content.
4. Salt and sodium build up should be monitored regularly (every 1 to 2 years). Development of a sodium hazard usually takes time and therefore soil tests for SAR or percent exchangeable sodium can detect changes before permanent damage occurs. Soil samples to be analyzed should represent the top soil and occasionally the sub soil.
5. Soluble calcium such as gypsum should be added to decrease the SAR to a safe value. The gypsum can be dissolved into the water or it can be broadcasted over the field. It should be broadcasted directly before irrigation or thoroughly incorporate into the tillage layer to avoid crusting problems. The soil can alternatively be tested for free lime; and when present elemental sulphur could be broadcasted. The sulphur solubilizes the calcium from the free lime already in the soil. If gypsum is used, the fresh water for leaching may have to be increased.

Table 2: General Irrigation Water Quality Parameters for the Watari Irrigation Scheme (Salinity and Cations)

Sample ID	pH	EC $\mu\text{S/m}$	Na (cmol/l)	Ca (cmol/l)	Mg (cmol/l)	K (cmol/l)	NH_4 (mg/l)	SAR	TDS (mg/l)
DAM	7.10	51.67	15.74	9.01	3.63	15.00	0.00	8.85	31.00
SECTOR 1	7.13	53.33	20.07	12.92	3.97	14.83	0.00	9.77	32.00
SECTOR 2	7.10	50.00	15.00	5.41	3.29	15.50	0.00	10.17	30.00
SECTOR 3	7.40	60.00	15.28	13.52	5.48	15.00	0.00	7.01	36.00
SECTOR 4	7.20	50.00	16.00	16.22	5.48	15.50	0.00	6.87	30.00
SECTOR 5	7.50	50.00	15.28	10.81	6.57	15.00	0.00	7.33	30.00
SECTOR 8	7.10	50.00	15.00	13.52	5.48	15.00	0.00	6.88	30.00

Source: Laboratory analytical data, 2012

Part 2: Anions

The quality of the irrigation water across the sectors in terms of anions is shown in Table 3. The mean carbonates concentration detected in the irrigation water was from 4.00 to 12.00cmol/l, while the mean bicarbonate content ranged from 22.00 to 55.00cmol/l. The ranges for chloride and nitrate were 9.87 to 31.58 and 1.00 to 1.65mg/kg respectively. The residual sodium carbonate (RSC) ranged from 8.00 to 30.69.

Interpretation

The normal safe ranking for carbonate (CO_3^{2-}) and bicarbonates (HCO_3^-) are 1.00 and 10.00cmol/l respectively (Landon, 1991). By this criteria therefore, the irrigation water in the sectors assessed could be described as being at severe risk with regards to carbonates and bicarbonates. High carbonate and bicarbonate in water essentially increases the sodium hazard of the water to a level greater than that indicated by the SAR. High CO_3^{2-} and HCO_3^- tend to precipitate calcium carbonate (CaCO_3) and magnesium carbonate (MgCO_3), when the soil solution concentrates during soil drying. If the concentrations of calcium and magnesium in soil solution are reduced relative to sodium the SAR of the soil solution tends to increase as stated above.

Another effect of carbonates and bicarbonates is on the alkalinity status of the soil. High alkalinity indicates that the water will tend to increase the pH of the soil or growing media, possibly to a point that is detrimental to plant growth. Low alkalinity could also be a problem in some situations. This is because many fertilizers are acid-forming and could, over time, make the soil too acid for some plant. Another aspect of alkalinity is its potential effect on sodium. Soil irrigated with alkaline water may, upon drying, cause an excess of available sodium. Several potential sodium problems as highlighted above could therefore result.

Among the components of water alkalinity, bicarbonates are normally the most significant concern. Typically, bicarbonates become an increasing concern as the water increases from a pH of 7.4 to 9.3. However, bicarbonates can be found in water of lower pH. Carbonates become a significant factor as the water pH increases beyond 8.0 and are a dominant factor when the pH exceeds about 10.3(cite).

Chloride (Cl^-) ions are one of the anions in irrigation water for the potential of the water for phytotoxicity. The normal and safe limit for chloride ions in irrigation water should not exceed 30cmol/l (Landon, 1991) by which standard only sector 8 could be described at any potential risk. If the chloride contamination in the leaves exceeds the tolerance of the crop, injury symptoms develop such as leaf burn or during leaf tissue (cite). These symptoms occur when leaves accumulate from 0.3 to 1.0 percent chloride.

Nitrate (NO_3^-) is also another important anion assessed for irrigation water. The normal ranking for nitrate nitrogen is a maximum of 10mg/l (Landon, 1991) by which standard all the sectors could be described as within safe limit. Although it may seem nitrogen in whatever form may be desirable for plants' growth, the risk associated with excess nitrogen, especially the nitrate form which is not adsorbed at exchange sites is the tendency for it to be leached into underground water or being washed away via drainage water to sundry water bodies where it can cause eutrophication.

The influence of bicarbonate and carbonate on the suitability of water for irrigation purpose is empirically assessed based on the assumption that all Ca^{2+} and Mg^{2+} precipitate as carbonate (Michael, 1985). Based on this, the concept of residual sodium carbonate (RSC) for the assessment of high carbonate waters is used. Waters with high RSC have high pH, and land irrigated with such water becomes infertile owing to deposition of sodium carbonate; as known from black colour of the soil. RSC values more than 2.5cmol/l are considered as unsuitable for irrigation (Landon, 1991). By this standard only sectors 2, 3 and 8 can be regarded as within safe limit for irrigation.

Management Implications

High levels of bicarbonates can be directly toxic to some plant species. Bicarbonate levels above 3.3cmol/l will cause lime (calcium and magnesium carbonate) to be deposited on soils and even on foliage especially when irrigated with overhead sprinklers. This may be undesirable for vegetable plants. Similar levels of bicarbonates may also cause lime deposits to form on roots, which can be especially damaging to many tree species. The most efficient corrective measure for high alkalinity is acidification of the water and the soil (cite). This can be achieved by direct controlled acid injection in the water; or the safer major of incorporation of high levels of organic matter in the soil which on decomposition releases organic acids into the soil that solubilise sodium and prevent its accumulation in the soil(cite).

By the most obvious indications, the soil is not calcareous which will have necessitated the calculation of an adjusted SAR value for the water because of the high bicarbonate and RSC values. The adjusted SAR is calculated for the surface soil and, if a leaching fraction is assumed, can be calculated for the subsoil at the bottom of the root zone. The adjusted SAR will also be useful in estimating the sodium build up in the soil from continued use of the water. The adjusted SAR and knowledge of soil properties help determine management practices when using high bicarbonate water. Further assessment of the soil therefore needs to take care of these factors.

Table 3: General Irrigation Water Quality Parameters for the Watari Irrigation Scheme (anions)

Sample ID	CO ₃ ²⁻ (cmol/l)	HCO ₃ ⁻ (cmol/l)	Cl ⁻ (cmol/l)	NO ₃ ⁻ (mg/l)	RSC (cmol/l)
Dam	6.67	36.67	9.87	1.00	3.69
Sector 1	6.67	41.67	16.45	1.65	3.44
Sector 2	4.00	20.00	8.88	0.90	1.30
Sector 3	12.00	15.00	14.80	1.50	0.80
Sector 4	8.00	55.00	14.81	1.50	4.13
Sector 5	6.00	40.00	12.83	1.30	2.86
Sector 8	8.00	25.00	31.58	3.16	1.40

Source: Laboratory analytical data, 2012

Part 3: Trace elements

The quality of the irrigation water in terms of trace elements presence in water is as shown in Table 6. No Cu and As were detected across all the sectors, but Cd and Pb were detected at sector 4 and 1 at 0.1cmol/l respectively. The ranges of Mn and Fe were 0.00 to 0.06 and 0.00 to 0.17cmol/l respectively.

Interpretation

The maximum levels (ML) allowed for these metals in irrigation water are 1.7, 10, 0.1, 20, 50 and 5.0mg/l for Cu, As, Cd, Mn, Fe and Pb respectively (Landon, 1991). By this standard therefore, none of the sectors is at any potential risk hazard except sectors 4 and 8 in terms of Cd.

This is not unexpected as high concentrations of trace elements are only expected in waste water. However, trace elements in all forms of irrigation water are assessed because they have the tendency to get into surface waters via runoff coming through agricultural fields in which agrochemicals and fertilizers are applied, because they form constituents of many of such chemicals. Monitoring trace elements in irrigation water is as important as monitoring salinity status because of their potential to build up in soil and be absorbed by plants thereby being introduced into food chain. When such happens, they constitute further risks to human and livestock in terms of health and wellbeing.

Management Implication

The fact that the levels in water is much lower than prescribed values does not translate into total safety of the water because the trace amounts detected for some elements is still worthy of consideration and further monitoring to ensure that levels do not exceed what has been detected. Monitoring should be on regular basis and different spatial and temporal settings because they are key factors with which concentrations vary.

Table 4: Concentrations of Trace Elements in the Waters of the Watari Irrigation Scheme

Sample ID	Cu (mg/l)	As (mg/l)	Cd (mg/l)	Mn (mg/l)	Fe (mg/l)	Pb (mg/l)
Dam	0.00	0.00	0.00	0.02	0.03	0.00
Sector 1	0.00	0.00	0.00	0.04	0.12	0.01
Sector 2	0.00	0.00	0.00	0.00	0.00	0.00
Sector 3	0.00	0.00	0.00	0.06	0.17	0.00
Sector 4	0.00	0.00	0.01	0.00	0.05	0.00
Sector 5	0.00	0.00	0.00	0.00	0.00	0.00
Sector 8	0.00	0.00	0.01	0.05	0.17	0.00

Source: Laboratory analytical data, 2012

Soil Assessment

The results of the soils analysis of the various sectors of the Watari Irrigation Scheme are presented in the following Tables 1, 2 and 3. The results are grouped into three sections namely physical properties, salinity and fertility statuses.

Soil Physical Properties of the Watari Irrigation Scheme

The physical condition of the soil was assessed for particle size distributions in the soil and subsequently translated into textural classes. These results are presented in Table 5. Across the eight sectors 3, means and values ranged between 63 – 85%, silt values ranged between 6.5 to 20% and clay values ranged between 10 – 18.5%. The highest sand content was recorded at sector, which correspondingly also had the least content of both sand and clay.

Interpretation

Going by these results, it is evidently clear that the soils in all the eight sectors have sand dominated texture. Furthermore, while Sectors 1, 4, 5, 6 and 7 have sandy loam texture; sectors 2 and 7 have sandy clay loam textures; while sector 3 having loamy sand texture. The predominance of sand particles in arid and semi-arid climates is not uncommon because many of them were formed from aeolian deposits blown from across several thousands of kilometers (Mortimore, 1989). Such deposits are commonly found covering the surfaces of underlying soils that may be formed from other parent materials such as the alluvial deposits common in *fadama* areas such as the one investigated. It may be the influence of the alluvium that must have raised the clay and silt values in sectors 2 and 7.

Management Implications

Sandy textured soils are prone to erosion because of the low silt and clay contents which play very important role in binding particles and creating stable structures that can resist erosive factors such as wind and water (Adamu 1997). Such soils are also prone to excessive leaching of nutrients because of low water holding capacity and limited binding sites for cations. Because of this low water holding capacity, the frequency of irrigation will also have to increase and this will affect water use economy and salinity status of the soil. The best management options for such soils would be conservation tillage which minimizes the impact of machines and tools, enhances structural grade thereby improving water retention as well as improving the overall organic matter content of the soil which will improve the nutrient retention ability of the soil (Omar, 2011). The practice may also benefit even those sectors with appreciable clay because it will reduce their proneness to compaction which is a possibility with increased machinery use.

Table 5: Physical Properties of the Watari Irrigation Scheme

Sector	CLAY	SILT	SAND	TEX.CLASS
1	13.5	18	68.5	Sandy loam
2	17	20	63	Sandy clay loam
3	8.5	6.5	85	Loamy sand
4	14.5	10	75.5	Sandy loam
5	12	13	75	Sandy loam
6	10	15	75	Sandy loam
7	18.5	17	64.5	Sandy clay loam
8	13	10.5	76.5	Sandy loam

Source: Lab. analytical data, 2012

Salinity Status of Soils of the Watari Irrigation Scheme

The mean values of the major indicators of soil salinity for the sectors are shown in Table 2. The mean pH in water ranged between 6.13 and 6.48 while in salt it ranged from 5.50 to 5.95. The EC ranged between 0.06 to 0.23dS/m. Na CO_3^{2-} was detected across the eight sectors. While the HCO_3^- mean ranged between 0.49 to 1.30cmol/kg, the Cl^- mean ranged between 0.53 to 1.13cmol/kg. Na mean ranged between 0.29 to 1.07cmol/kg and the SAR ranged between 0.13 and 0.72.

Interpretation

The pH readings across the eight sectors in both water and salt were all within the slightly acid (pH in salt) to very slightly acid (pH in water). The EC values are very much within safe limit, much lower than the 4dS/m prescribed for alkaline and salt affected soils (Landon, 1991). This corroborates the pH values further. The lack of carbonate in the soil and the low (for sectors 1, 2, 3, 4, 7 and 8) to very low (for sectors 5 and 6) concentrations of the bicarbonate further supports the acidity in the soil because it implies that most of the dissolved carbon dioxide and carbonates must have been reduced to either carbonic acid (H_2CO_3) or in the transitional state of bicarbonate. The low sodium (for sectors 1, 2, 3, 4 and 5) to medium (for sectors 6, 7 and 8) concentrations and a variable concentration of Chloride with sectors 1, 2, 3, 4, 7 and 8 having low and sectors 5 and 6 having very low concentrations. There was seemingly a fall in sodium concentration in areas with high chloride ions and a high sodium concentration in areas with low chloride ions; except in sector 7 which seems to have appreciably high concentrations of both. The probable explanation for this condition may be the fact that due to the slightly acid nature of the soil, sodium ions may have been solubilised as carbonates and bicarbonates and leached out of the soil, which explains the low SAR value in all the sectors except sector 7, which has highest amounts of sodium. It also further supports the low EC values across most of the sectors. The higher chloride ions could have originated from the use of chlorinated pesticides and agrochemicals, which are not uncommon in irrigated areas under cultivation year round.

Management Implication

As an area of land under irrigation, the parameters measured in relation to salinity have indicated a soil that is far from being saline or even alkaline. The slightly acid nature of the soil will enhance the availability of nutrients and as shown above may further facilitate the solubilisation of sodium ions which are the primary agents of salinization and alkalisation in irrigated soils (Alhasan, 1996).

Caution should however be exercised over the results shown here because of the delicate balance that exists between different soil properties. For example, the sandy textured nature of the soil as shown above may necessitate higher irrigation frequency which in semi-arid climate like the area under study may not be desirable because of the tendency of excessive evaporation which may precipitate salts on the surface of the soil and which may be disadvantageous to non-tolerant varieties. Furthermore, the tendency for chloride build up in the soil, especially in sector 7 where the sodium concentration is equally appreciable may, in addition to the probability of chloride ions approaching toxic levels, also lead to further salt formation, even in those sectors where the sodium ions are not very high.

There is also the added fear of pH falling further low for reasons associated with nitrogen forms in the soil as will be explained in the next section. When this happens, the tendency for exchangeable bases' concentration to fall and that of micro-nutrients such as Cl and Fe to rise may not be ruled out, and these will cause nutritional complications for crops being grown in the sectors.

Irrigation, fertilizer and agrochemicals management, as well as close monitoring of soil and water conditions should be adopted as strategies to maintain and/or improve the salinity status of the sectors. Extension should focus on water use efficiency, soil conservation practices such as incorporation of organic residues and conservation tillage practices.

Table 6: Soil Fertility Status of the Watari Irrigation Scheme

Sector	pH in H ₂ O	pH in CaCl ₂	EC (dS/m)	CO ₃ ²⁻ (cmol/kg)	HCO ₃ ⁻ (cmol/kg)	Cl ⁻ (cmol/kg)	Na ⁺ (cmol/kg)	SAR
1	6.35	5.95	0.20	0.00	0.68	1.05	0.29	0.17
2	6.13	5.50	0.17	0.00	1.30	1.13	0.36	0.23
3	6.50	5.90	0.06	0.00	0.70	1.00	0.20	0.13
4	6.48	5.85	0.09	0.00	0.85	1.33	0.28	0.19
5	6.28	5.78	0.06	0.00	0.60	0.48	0.32	0.22
6	6.48	5.93	0.12	0.00	0.49	0.53	0.72	0.49
7	6.45	5.88	0.18	0.00	0.83	0.80	1.07	0.72
8	6.48	5.88	0.23	0.00	1.00	1.08	0.59	0.37

Source: Lab. analytical data, 2012

The assessment of the fertility status of the soils of the Watari Irrigation Scheme was based on the parameters whose means are shown in Table 3. Organic carbon was used as indicator of organic matter content in the soil, and total nitrogen was further fractionated into ammonium and nitrate forms due to the implication of each to the soil and water. The CEC of the soils was determined and the concentrations of exchangeable bases was also determined as indicators of percent base saturation (PBS), being a more important fertility indicator than the total CEC.

The results shown in Table 4 indicate the mean organic carbon across the sectors to range between 0.62 to 1.42%. Total nitrogen ranged between 0.035 to 0.084% while the NH₄⁺ and NO₃⁻ forms of N ranged between 0.0043 to 0.0065cmol/kg and 0.0025 to 0.0065mg/kg respectively. The range of available P was between 10.20 to 52.94mg/kg. The CEC ranged between 9.04 to 12.68cmol/kg and the ranges for the exchangeable bases were 3.13 to 4.25; 1.06 to 1.73 and 1.28 to 2.08cmol/kg for Ca, Mg and K respectively. The Boron content in the soil across the sectors ranged between 4.09 to 6.34mg/kg.

Interpretation

The mean organic carbon content in most of the sectors could be considered as low because only sector 2 and sector 7 have their mean within the medium range. Generally values <1% are regarded as low and 1 – 1.5% are regarded as medium (Adamu, 1997). The direct implication of this low organic carbon content in the soil is that organic matter is also low. This is not unexpected in tropical environments because generally addition of organic residues which determines the organic matter content in the soil is low and their lost through mineralization is high (Binns et al, 2003).

In contrast however, the N content of all of the sectors were high because the range considered as high starts from 0.02% or 0.03% in extreme cases (Landon, 1991). Most of the N is however in the ammonium form as can be observed in Table 3. The high N content, despite the low levels of organic matter across the sectors indicate the probable effect of application of N-fertilizer especially the ammonium forms which explains the higher concentration of its form in soil as indicated by the result. The effect of the clay content and the little organic matter in the soils could be seen, especially in sector 2, in terms of retention of the ammonium form of nitrogen.

The conditions of the soil favour the retention of this form of N and the loss of the nitrate form through leaching. This also significantly relates to the pH of the soil because ammonium N is associated with acidification of soils.

The available P content for most of the sectors was within the medium range, except in sectors 5 and 7 where it is low. The P content in the soil is also another factor that disagreed with the organic matter content of the soil (Adamu, 2008). That is with low organic matter in the soil, the N and P may likely be low because mineralization of organic matter is known to significantly contribute to the concentrations of both. The most probable explanation for this deviation may also be attributed to fertilizer use, and in the case of the phosphorus, the mild pH might have significantly favoured its solubility from the various pools in the soils.

The CEC values in all the sectors could be regarded as medium despite the apparent variability from sector to sector which is not unexpected giving the nature of the soils especially in terms of clay and organic matter content which are the principal determinants of CEC. The soil CEC must have been significantly contributed to by the clay content, because of the poor state of the soil in terms of organic matter (Alhasan, 1996).

The Ca values across all the sectors are generally low because values of 5cmol/kg and below are generally considered low (Landon, 1991). The Ca values have slightly deviated from the fairly moderate to high values generally found in soils under irrigation. The low values recorded here are as result of the slightly acidic pH, because soils with pH values within the range of neutral to slightly alkaline are associated with high values. Furthermore, the sandy textured nature of the soils and the need for frequent irrigation encourages its leaching, which explains its deviation from the assertion of its accumulation in arid and semi-arid environments.

The Mg values are however within the medium range across all the sectors. The K values are however fairly high. The high amount of K in the soil may have also contributed to the low Ca and Mg values because of its better competitive ability for exchange sites, although their values are not however extremely bad (Folorunsho, 1998). Both Ca and Mg are hovering above the Na concentration the advantage of which is their effect in lowering the SAR values as shown in Table 2. This may significantly offset the salinity condition in the soil.

The theory of the CEC being contributed to by the clay content is further validated by the amounts of basic cations held in the exchange complex, which has translated into a very good index of percent base saturation (PBS) (Alhasan, 1996). The fact that all of the sectors have their PBS above 50% is an indicator of fertile soil only if the all the cations are within the medium to high range.

The boron condition in the soil is also mild. The major fear in the concentration of boron in irrigated soils is its toxicity in some crop varieties when it exceeds the maximum tolerable range (Folorunsho, 1998). This is why it is always one of the parameters being evaluated in irrigation water as well as the soil.

Management Implication

The result is indicative of only marginally fertile soil. This is not unexpected in areas under continuous cultivation. Fertility decline in those types of soils is accelerated with high loss of organic matter and insufficient fertilization (Young, 1976). Apart from phosphorus and potassium whose values in many of the sectors are medium to high respectively, either low or just marginally above the low values for virtually all the indices of fertility were recorded. The major implication of this is the tendency for crops grown to exhibit deficiency if not properly fertilized, especially with nitrogen fertilizer. Fertilizer application should however follow agronomic recommendations based on crops' needs and the physico-chemical properties of the soil. For example, it is shown above that a larger concentration of the soil N is in ammonium form and with further increase; there is the tendency for the mild pH to fall further low, thereby affecting the balances of other nutrients. As already mentioned, the soils of all the sectors would definitely benefit from addition of organic matter, with its advantage of slow release of nutrients, especially nitrogen and phosphorus.

Table 7: Soil Fertility Status of the Watari Irrigation Scheme

OC%	TN%	AP mg/kg	Ca cmol/kg	Mg cmol/kg	K cmol/kg	CEC cmol/kg	B mg/kg	NH ₄ ⁺ N cmol/kg	NO ₃ ⁻ N mg/kg
0.76	0.06	52.94	4.25	1.73	2.08	12.6775	5.34	0.007	0.006
1.43	0.08	42.66	3.43	1.37	1.64	10.2475	5.58	0.005	0.005
0.63	0.04	32.38	3.73	1.30	1.56	10.435	5.29	0.005	0.004
0.62	0.04	23.63	3.13	1.09	1.30	9.035	5.00	0.005	0.005
0.63	0.05	11.81	3.40	1.07	1.28	9.5275	4.09	0.005	0.004
0.75	0.05	24.06	3.28	1.06	1.28	9.8475	4.66	0.004	0.003
1.02	0.05	10.50	3.18	1.22	1.46	10.23	4.85	0.005	0.004
0.52	0.04	36.75	3.80	1.37	1.65	11.4	6.34	0.007	0.006

Source: Lab. analytical data, 2012

REFERENCES

- [1] Alhasn, J. (1996). Determination of CEC and exchangeable bases (Ca, Mg, K and Na) of soils from Sokoto-Rima River Basin at Kwakwalawa: A B Sc. project submitted to the department of soil science and Agric. Usman Dan Fodio University, Sokoto.
- [2] Ajayi, F., M. Nduru and A. Onigwe, (1990). Halting the salt that kills crops African Farmer No.4, pp 10-12
- [3] Adamu G.K. (1997). An assessment of erodibility of selected soils under different land management systems at Bayero University, Kano New campus: Unpublished PGD Project Soil evaluation: BUK.
- [4] Adamu G. K. (2008). N P K level in multiple crop land in a small holder farmland in Kano closed settled zone: Biological and environmental sciences journal for the tropics. Vol.5. BUK.
- [5] Adepetu, J. A., Nabhan, H., Osinubu A. (2000) : Simple soil, water and plant testing techniques for soil resources management: proceedings of a training course held in Ibadan, Nigeria, 16-27 september 1996: Ibadan, IITA, 168pp
- [6] Belan F. I. (1985). Water treatment. Mir Publishers Moscow, USSR, 232P.
- [7] Blum, W. E. H. (1988). Problems of Soil Conservation. Nature and Environment, 40.
- [8] Strasbourg: Council of Europe.
- [9] Binns J. A., Machonachie, R. A., and Tanko A. I. (2003). Water, Land and Health in Urban and Peri-urban food production: The case Kano, Nigeria; www.cityfarmer.org. Accessed June, 2005.
- [10] Bello, S. (2001). Quality of irrigation water and soil characteristics of wetlands in sokoto metropolis. Unpublished B.Sc. Project. Department of Soil Science and Agricultural Engineering, Usman Danfodio University, Sokoto. Pp 69.
- [11] Christenson, J.E., E.C. Olsen, and L.S. Willardson, (1977). Irrigation water quality evaluation. Journal of irrigation and Drain Div. A and CIR 2, proc. paper 13015
- [12] Danko, M.M (1997). Comparative analysis of variables of irrigation water quality along river Rima. B. Agricultural project, Department of soil science and Agricultural engineering, Usman Danfodio Sokoto. pp.45
- [13] Davis, S W. and Dewest, R.J.M. (1966). Hydrology John Wiley and Sons. New York 463p.
- [14] Dawaki U.M. (1996). Determination of organic carbon, available Nitrogen, available Phosphorus, pH Textural class of irrigated soils along the Rima River Basin at Kwakwalawa, Sokoto, A B Sc. Agric. Research project submitted to the department of soil science and Agric. Usman Dan Fodio University, Sokoto.
- [15] EEA/UN EP (2000). Down to Earth: Soil degradation and Sustainable Development in Europe – a Challenge for the 21st Century. Environmental Issue Report 16. Copenhagen: EEA and United Nations Environment Programme Regional Office for Europe.
- [16] FAO, (1985). Guidelines. Land evaluation for Irrigated Agriculture. Soil Bull. No 55, FAO Room Italy.
- [17] Folorunsho, E. (1998). Evaluation of soil fertility status Under Irrigation in Jakara River Valley: A case study of Air-Port Road-Katsina Road, Kano Metropolis; Post Graduate Diploma in Land Resources Thesis; Geography department, Bayero University, Kano
- [18] Hesse, P.R. (1970): A textbook of soil chemical analysis. John Murray Ltd, London Kano Agricultural and Rural Development Authority (KNARDA, 2011)
- [19] Landon, J. R. (ed) (1991). Booker Tropical Soil Manual, John Wiley and Sons Inc.; New York.
- [20] Mortimore M. (1989). Adapting to drought: farmers, famine and desertification in West Africa: Cambridge University Press.
- [21] Machael, A. M. (1978). Irrigation principles and practices. Vikas publishing house Ltd. New Delhi, India Pp702-720.
- [22] Machael, A. M. (1985). Irrigation principles and practices. Vikas publishing house Ltd. New Delhi, India. Pp702-720.
- [23] Omar, G. (2011). Assessment of the Fertility Status of some Irrigated Fluvisols in Northern Guinea Savannah of Nigeria: Department of Soil Science, Faculty of Agriculture, Bayero University, Kano.
- [24] Shoenberger, P. J., D. A Wysocki, E. C. B enham., W.D. Broderson (Eds). (2002). Field Book for Describing and Sampling soils Version 2.0 National soil Survey Center , National Resources Conservation Services, U. S. Department of Agriculture, Lincoln.
- [25] Singah, B. R. (2000). Quality of irrigation water in Fadama lands North-western Nigeria. I. Ground and Surface Water in Kebbi State. Nig. J. Basic. And Apl. Sci. 9:133-148
- [26] U. S. Salinity Laboratory Staff (1954). Diagnosis and Improvement of saline and alkali soil .L.A. Richard (Ed,) Agricultural Handbook No. 60. United State Dept. of Agriculture, US Government printing office, Washington DC., USA. Young, A. (1976). Tropical soils and soil survey; Cambridge University press.